AN ANALYTICAL STUDY
ON
RIVERBED AND RIVERBANK FILTRATION

A THESIS

Submitted in partial fulfilment of the
requirements for the award of the degree
of
DOCTOR OF PHILOSOPHY
in
WATER RESOURCES DEVELOPMENT

by
KAILASH BISHNOI

DEPARTMENT OF WATER RESOURCES DEVELOPMENT & MANAGEMENT
INDIAN INSTITUTE OF TECHNOLOGY ROORKEE
ROORKEE-247 667 (INDIA)
JUNE, 2015

INDIAN INSTITUTE OF TECHNOLOGY ROORKEE
ROORKEE

CANDIDATE'S DECLARATION

I hereby certify that the work which is being presented in the thesis entitled **AN ANALYTICAL STUDY ON RIVERBED AND RIVERBANK FILTRATION** in partial fulfillment of the requirements for the award of the Degree of Doctor of Philosophy and submitted in the Department of Water Resources Development and Management of Indian Institute of Technology Roorkee, Roorkee is an authentic record of my own work carried out during a period of July, 2010 to June, 2015 under the supervision of Dr. M. L. Kansal, Professor, Department of Water Resources Development and Management, Indian Institute of Technology Roorkee, Roorkee.

The matter presented in this thesis has not been submitted by me for the award of any other degree of this or any other institute.

Signature of the Candidate

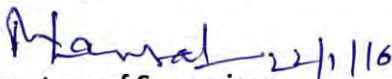This is to certify that the above statement made by the candidate is correct to the best of my knowledge.

Signature of Supervisor

The Ph. D. Viva-Voce Examination of Kailash Bishnoi, Research Scholar, has been held on 22-01-2016.

Chairman, SRC

Signature of External Examiner

This is to certify that the student has made all the corrections in the thesis.

Signature of Supervisor   22/1/16
Dated:

Head of the Department

ABSTRACT

Surface water as a source of drinking water requires costly treatment to make it free from physical, chemical, and bacteriological contamination. Therefore, the managers of various water utilities are exploring the other sources, wherein, the cost of treatment is low. Groundwater is considered as a sustainable source of drinking water in many parts of the world as it requires minimal treatment. Most of the urban areas are located on the banks of the river which are generally contaminated due to various anthropogenic activities. Rivers are the main source of water supply to various cities especially in the Indo-Gangetic plain. In such cases, as the rivers are mostly polluted, it results in heavy treatment cost. Therefore, in such situations, water collected through a collector pipe laid under a riverbed or through a radial well constructed adjacent to the river is a better choice. The flow through collector pipes in such cases shall be free from suspended particles as well as from bacterial contamination as the riverbed/ riverbank filtration work as slow sand filter.

Riverbank filtration (RBF) is a process during which surface water is subjected to subsurface flow prior to extraction from the wells. In RBF process, surface water is subject to a combination of physical, chemical, and biological processes such as filtration, dilution, sorption, and biodegradation that significantly improve the raw water quality. RBF is widely used for drinking water purposes as the water utilities strive to meet increasingly stringent drinking water regulations, especially with respect to the provisions of multiple barriers for protection against microbial pathogens and tighter regulations related to Disinfestation By Products (DBPs).

It has been noticed that only a few studies have been carried out to model such systems mathematically which resulted in analytical solutions. In this study, an attempt has been made to analyse the system of riverbed and riverbank filtration mathematically and to derive the analytical solutions corresponding to various flow characteristics under steady flow condition through such a system.

A radial collector well, commonly known as "Ranney Well", collects water from underground aquifer through slotted radial pipes extended horizontally outward from a caisson. Like infiltration galleries, they are located in or close to rivers and other surface-water bodies. A collector pipe is the primary component of a radial collector well constructed either for riverbed or riverbank filtration. Assuming the collector pipe as a line sink and applying the conformal mapping technique, Aravin and Numerov (1965) have derived an analytical solution for computing potential and flow to the collector pipe laid under riverbed under steady state flow condition. They have considered the origin of the physical domain at the centre of the collector pipe, which restricts the convenience of analysis. In this study, the origin of the physical flow domain is considered at the lower impervious base of the aquifer, which makes the analysis easier as compared to Aravin and Numerov (1965). Analytical expressions have been derived for

i) the potential at different location in the flow domain,

ii) quantity of flow to the collector pipe,

iii) entrance velocity, and

iv) travel time of a parcel of water from the riverbed to the collector pipe along the shortest path.

Further, using the travel time and the logistic function approach, the number of log cycle reduction in bacterial concentration has been found out. It has been noticed that this expression is non-linear in nature which depends on the reproduction and decay rate of micro-organisms. Based on the dimensionless parameters obtained and the analysis related to flow characteristics, following conclusions are drawn:

Yield of a collector pipe is linearly proportional to

(i)   hydraulic conductivity of the riverbed material,

(ii)   drawdown in the well caisson,

(iii)   length of the collector pipe, and

Nonlinearly dependent on

(i)   the diameter of the collector pipe,

(ii) thickness of the aquifer,

(iii) height above the impervious base at which the collector pipe laid.

Further, the present study has been extended to two more cases, i.e.,

(i)   assuming the collector pipe as a line slit, and

(ii) collector pipe with a square cross-section having constant finite head boundary condition at their periphery.

In both the cases, collector pipe is laid under fully penetrating riverbed.

It is found that whether the collector pipe is assumed as a line sink with infinite head boundary or as a line slit or as a collector pipe with square cross-section with finite head boundary; there is no appreciable difference in the estimated flow to the collector pipe.

In case of riverbank filtration, Zhan and Cao (2000) have put forward the philosophy that during late pumping stage, horizontal pseudo-radial flow takes place towards a horizontal collector pipe. This postulation supports the assumption of sheet flow condition in a thin aquifer system with horizontal collector pipe(s). In the present study, using this philosophy for applying Schwartz-Christoffel conformal mapping technique, radial collector well systems having several coplanar laterals located near a straight river reach have been analyzed. The collector well systems with different lengths of laterals, orientation of laterals and distance of the collector well from the river, etc, have been analyzed for safe yield.

In case of a collector well with 4 laterals of equal length, it has been found that the maximum flow occurs when angle between the laterals oriented towards the river is $\pm\frac{\pi}{3}$ and π for $\frac{R}{l_2} < 5$ (see Fig. 5.2 (a)). For $\frac{R}{l_2} \geq 5$, flow to the collector well is maximum for $\gamma = 0.5$.

A radial collector well with 3 radials is a particular case of 4 laterals in which one of the collectors (l_3) (which is perpendicular to the river axis but away from river) is zero. The flow

iii

in such well system is maximum, if the other two laterals are oriented at an angle $\gamma = 0.5$ for $R/l_2 < 5$. For $\dfrac{R}{l_2} \geq 5$, the flow to the collector well is maximum if $\gamma = \dfrac{2}{3}$. In case of a collector well with three radials of equal length in which one of them orient away from the river, the other two should be oriented at an angle $0.2 \leq \gamma \leq \dfrac{1}{3}$ for $\dfrac{R}{l_2} \leq 5$ to obtain near maximum yield. For $\dfrac{R}{l_2} > 5$, their orientation should be $\dfrac{1}{3} \leq \gamma \leq \dfrac{1}{2}$.

In order to validate the results using the concept of sheet flow, an exact solution of flow computation to a line sink in a confined aquifer with collector pipe laid parallel to the river is suggested. In the study, using the conformal mapping technique, an exact analytical solution for two-dimensional flow in vertical plane normal to a collector pipe laid parallel to a fully penetrating river in the middle of a confined aquifer is obtained. While estimating flow to a radial collector well with sheet flow condition, the thickness of aquifer and diameter of the collector pipe are not considered. Therefore, in order to account for thickness of the aquifer, it is suggested to multiply the estimated flow by the thickness of aquifer. As the flow does not increase linearly with thickness of the aquifer, a correction factor needs to be applied. It has been found that the correction factor increases marginally as the thickness of the aquifer decreases. It decreases as the distance of the collector pipe from the riverbank increases. It has been noticed that as the correction factor is very much less than 1, Broom's postulation $\phi = -kD\left(\dfrac{p}{\gamma_w} + y\right) + C^*$ of flow estimation using sheet flow concept overestimates the collector pipe yield, and hence need a correction factor. It may be noticed that the derived correction factors may be applied to estimate the collector well yield with more than 2 collector pipes. Further, yield of collector well increases as it is located nearer to the water body but will decrease the travel time and hence the number of log cycle reduction. It also increases with increase in length and diameter of the collector pipe.

ACKNOWLEDGEMENTS

कैलाश बिश्नोई

(Kailash Bishnoi)

LIST OF CONTENTS

NOTATIONS

C	=	concentration of a bacteria;
C_0	=	initial concentration of a bacteria at $t = 0$;
C_f	=	correction factor;
C_r	=	bacteria concentration in river water;
d	=	median diameter of particle;
D	=	thickness of aquifer;
d_1	=	depth of collector pipe from impervious base;
d_p	=	diameter of horizontal collector pipe or lateral;
D_s	=	scour depth;
d_s	=	side of square collector pipe;
D_w	=	$h_R - h_w$ = drawdown in caisson;
f_a	=	fraction of opening area;
f_L	=	Lacey's silt factor;
h_1	=	piezometric head in the collector pipe;
h_R	=	water level in river;
h_w	=	water level in well caisson;
i	=	imaginary number $= \pm\sqrt{-1}$;
k	=	hydraulic conductivity;
l	=	length of lateral;
l_1, l_2, l_3	=	length of laterals 1, 2 and 4, and 3 respectively;
M	=	conformal mapping constant in z-plane;
M_1	=	conformal mapping constant in w-plane;
N	=	conformal mapping constant in z-plane;
n	=	number of log cycle reduction in bacterial concentration;
N_1	=	conformal mapping constant in w-plane;

p	=	water pressure;
Q	=	design flood discharge;
q	=	flow per unit length from one side of the flow domain;
r	=	reproduction rate of bacteria;
t	=	time parameter;
t_r	=	travel time of a parcel of water;
t_{rf}	=	dimensionless time factor;
u	=	velocity component in x-direction;
v	=	velocity component in y-direction;
w	=	complex potential$= w(= \phi + i\psi)$;
y	=	elevation head;
C^*	=	arbitrary conformal mapping constant;
$\bar{v}_e$	=	average entrance velocity;
λ_L	=	decay rate of bacteria;
$\bar{v}_{ef}$	=	dimensionless average entrance velocity factor;
α, β, γ	=	interior angles of the polygon in z-plane;
π	=	$pai = 3.14159265\ldots$;
η	=	porosity of aquifer materials;
p/γ_w	=	pressure head;
ψ	=	stream function;
γ_w	=	unit weight of water$= 9810 \; N/m^3$;
ϕ	=	velocity potential function;

Other notations are locally defined wherever these appear

LIST OF FIGURES

LIST OF TABLES

INTRODUCTION

1.1 GENERAL

Continued population growth and uneven distribution of water resources have forced the water resources agencies to search for innovative and sustainable sources of water for domestic, industrial, and irrigation purposes. As the surface water sources are becoming more and more inadequate and unsafe due to contamination, the decision makers are looking towards ground water as a sustainable source of drinking water in many parts of India and in other countries, Ray et al. (2002).

The oldest method of ground water tapping is digging hole into the earth to a certain depth below the water table but a little can be abstracted in this way. When a large quantity of water is required, the area of contact with the aquifer must be increased. This is carried out by increasing the horizontal or vertical dimension or both depending upon the local conditions; i.e. mainly the thickness of the aquifer and depth of the water table below the ground surface. The horizontal means of groundwater recovery are called infiltration galleries or in case there exits only one or two co-linear collector pipes, the arrangement is termed as an infiltration or drainage gallery and the vertical means of ground water recovery are called wells. In wells, water is admitted from the sides as well as from the bottom of the wells; the velocity of inflow is kept low. In order to increase the flow, these wells are generally connected to each other by means of porous pipes. In some groundwater basins, the alluvial deposit in the vicinity of a river may contain boulders. Pushing horizontal collector pipes into such deposits is very difficult. In such aquifers, infiltration galleries are laid at a shallow depth after making an open excavation and top covered by rubble. A gallery may be laid under the riverbed or in the vicinity of the riverbank. A significant quantity of water can be pumped from an infiltration gallery because the hydraulic conductivity of the natural material and the filter pack surrounding the screens is so high that recharge is sufficient to meet required pumping rate with permissible drawdown. A gallery laid under a riverbed is oriented perpendicular to the river flow direction whereas a gallery installed near the riverbank is placed parallel to the river i.e. perpendicular to the groundwater flow direction. The galleries located adjacent to a water body usually receive water that has lower turbidity and fewer bacteria than bed-mounted galleries, because the water gets filtered more extensively, Ray et al. (2002).

1

A collector pipe is the primary component of a radial collector well constructed either for riverbed or riverbank filtration (RBF). In riverbed filtration a collector pipe is laid as per requirement from consideration of scour depth and minimum filtration depth. A collector pipe is a part of a riverbed or bank filtration technique. Riverbed or bank filtration is cost effective, well established technique that is used as an important component of water treatment system. Underground water passage provides several benefits for drinking water treatment. The underground aquifers act as natural slow sand filters. Underground water passage results in suspended particle, organic and inorganic chemical, and pathogen removal as well as temperature equalization and reduction in disinfection by-products (DBPs) formation and production of more biologically stable water. However, persistent organic substances are not often completely removed during underground passage. Elimination of these substances depends on the residence or travel time and the subsoil passage. The cities which are situated along the banks of rivers have taken advantages of RBF. It may contribute to a more suitable water cycle by recharging stressed groundwater bodies with filtered surface water. RBF technique comes into picture when the water quality in the river is not matching the drinking water quality standards due to intermittent or chronic pollution. The riverbed deposits and aquifer ingredients provide 'slow-rate filtration' and the improved water is of higher and more consistent water quality than water drawn directly from the river. RBF produces water that is relatively consistent in water quality and easier to treat to higher levels of finished quality. Riverbed filtration / RBF are suitable as a water purification tool in developing countries.

In case the surface water is contaminated, water should not be directly taken from the surface water source. In such situation, a collector well or a drainage gallery is constructed in the vicinity of the surface water body to take the advantage of RBF. If the collector well or the drainage gallery is place very near to the water body, the bacteria present in the water body would enter the collector well or infiltration gallery, thereby making the water unsafe for drinking and leading to high water treatment cost. There is a safe distance from the water body within which the concentration of bacteria will get reduced by several times and ground water extracted beyond this distance from the water body will satisfy the water quality standard. Moreover a gallery placed under a riverbed is to be safeguarded against scour problem. Because of greater depth, the galleries cannot be used and because of small saturated thickness of water bearing stratum the vertical well cannot be proved a feasible solution.

However, riverbed/riverbank filtration has its potential disadvantages. Enhanced clogging of the infiltration zone is likely to be observed with high levels of suspended solids (especially in equatorial countries) that may render bank filtration unsustainable, Huelshoff et al. (2009).

High organic pollution and higher mean temperatures (often found in developing countries) both promote microbial growth and may lead to oxygen depletion, thereby lowering the removal efficiency of RBF systems, Huelshoff et al. (2009). The presence of dissolved heavy metals (e.g. arsenic) may severely impair bank filtration quality, Huelshoff et al. (2009). Polar, persistent organic substances are often not completely removed during underground passage (dependent on residence time, length of subsoil passage, redox status), Schmidt et al. (2003). Other post-treatment methods are necessary such as oxidation and adsorption to reach drinking water quality.

A collector pipe is a component of a radial collector well system. A collector pipe is a perforated conduit laid in an aquifer layer to intercept or collect filtered water. Generally, a number of such collector pipes are connected to a circular vertical caisson plugged at the bottom. This water collection system is known as a radial collector well. While installing the collector pipe one should keep in mind that the collector pipe should be located at a total depth of scour plus the minimum filtration depth required for natural filtration. The scour depth is related to the silt factor, which depends on the particle size and type of riverbed materials. Accordingly, the collector pipe is designed.

1.2   TECHNICAL BACKGROUND AND RESEARCH GAP

The ground water flow problem near a horizontal or radial collector well can be described as a three-dimensional flow problem. The safe yield of a radial collector well can be estimated by solving Boussinesq's equation for 3-D flow with appropriate initial and boundary conditions. The flow to the radial collector well can be estimated using a numerical modelling approach by assuming the hydraulic head along the laterals as the same as that in the caisson. Though, the numerical methods are versatile for analyzing both steady and unsteady flow in non-homogeneous flow domain, they need more effort to discretize the flow domain for any parametric study. For example, a study on flow to radial collector well with several laterals would require fine grid size to compute the hydraulic gradient near the laterals with precision. Further, numerical models have their own limitations due to truncation error, convergence and stability problems.

Alternately, the flow characteristics in collector pipe can be based on steady state flow condition satisfying Laplace equation and the pertinent boundary condition, Harr (1962). In order to restrict the movement of fine particles in the collector pipe, depending upon the type of aquifer medium, the entrance velocity to the collector should be restricted below a particular value. Such entrance velocity to the collector pipe is linearly proportional to the drawdown in

the well caisson and the hydraulic conductivity of the aquifer medium, and inversely proportional to the open area fraction in the collector pipe. Blair A. H. (1970) has suggested the maximum entrance velocity of 3cm/s and Huismann (1972) has recommended the maximum entrance velocity as 4cm/s. Larger available length of collector pipe lowers the entrance velocity of the groundwater through the collector pipe reducing the rate of clogging and minimizing the head loss between the aquifer and the collector pipe, Hunt et al. (2003). Further, the axial velocity inside the screen should be less than 0.9m/sec, Ray et al. (2002) and Driscoll (1986). The advantage of homogeneity is taken for solving the flow characteristics to the collector pipe analytically. If the objective is to estimate the flow to a collector pipe, flow field can be considered as two-dimensional (*x-y* horizontal plane) neglecting the resistance to vertical flow. If the well is located near to a surface water body, the flow to the well could be treated as steady state flow during the later stage of long pumping. Thus, the flow can be estimated by solving well-known Laplace equation for 2D flow field $\left(d^2\phi/dx^2 + d^2\phi/dy^2\right)$under steady state conditions and, thereafter, a correction factor can be applied on account of resistance to vertical flow.

Hantush and Papadopulos (1962) have derived analytical solutions for drawdown distribution around a collector well with several horizontally laid collectors in confined and unconfined aquifer located near or under a stream channel satisfying uniform-flux boundary condition along the collector pipes. Milojevic (1963) had carried out an experimental study using electro-dynamic analog model to investigate the yield of a radial collector well for the constant head boundary condition along the pipes.

Hantush (1964) had suggested that instead of assuming each of the collector pipes to be the line sink of uniform strength, Dirichelt type of boundary condition (uniform head condition) needs to be imposed along the collector pipes. Also, Hantush (1964) has analysed the unsteady three dimensional flows to a collector well system located under a streambed for prescribed drawdown at the well face using a finite difference numerical method.

Aravin and Numerov (1965) have derived an analytical solution for computing potential and flow to the collector pipe is treating as a line sink under steady state flow condition. In order to determine the potential and flow to the collector pipe, they have chosen the center of the collector pipe as the origin and it is laid under riverbed.

Debrine (1970) had conducted an experiment on electrolytic model to check the validity of the condition if the flux or the head should be uniform along the collector pipe. The results of his model study agreed with the solutions of Hantush and Papadopulos (1962) with relative deviation of about 2.2%. He concluded that the flow to a collector well could be

4

estimated using the assumptions of either uniform flux or uniform head along the collector pipes.

Zhan and Cao (2000) put forward that at late pumping stage, horizontal pseudo-radial flow takes place towards a horizontal collector pipe. This postulate supports the assumption of sheet flow condition in a thin aquifer and horizontal collector well system.

Zhan and Park (2003) have assumed uniform flux distribution along the lateral axis for solving unsteady flow to the well under various aquifer conditions. Bakker et al. (2005) have applied multi-layer analytic element modelling to estimate the flow to a two-tier radial collector well with several collector pipes under steady state conditions.

Mishra and Kansal (2005) have studied the specific capacity of a radial collector well having 2-tier of 12 numbers of collector pipes in each tier. Mohammed and Rushton (2006) have carried out field experiment and numerical model to analyze the flow in a shallow aquifer before entering into a horizontal well, the flow from the aquifer into the horizontal well and flow inside the horizontal well. They conclude that the hydraulic losses are significant for the longer horizontal collector pipe.

Fahimuddin (2007) applying Schwartz-Christoffel conformal mapping had analysed steady flow to an infiltration galleries and laterals of radial collector well near straight and meandering river reach.

Patel et al. (2010) have performed a steady state simulation model based on analytic element method. The model was used to study the effects of different lateral configurations, hydraulic conductivity of river-bed aquifer, radius of influence and conductance of laterals on the well-discharge, and consequent drawdown. Further based on the results of simulation (using the analytic element method), an approximate empirical equation was developed to obtain the discharge of radial collector well for design purpose.

In order to estimation of flow to a radial collector well assuming sheet flow concept to account for the thickness of the aquifer, one has to multiply the flow to a collector pipe by the thickness of the aquifer. Broom's postulation $\phi = -kD(p/\gamma_w + y) + C^*$ for computation of flow characteristics estimated using sheet flow concept overestimates the yield of collector pipe and needs a correction factor (Broom, 1968). As the flow does not increase linearly with thickness of the aquifer, a correction factor needs to be applied.

Yield of a collector well is influenced by length, orientation, number and diameter of collectors, etc. and can be studied through analytical technique such as the conformal mapping technique. Conformal mapping technique is one of the classical methods available to solve the 2-dimensional groundwater flow. Hunt (1983), applying Schwarz Christoffel conformal

5

mapping, has analyzed steady flow to the collector pipe either laid under riverbed or placed adjacent to riverbank, for different orientation of the collector pipe implementing constant head boundary condition along the pipe. Assumption of two-dimensional flow in a horizontal plane implies that the lateral as well as the river penetrates the entire thickness of aquifer. Applications of the classical Schwartz Christoffel conformal mapping technique in solving two-dimensional saturated steady flow in homogeneous flow domain are well documented in several text books (Polubarinova-Kochina, 1962; Harr, 1962; Bear, 1972; Halek and Svec, 1979; Hunt, 1983; Raghunath, 2007).

The Schwarz-Christoffel conformal mapping technique is applicable to a simply connected polygon with straight-line boundaries having a finite number of vertices one or more of which may be at infinity and the vertex that is taken to infinity does not take part in the transformation there by the complexity of transformation is reduced. Use of conformal mapping technique generally results in multivariable non-linear equations. The non-linear equations are proposed to be solved by Newton-Raphson technique.

The quality of water produced by the well in terms of presence of pathogenic bacteria needs to be assessed. Hence, it is important to estimate the travel time for a parcel of water from river to the collector pipe so that it is more than the survival life of the bacteria. Gerba et al. (1975) have presented the survival lives of pathogenic bacteria in porous medium in different conditions. Lesser bacterial concentration in produced water will require lesser amount of chlorination and hence lesser quantity of Disinfection-by-Products (DBPs) production in the treated water and lesser risk of carcinogenic disease.

The minimum travel time would be the time taken by a parcel of water particle to reach the nearest part of the collector pipe along stream line. It should be more than the survival time of particular pathogenic bacteria in concern.

Overall, the technical background shows that efforts have been made to understand the flow characteristics to collector pipe, particularly for flow estimation. However, no analytical expressions exist for entrance velocity, travel time for a parcel of water, and number of log cycle reduction in bacterial concentration for various shapes likes line sink, vertical slit, and square cross-section pipe for riverbed filtration. Further, it has been assumed that the flow to collector pipe can be considered as sheet flow but no analysis has been carried out for estimating the correction factor for such assumption. There is no relationship between the number of the log cycle reduction in bacteria concentration and the travel time for a parcel of water.

1.3 OBJECTIVES OF THE PRESENT STUDY

In light of the above-indicated research gaps in the area of riverbed and riverbank filtration, the present research has been carried out with the following objectives:

1. To derive expressions for flow estimation through a collector pipe with different boundary conditions.

2. To determine mathematically the entrance velocity to a collector pipe placed under riverbed and adjacent to fully penetrating river.

3. To determine mathematically the travel time of a parcel of water through the shortest path for a collector pipe laid under the riverbed as well as the riverbank system.

4. To find the number of log cycle reduction in bacterial concentration using the logistic function.

1.4 ORGANIZATION OF THE THESIS

The presentation of the work in the thesis has been organized as follows:

Chapter 1 introduces the importance of riverbed and riverbank filtration processes. It highlights the basic flow characteristics (flow, entrance velocity, travel time of a parcel of water and number of log cycle reduction in bacteria concentration) in a collector pipe placed either under or adjacent to fully penetrating river. It further highlights the technical background of the subject matter and describes the research gaps. On the basis of research gaps, objectives of the present study are fixed and the organization of thesis has been presented.

Chapter 2 highlights the various important studies carried out in the area of riverbed filtration, design of radial collector well, riverbank filtration, number of log cycle reduction, entrance velocity, travel time of a parcel of water that travels from riverbed to collector pipe and natural attenuation of contaminant in the porous medium.

Chapter 3 describes the estimation of flow to a collector pipe by applying Schwartz-Christoffel transformation conformal mapping technique. Flow has been estimated for (i) The collector pipe laid under riverbed and treating it as a line sink, and (ii) The collector pipe placed under riverbed and considering the collector pipe is a vertical slit. Definition of line sink has been introduced. In this chapter, the concept of scour depth and suitable place of its placement has been described. Further, for both cases, dimensionless factors for the entrance velocity, travel time and number log cycle reduction in bacteria concentration have also been estimated.

7

Chapter 4 discusses the flow characteristics through a square cross-sectional collector pipe installed under the riverbed at different vertical positions in the aquifer. The chapter also explores the application of Newton-Raphson and Gaussian-Quadrature numerical techniques for solution of non-linear equations. These equations are explicit in nature, and the solution of these equations is useful in determining the conformal mapping parameters. Further, a computer program has been written to solve the Jacobian matrix. The dimensionless entrance velocity factor and minimum travel time along shortest path of a parcel of water taken to reach from riverbed to collector pipe have been carried out. In this case, the corner points of square cross-section are called singular point. The singularities are removed by using Gaussian-quadrature numerical technique considering 96 weights.

Chapter 5 describes the assessment of the flow characteristics for a multi collector pipes with different orientation placed adjacent to a fully penetrating river. In this chapter the concept of sheet flow has been described. Best orientation angles for three and four equal length collector pipes placed parallel to fully penetrating river have been presented. Besides this, the yield of two collector pipes of equal lengths running parallel to the river has also been presented.

Chapter 6 describes the exact analytical solution for computing flow to a line sink in a confined aquifer laid parallel to the river. Also, need of a correction factor has been highlighted and the same is estimated using the estimated flow analytically and the same estimated with sheet flow assumption as carried out in chapter 5.

Chapter 7 describes the summary and conclusions of the work. It also highlights the limitations and the scope for future work.

Finally, a list of the important references has been provided.

The thesis also includes four appendices at the end.

Appendix A mentions the Lacey's scour depth formula and the silt factors for various types of soils.

Appendix B describes the derivation of expression for the number of log cycle reduction in bacterial concentration.

Appendix C describes the Scwartz-Cristoffel transformation used in the thesis.

Appendix D describes the Newton-Rapshon iterative method used in the thesis.

Symbols and notations are defined wherever these are first used. Lists of notations, figures and tables have been provided before the first chapter.

8

LITERATURE REVIEW

2.1   INTRODUCTION

Ground water is used as a potential source of drinking water supply. In comparison to surface water, ground water is well protected against microbial type of pollution and relatively is of good quality. However, exploitable ground water sources are limited as regard to quantity. Inadequate treatment and prohibitive cost of treatment of contaminated surface water have led planners and decision makers to innovate techniques for sustainable and continuous water supply. In regions where rivers are not perennial or have low flows during most part of the year, collector pipes are placed below the riverbed to obtain un-interrupted supply of water naturally filtered through highly permeable saturated riverbed sediments. If a river, which has scarce surface water, underlies alluvial deposits, the exploitation of saturated riverbed aquifer becomes necessary. Under these circumstances, a collector pipe installed under riverbed at suitable depth is a solution of drinking water supply problem. In comparison to most ground water sources, alluvial aquifers that are hydraulically connected to rivers are typically easier to exploit and more highly productive for drinking water supplies, Doussan et al. (1997).

A collector pipe is a special type of water abstraction structure and it is an integral part of radial collector well. A radial collector wells with several horizontal radial infiltration pipes emanating from a central caisson and under favorable hydro-geological conditions are a convenient means for groundwater recovery. Estimation of flow characteristics (flow, entrance velocity, travel time, and number of log cycle reduction etc.) in a collector pipe is a complex problem as compare to vertical well or other means of ground water extraction, which is based on the theory of flow characteristics in a horizontal collector pipe. The theory of flow characteristics of collector pipe are expressed by (i) analytical studies, (ii) experimental studies, and (iii) empirical field studies. Various researchers suggested theories based on these characteristics.

Hantush and Papadopulos (1962) have derived analytical solution for drawdown distribution around a collector well. They analyzed several horizontally laid collectors in confined and unconfined aquifer located near or under a stream channel satisfying uniform-flux boundary condition along the collector pipe. The flow estimation to a collector pipe is based on the solution of Boussinesq's equation for three-dimensional flow satisfying the existing initial

and boundary conditions. Alternately, Harr (1962) suggested the flow through collector pipe may be estimated based on steady state flow condition satisfying Laplace equation and pertinent boundary condition.

An experimental study using electro-dynamic analog model to investigate the yield of a radial collector well for the constant head boundary condition along the collector pipes is carried out by Milojevic (1963). Hantush (1964) has suggested that instead of assuming each of the collector pipes to be line sink of uniform strength, first kind (Dirichelt type) of boundary condition needs to be imposed along the collector pipes.

Based on concept of line sink under steady state flow condition, Aravin and Numerov (1965) have derived an analytical solution for computing potential and flow to the collector pipe. In order to determine the potential and flow to the collector pipe, they have chosen the center of the collector pipe as the origin and collector pipe is laid under riverbed.

In an experimental model using an electrolyte, to check the validity of the condition if the flux or the head should be uniform along the collector pipe or not, Debrine (1970) conducted a study. The results of his model agreed with the solutions of Hantush and Papadopulos (1962) having relative deviation of about 2.2%. He also concluded that the flow to a collector well could be estimated using the assumptions of either uniform flux or uniform head along the collector pipes.

In a review work Hunt (2003) elaborated the advantages of the horizontal collector pipe like (*i*) its installation depth allows large permissible drawdown as a collector pipe can be installed at a lower elevation in the aquifer (*ii*) complete length of the collector pipe screen in an aquifer contributes to groundwater production (*iii*) they suggested that available collector pipe length should be larger in order to lower the entrance velocity of the groundwater through the collector pipe. It also helps in reducing the rate of clogging and minimizing the head loss between the aquifer and the collector pipe.

Zhan and Cao (2000) put forward that at late pumping stage, horizontal pseudo-radial flow takes place towards a horizontal collector pipe. This postulate supports the assumption of sheet flow condition in a thin aquifer and horizontal system. Based on the assumption of uniform flux distribution along the lateral axis for solving unsteady flow to the collector well, Zhan and Park (2003) have carried out experimentation under various aquifer conditions.

In another study based on multi-layer analytic element modeling Bakker et al. (2005) have estimated flow for a two-tier radial collector well with several collector pipes under steady state conditions. In their study they took in consideration the three natures of flow and non-

homogeneous properties of aquifer. They computed the horizontal flow inside a layer analytically and the vertical flow is approximated with a standard finite-difference scheme.

Mishra and Kansal (2005) and Kansal et al. (2012) have studied the specific capacity of a radial collector well having 2-tier of 12 numbers of collector pipes in each tier and also correction factor is derived using sheet flow concept.

Mohammed and Rushton (2006) have carried out field experiment and numerical model to analyse the flow in a shallow aquifer before entering into a horizontal well, the flow from the aquifer into the horizontal well and flow inside the horizontal well. They conclude that the hydraulic losses are significant for the longer horizontal well.

Fahimuddin (2007), applying Schwartz-Christoffel conformal mapping, has analysed steady flow to an infiltration galleries and laterals of radial collector well near river (straight and meandering reach).

Patel et al. (2010) performed a steady state simulation model based on analytic element method. The model was used to study the effects of different lateral configurations, hydraulic conductivity of river-bed aquifer, radius of influence and conductance of laterals on the well-discharge, and consequent drawdown. Further based on the results of simulation (using the analytic element method), an approximate empirical equation was developed to obtain the discharge of radial collector well for design purpose.

Petroleum engineers have also done extensive work on horizontal well problems. Joshi (1991) has presented a comprehensive detail on the flow to horizontal well from the petroleum literature. Kawecki (2000) presented a study to correlate the equations that relate the transient head in a horizontal well to a constant well discharge obtained from the petroleum literature to groundwater hydrology.

Several investigators have carried out mathematical studies to analyze the flow to a horizontal well with their different objectives and under different hydro-geologic conditions. Some recent studies are cited (Zhan, 1999; Zhan et al., 2001; Steward and Jin, 2001; Park and Zhan, 2002; Zhan and Zlotnik, 2002; Park and Zhan, 2003; Hunt, 2005; Kompani-Zare et al., 2005; Sun and Zhan, 2006, etc).

2.2   THE RIVERBED AND RIVERBANK FILTRATION

In case of riverbed filtration the collector pipe should be installed beyond the minimum filter thickness plus scour depth. The scour depth is the function of peak flood discharge and silt factor of various types of soils. When the collector pipe is installed above the scour depth, it

is dislodged and gets turbid water. The riverbank filtration (RBF) technique takes advantage of existing geological formation adjacent to water bodies to filter drinking water. Wells are dug in fine, sandy sediments next to water bodies and water is extracted from these wells. Water in the water bodies filters through the sediment removing contaminants. The water obtained is often of much higher water quality than the raw surface water. The performance of riverbank filtration system using vertical production and radial collector wells in terms of reduction of contaminants (microorganism, organic) that occur during passage of water through porous medium between the productions well and the river. Removal of dissolved organic carbon (DOC) in RBF water utilities with different retention is found in bank filtration by Sontheimer (1980).

The portion of riverbank filtration in the pumped raw water would depend on source water quality, geo-hydrologic conditions of the aquifer, river-aquifer interface, hydraulic gradient, infiltration rates, hydraulic conductivity and distance between the riverbank and the pumping wells. Reduction of contaminant levels in riverbank filtrate is attained by physical filtering, microbial degradation, ion exchange, precipitation and sorption, Gerritse (1998).

During RBF process, which has many similarities to slow-sand filtration, river water contaminants are attenuated from a combination of processes such as filtration, microbial degradation, sorption to sediments and aquifer sand, and dilution with background groundwater (Hiscock and Grischek, 2002; Ray et al., 2002, Ray and Shamrukh, 2010)

The effectiveness of RBF for water quality improvement depends on a number of variables such as the characteristic and composition of the alluvial aquifer materials, river water quality, groundwater dilution, filtration velocity and the distance of the well from the river, temperature of river water, pumping rate, and sediment characteristic at the river-aquifer interface (Ray et al., 2003; Ray et al., 2008).

Riverbank filtration wells can either be horizontal or vertical well depending upon hydro-geologic setting, require production rate and utility's preference. Shallow alluvial deposits and a higher rate of pumping from a given location often favour horizontal wells called drainage galleries. The collector pipes of the collector wells can all be directed towards the river or distributed in all direction (Mishra, 2005; Grischek et al., 2003; Grischek et al., 2005).

In addition, dispersion of surface water chemicals in aquifers and further dilution of chemicals with groundwater help to reduce the contaminant concentration in the pumped water.

12

Water turbidity is often used as an indicator of suspended matter, which in turn is used as an indicator of microbial contamination. Particle removal can be considered a combined effect of straining, adsorption and biodegradation. In riverbank filtration, all three processes can occur Knappett (2006) and Knappett et al. (2008).

Geographic conditions impact the effectiveness of riverbank filtration. The permeability of the sediment affect the seepage velocity and often internal clogging is associated with sediments having low hydraulic permeability and small hydraulic gradients. Sediments that have excessively high conductivity will not be efficient in removing contaminants. Microbial activity may decrease the permeability at the surface water – groundwater interface as a result of biofilm formation. The accumulation of biofilm extra cellular polymeric substances as well as bacterial cells and their gaseous degradation products, can reduce the hydraulic conductivity of sediment layers. The retention of the fine particles (<2mm) in hyporheic interstices is another major contributor to the clogging of riverbank sediments. Under low flow condition, the setting of the fine particles can cause external clogging of riverbed. Although clogged riverbank sediments may increase the efficiency of natural filtration, the loss in conductivity can significantly reduce the productivity of well fields Goldschneider et al. (2007).

2.3 TRANSPORT OF MICROBIAL CONTAMINATIONS

Transport of microbial contaminations in a variety of RBF systems with different characteristics such as travel time, aquifer material, climate, water chemistry and river flow conditions are important from water quality aspects. Some of researchers have described the attenuation and travel of micro-organisms. Berger (2002) has discussed about the various aspects and hydro- geological parameters on which the microorganism removal capacity of a riverbank filtration system depends. The removal process performs most efficiently when groundwater velocity is slow or retention time, i.e., travel time is more. In the granular porous aquifers, the flow path is tortuous and hence organism gets more chances to come in contact with and attached to a grain surface. Detachment also occurs with very slow rates when the water velocity is very slow and organism remains attached for long time and become inactivated or died before reaching the producing well. The efficiency of riverbank filtration to remove microorganism from the infiltrating surface water depends on (1) attachment of the microorganism to the soil or sand and inactivation, (2) the climate and hydrological conditions (temperatures, heterogeneity, flood), (3) the geometry of production well (horizontal well or vertical well) and surface water body (lake, river, island), (4) the character of the bank materials

and streambed, and (5) groundwater flow field. Aquifer materials with significant fracturing are capable of transmitting groundwater at high velocity in a direct flow path with less travel time, i.e., less opportunity for inactivation or removal of microbial pathogens.

Several researcher caries out simulation work on MODFLOW for flow and transport modeling in various flow conditions ((Kelson, 2012, Patel et al. 1998). Dillon et al. (2002) have considered two basic factors which are most important for the assessment of quality of recovered water from a well pumping nearby a river as a part of RBF for drinking water supplies from brackish aquifers. These two factors are (i) minimum travel time from the river to the well, t_{min}, and (ii) the proportion of the recovered water which is derived from the river (q_1/Q_1), where q_1 is the rate of induced infiltration from the river and Q_1 is the discharge rate of the pumping well. The first factor allows an estimate of contamination attenuation through adsorption and biodegradation and the second factor contribute to the further reduction in contaminant concentration through dilution. For well close to the river, t_{min} is small and q_1/Q_1 is large, and with increasing distance from the river t_{min} increase and q/Q may decline. They have considered only vertical well for the study and used MODFLOW for simulation. There results show that a well located 50m from the bank would pump 94% water from the closest reach at steady state and will have a t_{min} of about 84 days for initially horizontal water table taking adsorption and biodegradation into consideration. Further, to minimize the risk of bacterial contamination of produced water, the t_{min} should be more than the survival time of pathogenic bacteria in concern.

Several researcher (Schubert (2002); Schmidt et al., 2003; Schubert, 2003; Schmidt et al., 2004) are reported the field studies conducted in the lower Rhine region to know the flow and transport phenomena of riverbank filtration and to develop numerical models for dynamic simulation of flow and transport. In this study, the important finding was about the age stratification of the bank filtrate between the river and the wells. Age stratification means that water enters a well near a river at widely different times. This difference in time is the reason for equalization of the fluctuating concentrations between the river and the wells. From 3D modeling under steady state condition, results of the flow path, flow time and mean flow velocity were reported and are reproduced as:

Table 2.1 Flow Path, Flow Time and Mean Flow Velocity

Flow path (m)	Flow time (days)	Mean flow velocity (m/day)
290	157	0.25
162	120	1.35
108	33	3.27
68	20	3.4

Several researchers try to provide effective solutions for river bed filtrations. There is several work carried out for monitoring and management of the pathogens, contaminants, dissolved organic and in organic contaminants, carbon content, turbidity, pesticides and Disinfection Byproduct (DBP) Precursors etc. (Kuehn and Mueller, 2000; Hiscock and Grischek, 2002; Ray, 2002; Ray et al., 2002; Verstraeten et al., 2002; Weiss et al., 2003; Weiss et al., 2003a; Weiss et al., 2003b; Ray et al., 2003; Ray, 2004; Weiss et al., 2005; Ray, 2008). Other notable work on RBF technique provides inside for flow and contaminants control (Irmscher and Teermann, 2002; Tufenkji et al., 2002; Weiss et al., 2003a; Gollnitz et al., 2003; Schijven et al., 2003).

Weiss et al., (2004) discussed the significance of RBF in removing natural organic matter (NOM) present in surface water. NOM present in water reacts with chlorine used for disinfection and halogenated DBPs such as trihalomethanes (THMs) and haloacetic acid (HAAs) are formed, many of which are suspected or known human carcinogens (Singer, 1999). Possible approaches for controlling DBPs formation include (1) use of alternative disinfectants, such as ultraviolet radiation or mono-chloramines which do not react readily with NOM, (2) removal of DBPs from finished water through such process as granular activated carbon adsorption or stripping, and (3) better control of source water quality through removal of precursor NOM to prevent DBP formation. RBF's value for controlling DBPs lies in its ability to achieve this last benefit, namely removal of NOM through ground passage.

2.4 ENTRANCE VELOCITY AND TRAVEL TIME OF A PARCEL OF WATER ALONG A STREAM LINE

The range of an entrance velocity to the collector pipes is a conflicting issue among the researchers; Blair (1970) has suggested the maximum entrance velocity to 3 cm/s and Huisman (1972) has recommended the maximum entrance velocity to be 4 cm/s. While installing a collector pipe, one has to check the entrance velocity. Further, the axial velocity inside the screen should be less than 0.9 m/sec Driscoll (1986), Ray (2002). Larger available length of

15

collector pipe lowers the entrance velocity of the groundwater through the collector pipe reducing the rate of clogging and minimizing the head loss between the aquifer and the collector pipe Hunt (2003). The critical axial velocity was determined to be 1m/s Kim et al. (2008) and the concept of entrance and axial velocity also elaborated by Mishra and Fahimuddin (2005). The theory behind this criterion is that at such low velocities flow is entirely laminar, thus turbulence will not contribute to well loss. However, the average entrance velocity concept may be misleading. In screened well, part of the entrance area is blocked by the screen and aquifer material or gravel pack. Soliman(1965) and Li(1954) analyzed flow to a well and they showed that the entrance velocity in the upper 10% of screen was about 70 times that of the lower 10% in an ideal aquifer. In every screened well, part of the entrance area is blocked by the screen and gravel pack. Depending upon the type of soil an aquifer medium is comprised of, the entrance velocity to a collector pipe laid in the aquifer is to be maintained in order to restrict the movement of fine sediments to the collector pipe. The entrance velocity to a collector pipe is linearly proportional to the drawdown in the well caisson, and hydraulic conductivity of the aquifer medium and inversely proportional to the open area fraction in the collector pipe.

Using concept of unsteady flow condition based on hydrodynamic equation, Sende S. (2008) had derived an analytical expression for safe distance of abstraction point from the river. He also derived the expression for travel time of a parcel of water to a drainage gallery under. The collector pipe is installed below the scour depth (Kothyari et al, 1992, Kothyari, 2007) and minimum filtration thickness. The scour depth the function of silt factor is given by lacey (Lacey, 1946, (Lacey, 1929). The value of silt factors for different size of particles is given in appendix A (IS: 3955, 1967).

2.5 CONCLUDING REMARKS

From the literature review on the work carried out by various researchers, it is observed that very little analytical works have been carried out on the flow characteristics of collector pipe in both cases of the riverbed or riverbank filtration. From the technical background reported earlier one can conclude that though efforts have been made to assess the flow through a collector pipe under steady state condition, still analytical studies are required to understand the other flow characteristics through the collector pipe laid under riverbed and in case of riverbank filtration. Further, it has been assumed that the flow to collector pipe can be considered as sheet flow but no analysis has been carried out for estimating the correction factor for such assumption.

considered as sheet flow but no analysis has been carried out for estimating the correction factor for such assumption.

Furthermore, the numerical modeling of collector pipe reported by researchers is quite cumbersome and has its own limitations. There is no relationship between the number of the log cycle reduction in bacteria concentration and the travel time for a parcel of water. In view of the existing gaps in the literature, the present research work has been undertaken. Attempt has been made to derive analytical expressions for various flow characteristics such as yield, entrance velocity, travel time and number of log cycle reduction for collector pipe of various shapes located at various locations in the aquifer system. Further, flow characteristics for multi-lateral collector system installed adjacent to the river under steady state condition have been studied.

ESTIMATION OF FLOW TO A COLLECTOR PIPE PLACED BELOW THE RIVERBED

3.1 INTRODUCTION

Water supplies for drinking, irrigation and industrial purposes have been traditionally drawn from different surface and sub-surface sources like rivers, streams, ponds, lakes and aquifers. However, surface water sources are becoming more and more inadequate and unsafe due to contamination. The contamination problem arises due to sewage effluent discharged into the surface water sources besides due to discharge of effluents from slum dwelling on the river banks. Drinking water supplies from surface water sources require costly water treatment to make it safe for consumption. Ground water is used as a potential source of drinking water supply. In comparison to surface water, ground water is well protected against microbial type of pollution and relatively is of good quality. However, exploitable ground water sources are limited as regard to quantity. Inadequate treatment and prohibitive cost of treatment of contaminated surface water have led planners and decision makers to innovate techniques for sustainable and continuous water supply. In regions where rivers are not perennial or have low flows during most part of the year, collector pipes are placed below the riverbed to obtain un-interrupted supply of water naturally filtered through highly permeable saturated riverbed sediments.

The flow estimation to a collector pipe is based on the solution of Boussinesq's equation for three-dimensional flow satisfying the existing initial and boundary conditions. Alternately, the flow through collector pipe can be based on steady state flow condition satisfying Laplace equation and pertinent boundary condition Harr (1962).

A collector pipe is the primary component of a radial collector well constructed either for river bed or river bank filtration. In river bed filtration a collector pipe is laid as per requirement from consideration of scour depth and minimum filtration depth. Assuming the collector pipe as a line sink and applying conformal mapping technique. Aravin and Numerov (1965) have derived an analytical solution for computing potential and flow to the collector pipe under steady state flow condition. The collector pipe is laid below the river bed perpendicular to the river axis shown in Fig. 3.2 (a) and (b).Such a layout is appropriate if the

well caisson is constructed on the river bank. To derive the flow characteristics, Aravin and Numerov (1965) have chosen the centre of the collector pipe as the origin. In conformal mapping technique, there is no restriction in selecting the location of origin in the physical flow domain. Choosing conveniently the origin at the impervious base below the collector axis, alternate analytical expressions to determine i) the potential at different location in the flow domain, ii) quantity of flow to the collector pipe, iii) entrance velocity, iv) and the travel time of a parcel of water from the river bed to the collector pipe along the shortest path have been derived in this section. Using the travel time, the log cycle reduction in bacteria concentration has been found using logistic function.

3.2   STATEMENT OF THE PROBLEM FOR A LINE SINK

A section of the flow domain in a vertical plane normal to the axis of the lengthy collector pipe is shown in Fig. 3.2 (a) and (b). It is required to estimate the flow characteristics, such as yield, entrance velocity, travel time, and number of log cycle reduction of bacterial concentration through this collector pipe. In order to solve this problem, following assumptions are made:

(i)   The flow is considered to be steady and two-dimensional.
(ii)   The aquifer is homogeneous and isotropic.
(iii) The aquifer thickness is finite.
(iv)   The head loss along the collector pipe is negligible.

In order to derive the solution, conformal mapping technique is suggested in this study. It can be used to solve the Laplace equation provided the flow boundaries are straight. The plan and section of collector pipe are shown in Fig. 3.1.
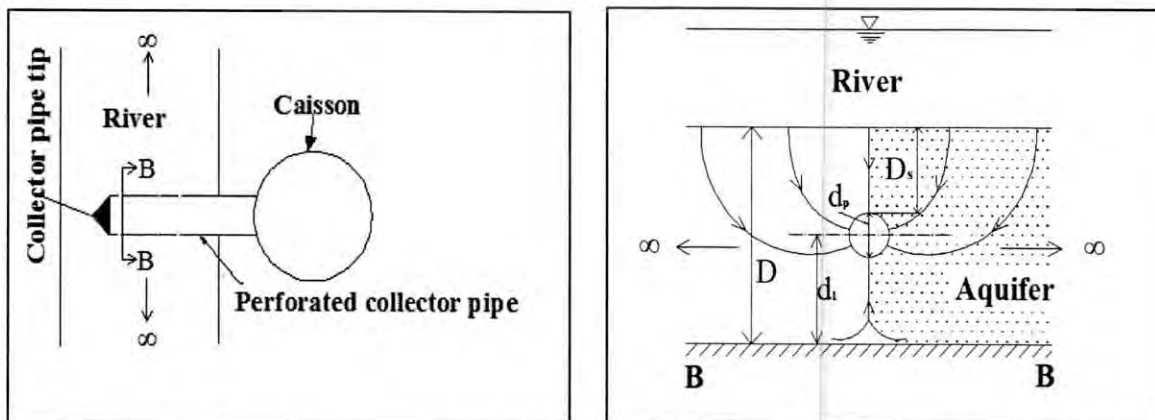
Fig. 3.1: (a) Plan and (b) Section at B-B of a typical collector pipe (not to scale)

The flow is assumed as two dimensional in a vertical plane perpendicular to the collector pipe axis. Further, solutions have been derived assuming the circular section as the followings:

i)   As a line sink as shown in Fig. 3.2 (a)

ii) As a narrow vertical slit of length 'd_p' equal to the diameter of the collector pipe as shown in Fig. 3.2 (b).
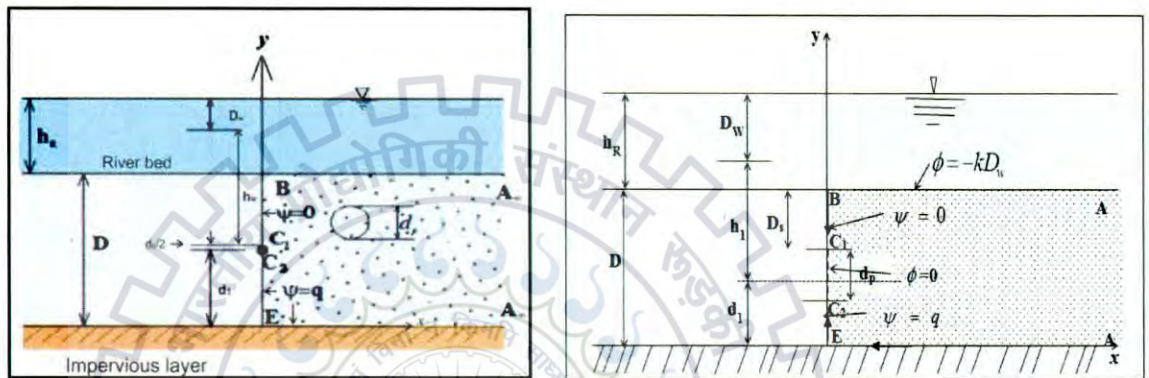
Fig. 3.2 Physical flow domain of (a) line sink and (b) Vertical narrow slit
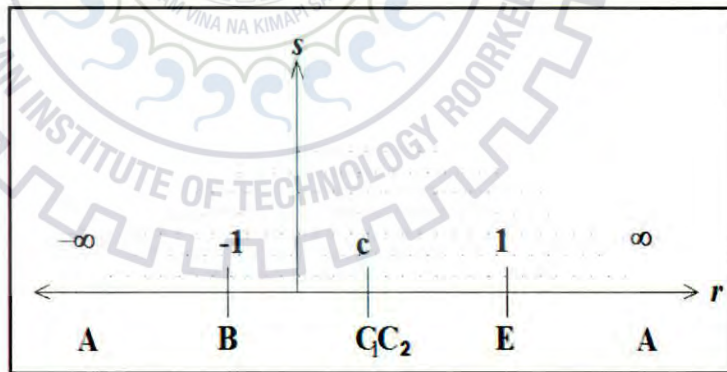
Fig. 3.3 Auxiliary $t (= r + i s)$ **plane of Fig. 3.2 (a)**

AB is the river bed and AE is the horizontal impervious base of the long river reach. D is the thickness of aquifer medium below the river bed. The flow is two dimensional in the vertical plane normal to the collector axis. We take into account the symmetry of the flow domain about y axis and consider half the flow domain for mapping to evaluate the flow characteristics.

3.3 COMPLEX POTENTIAL

The velocity potential function ϕ is defined as:

$$\phi = -k\left(\frac{p}{\gamma_w} + y\right) + C* \tag{3.1}$$

where, k is the saturated hydraulic conductivity of the sediments deposit; p=water pressure; γ_w=unit weight of water; y=elevation head; C^*=a constant conveniently chosen for vertical narrow slit as $C* = k(h_1 + d_1)$, where h_1 is piezometric head in the collector pipe and d_1 is the elevation head at the collector pipe axis. The velocity potential function ϕ is such that $\frac{\partial \phi}{\partial x} = u$, and $\frac{\partial \phi}{\partial y} = v$, where, u and v are the velocity components in x and y direction respectively. The velocity potential function ϕ satisfies the Laplace equation $\frac{\partial^2 \phi}{\partial x^2} + \frac{\partial^2 \phi}{\partial y^2} = 0$. The stream function ψ also satisfies Laplace equation. The velocity potential function ϕ and stream function ψ satisfy Cauchy-Riemann condition that is $\frac{\partial \phi}{\partial x} = \frac{\partial \psi}{\partial y}$ and $\frac{\partial \phi}{\partial y} = -\frac{\partial \psi}{\partial x}$.

3.4 CONFORMAL MAPPING ANALYSIS FOR A LINE SINK

Mapping of the z-plane onto t-plane of a line sink

The vertices A, B, E, and A of the flow domain have been mapped onto $-\infty$, -1, 1, ∞ on the real axis of the auxiliary t plane and plane is shown in Fig. 3.3. Accordingly, the Schwarz-Christoffel conformal mapping of the flow domain (Harr, 1962) in $z(= x + iy)$ plane onto upper half of the auxilliary $t(= r + is)$ plane is given by:

$$\frac{dz}{dt} = \frac{M}{\sqrt{(1+t)(1-t)}} \tag{3.2}$$

Integrating, equation (3.2) reduces to

$$z = M \sin^{-1} t + N \tag{3.3}$$

where, M and N are complex constants, which depend upon the geometry of flow domain. For vertex E, t=1, and $z = 0$; hence,

$$0 = M\sin^{-1}(1) + N = M\frac{\pi}{2} + N \tag{3.4}$$

22

For vertex $B, t = -1$, and $z = iD$. Therefore,

$$iD = M \sin^{-1}(-1) + N = -M\frac{\pi}{2} + N \qquad (3.5)$$

Equations (3.4) and (3.5) yield, $N = \dfrac{iD}{2}$ and $M = -\dfrac{iD}{\pi}$.

The transformation of z-plane onto the auxiliary t-plane is thus given by:

$$z = \frac{-iD}{\pi} \sin^{-1}(t) + \frac{iD}{2} \qquad (3.6)$$

or $\qquad t = \cos\left(i\frac{\pi z}{D}\right) \qquad (3.7)$

At point $C_1 C_2, t = c$ and $z = id_1$. Applying this correspondence in (3.7)

$$c = \cos\left(-\frac{\pi d_1}{D}\right) = \cos\left(\frac{\pi d_1}{D}\right) \qquad (3.8)$$

Mapping of the complex potential w $(= \phi + i\psi)$ plane onto t-plane for a line sink:

The complex potential plane pertaining to the flow domain is shown in Fig. 3.4. The w-plane has been constructed assuming the constant C, which appears in velocity potential function $\phi = -k(p/\gamma_w + y) + C$, is equal to $k(h_R + D)$.
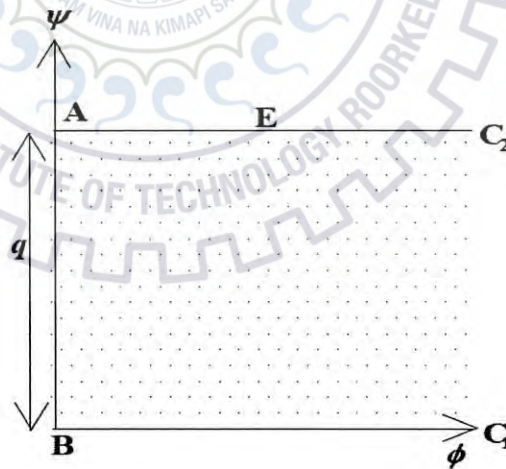
Fig. 3.4 Complex potential w $(= \phi + i\psi)$ plane of Fig. 3.2 (a)

The mapping of the complex potential plane onto the upper half of the auxiliary plane is given by

$$\frac{dw}{dt} = \frac{M_1}{(c-t)\sqrt{(1+t)}} \qquad (3.9)$$

23

Integrating, equation (3.9) reduces to

$$w = M_1 \int \frac{dt}{(c-t)\sqrt{(1+t)}} + N_1 \tag{3.10}$$

Expressing, $t+1 = v^2$, and $dt = 2vdv$ and integrating

$$w = M_1 \int \frac{2vdv}{(c+1-v^2)\sqrt{v^2}} + N_1 = 2M_1 \int \frac{dv}{(c+1-v^2)} + N_1 = \frac{M_1}{\sqrt{c+1}} \ln\left(\frac{\sqrt{c+1}+v}{\sqrt{c+1}-v}\right) + N_1 \tag{3.11}$$

Replacing back v by $\sqrt{(t+1)}$

$$w = \frac{M_1}{\sqrt{c+1}} \ln\left(\frac{\sqrt{c+1}+\sqrt{(t+1)}}{\sqrt{c+1}-\sqrt{(t+1)}}\right) + N_1 \tag{3.12}$$

M_1 and N_1 complex constants to be determined from the complex potential plane. At vertex B, $t = -1$ and $w = 0$, therefore, the constant $N_1 = 0$. At vertex A, $t = \infty$ and $w = iq$. Applying this condition in (3.12):

$$iq = \frac{M_1}{\sqrt{c+1}} \ln\left[\frac{\sqrt{c+1}+\sqrt{t+1}}{\sqrt{c+1}-\sqrt{t+1}}\right]_{t\to\infty} = \frac{M_1}{\sqrt{c+1}} \ln[-1] = \frac{M_1}{\sqrt{c+1}} \ln\left(e^{i\pi}\right) = \frac{M_1 i\pi}{\sqrt{c+1}}$$

Hence, $M_1 = \frac{q}{\pi}\sqrt{c+1}$. Finally, w-t relation is given by:

$$w = \frac{q}{\pi} \ln\left(\frac{\sqrt{c+1}+\sqrt{t+1}}{\sqrt{c+1}-\sqrt{t+1}}\right) \tag{3.13}$$

Substituting t and c in (3.13) by equations (3.7) and (3.8) respectively, the relation between w and z is obtained as:

$$w = \frac{q}{\pi}\ln\left(\frac{\sqrt{\cos\left(\frac{\pi d_1}{D}\right)+1}+\sqrt{\cos\left(i\frac{\pi z}{D}\right)+1}}{\sqrt{\cos\left(\frac{\pi d_1}{D}\right)+1}-\sqrt{\cos\left(i\frac{\pi z}{D}\right)+1}}\right) = \frac{q}{\pi}\ln\left(\frac{\sqrt{\cos^2\left(\frac{\pi d_1}{2D}\right)-1+1}+\sqrt{\cos^2\left(i\frac{\pi z}{2D}\right)-1+1}}{\sqrt{\cos^2\left(\frac{\pi d_1}{2D}\right)-1+1}-\sqrt{\cos^2\left(i\frac{\pi z}{D}\right)-1+1}}\right)$$

$$= \frac{q}{\pi}\ln\left\{\frac{\cos\left(\frac{\pi d_1}{2D}\right)+\cos\left(i\frac{\pi z}{2D}\right)}{\cos\left(\frac{\pi d_1}{2D}\right)-\cos\left(i\frac{\pi z}{2D}\right)}\right\} \tag{3.14}$$

At location, $z = 0$, the complex potential is

24

$$w(0) = \frac{q}{\pi} \ln \left[\frac{\cos\left(\frac{\pi d_1}{2D}\right) + \cos(0)}{\cos\left(\frac{\pi d_1}{2D}\right) - \cos(0)} \right] = \frac{q}{\pi} \ln \left[\frac{\cos\left(\frac{\pi d_1}{2D}\right) + 1}{\cos\left(\frac{\pi d_1}{2D}\right) - 1} \right]$$

$$= \frac{q}{\pi} \ln \left[-\cot^2\left(\frac{\pi d_1}{4D}\right) \right] = \frac{q}{\pi} \ln \left[e^{i\pi} \cot^2\left(\frac{\pi d_1}{4D}\right) \right] \qquad = \frac{q}{\pi} \left[\ln e^{i\pi} + \ln\left\{ \cot^2\left(\frac{\pi d_1}{4D}\right) \right\} \right]$$

$$= \frac{q}{\pi} \ln \left\{ \cot^2\left(\frac{\pi d_1}{4D}\right) \right\} + iq$$

Thus at $z = 0$, $\phi(0,0) = \frac{q}{\pi} \ln \left\{ \cot^2\left(\frac{\pi d_1}{4D}\right) \right\}$; and $\psi(0,0) = q$.

Further, separated the complex potential $w(z)$ into real and imaginary parts as described below and derive $\phi(x, y), \psi(x, y)$. Substituting $z = x + iy$ in equation (3.14)

$$\phi(x,y) + i\psi(x,y) = \frac{q}{\pi} \ln \left\{ \frac{\cos\left(\frac{\pi d_1}{2D}\right) + \cos\left(i\frac{\pi x}{2D} - \frac{\pi y}{2D}\right)}{\cos\left(\frac{\pi d_1}{2D}\right) - \cos\left(i\frac{\pi x}{2D} - \frac{\pi y}{2D}\right)} \right\}$$

$$= \frac{q}{\pi} \ln \left\{ \frac{\cos\left(\frac{\pi d_1}{2D}\right) + \cos\left(i\frac{\pi x}{2D}\right)\cos\left(\frac{\pi y}{2D}\right) + \sin\left(i\frac{\pi x}{2D}\right)\sin\left(\frac{\pi y}{2D}\right)}{\cos\left(\frac{\pi d_1}{2D}\right) - \cos\left(i\frac{\pi x}{2D}\right)\cos\left(\frac{\pi y}{2D}\right) - \sin\left(i\frac{\pi x}{2D}\right)\sin\left(\frac{\pi y}{2D}\right)} \right\}$$

$$= \frac{q}{\pi} \ln \left\{ \frac{\cos\left(\frac{\pi d_1}{2D}\right) + \cosh\left(\frac{\pi x}{2D}\right)\cos\left(\frac{\pi y}{2D}\right) + i\sinh\left(\frac{\pi x}{2D}\right)\sin\left(\frac{\pi y}{2D}\right)}{\cos\left(\frac{\pi d_1}{2D}\right) - \cosh\left(\frac{\pi x}{2D}\right)\cos\left(\frac{\pi y}{2D}\right) - i\sinh\left(\frac{\pi x}{2D}\right)\sin\left(\frac{\pi y}{2D}\right)} \right\}$$

$$= \frac{q}{\pi} \ln \left\{ \frac{\cos^2\left(\frac{\pi d_1}{2D}\right) - \cosh^2\left(\frac{\pi x}{2D}\right)\cos^2\left(\frac{\pi y}{2D}\right) - \sinh^2\left(\frac{\pi x}{2D}\right)\sin^2\left(\frac{\pi y}{2D}\right) + i\,2\cos\left(\frac{\pi d_1}{2D}\right)\sinh\left(\frac{\pi x}{2D}\right)\sin\left(\frac{\pi y}{2D}\right)}{\left\{ \cos\left(\frac{\pi d_1}{2D}\right) - \cosh\left(\frac{\pi x}{2D}\right)\cos\left(\frac{\pi y}{2D}\right) \right\}^2 + \sinh^2\left(\frac{\pi x}{2D}\right)\sin^2\left(\frac{\pi y}{2D}\right)} \right\}$$

$$= \frac{q}{\pi} \ln \left[\frac{\left[\left\{ \cos^2\left(\frac{\pi d_1}{2D}\right) - \cosh^2\left(\frac{\pi x}{2D}\right)\cos^2\left(\frac{\pi y}{2D}\right) - \sinh^2\left(\frac{\pi x}{2D}\right)\sin^2\left(\frac{\pi y}{2D}\right) \right\}^2 + \left\{ 4\cos^2\left(\frac{\pi d_1}{2D}\right)\sinh^2\left(\frac{\pi x}{2D}\right)\sin^2\left(\frac{\pi y}{2D}\right) \right\} \right]^{1/2}}{\left\{ \cos\left(\frac{\pi d_1}{2D}\right) - \cosh\left(\frac{\pi x}{2D}\right)\cos\left(\frac{\pi y}{2D}\right) \right\}^2 + \sinh^2\left(\frac{\pi x}{2D}\right)\sin^2\left(\frac{\pi y}{2D}\right)} e^{i\theta} \right]$$

$$= \frac{q}{\pi} \ln \left[\frac{\left[\left\{ \cos^2\left(\frac{\pi d_1}{2D}\right) - \cosh^2\left(\frac{\pi x}{2D}\right)\cos^2\left(\frac{\pi y}{2D}\right) - \sinh^2\left(\frac{\pi x}{2D}\right)\sin^2\left(\frac{\pi y}{2D}\right) \right\}^2 + \left\{ 4\cos^2\left(\frac{\pi d_1}{2D}\right)\sinh^2\left(\frac{\pi x}{2D}\right)\sin^2\left(\frac{\pi y}{2D}\right) \right\} \right]^{1/2}}{\left\{ \cos\left(\frac{\pi d_1}{2D}\right) - \cosh\left(\frac{\pi x}{2D}\right)\cos\left(\frac{\pi y}{2D}\right) \right\}^2 + \sinh^2\left(\frac{\pi x}{2D}\right)\sin^2\left(\frac{\pi y}{2D}\right)} \right] + i\frac{q}{\pi}\theta \quad (3.15)$$

25

where,

$$\theta = \tan^{-1}\frac{2\cos\left(\frac{\pi d_1}{2D}\right)\sinh\left(\frac{\pi x}{2D}\right)\sin\left(\frac{\pi y}{2D}\right)}{\cos^2\left(\frac{\pi d_1}{2D}\right)-\cosh^2\left(\frac{\pi x}{2D}\right)\cos^2\left(\frac{\pi y}{2D}\right)-\sinh^2\left(\frac{\pi x}{2D}\right)\sin^2\left(\frac{\pi y}{2D}\right)}.$$

hence,

$$\phi(x,y)=\frac{q}{\pi}\ln\left[\frac{\left[\left\{\cos^2\left(\frac{\pi d_1}{2D}\right)-\cosh^2\left(\frac{\pi x}{2D}\right)\cos^2\left(\frac{\pi y}{2D}\right)-\sinh^2\left(\frac{\pi x}{2D}\right)\sin^2\left(\frac{\pi y}{2D}\right)\right\}^2+\left\{4\cos^2\left(\frac{\pi d_1}{2D}\right)\sinh^2\left(\frac{\pi x}{2D}\right)\sin^2\left(\frac{\pi y}{2D}\right)\right\}\right]^{1/2}}{\left\{\cos\left(\frac{\pi d_1}{2D}\right)-\cosh\left(\frac{\pi x}{2D}\right)\cos\left(\frac{\pi y}{2D}\right)\right\}^2+\sinh^2\left(\frac{\pi x}{2D}\right)\sin^2\left(\frac{\pi y}{2D}\right)}\right] \quad (3.16)$$

and

$$\psi(x,y)=\frac{q}{\pi}\tan^{-1}\left\{\frac{2\cos\left(\frac{\pi d_1}{2D}\right)\sinh\left(\frac{\pi x}{2D}\right)\sin\left(\frac{\pi y}{2D}\right)}{\cos^2\left(\frac{\pi d_1}{2D}\right)-\cosh^2\left(\frac{\pi x}{2D}\right)\cos^2\left(\frac{\pi y}{2D}\right)-\sinh^2\left(\frac{\pi x}{2D}\right)\sin^2\left(\frac{\pi y}{2D}\right)}\right\} \quad (3.17)$$

Along $y=0$, i.e. line EA_∞, $\psi(x,0)=\frac{q}{\pi}\tan^{-1}(0)=\frac{q}{\pi}\pi=q$. It is to be noted that $\tan^{-1}(0)$ has

multiple values; $\tan(0)$ as well as $\tan(\pi)$ is equal to 0 and; we have considered the latter value.

Along BC_1, $x=0$; $\psi\left(0,y>(d_1+0.5d_p)\right)=\frac{q}{\pi}\tan^{-1}(0)=\frac{q}{\pi}0=0.$

Along $y=D$, the velocity potential is:

$$\phi(x,D)=\frac{q}{\pi}\ln\left[\frac{\left[\left\{\cos^2\left(\frac{\pi d_1}{2D}\right)-\sinh^2\left(\frac{\pi x}{2D}\right)\sin^2\left(\frac{\pi y}{2D}\right)\right\}^2+\left\{4\cos^2\left(\frac{\pi d_1}{2D}\right)\sinh^2\left(\frac{\pi x}{2D}\right)\sin^2\left(\frac{\pi y}{2D}\right)\right\}\right]^{1/2}}{\cos^2\left(\frac{\pi d_1}{2D}\right)+\sinh^2\left(\frac{\pi x}{2D}\right)\sin^2\left(\frac{\pi y}{2D}\right)}\right]$$

$$=\frac{q}{\pi}\ln\left[\frac{\cos^2\left(\frac{\pi d_1}{2D}\right)+\sinh^2\left(\frac{\pi x}{2D}\right)\sin^2\left(\frac{\pi y}{2D}\right)}{\cos^2\left(\frac{\pi d_1}{2D}\right)+\sinh^2\left(\frac{\pi x}{2D}\right)\sin^2\left(\frac{\pi y}{2D}\right)}\right]=0$$

At x=0, and $y=d_1$

$$\phi(0,d)=\frac{q}{\pi}\ln\left[\frac{\left[\left\{\cos^2\left(\frac{\pi d_1}{2D}\right)-\cos^2\left(\frac{\pi d_1}{2D}\right)\right\}^2+\left\{4\cos^2\left(\frac{\pi d_1}{2D}\right)\right\}\right]^{1/2}}{\left\{\cos\left(\frac{\pi d_1}{2D}\right)-\cos\left(\frac{\pi d_1}{2D}\right)\right\}^2}\right]=\infty$$

At location x=0, and y=0,

26

$$\phi(0,0)=\frac{q}{\pi}\ln\left[\frac{\left[\left\{\cos^2\left(\frac{\pi d_1}{2D}\right)-1\right\}^2\right]^{1/2}}{\left\{\cos\left(\frac{\pi d_1}{2D}\right)-1\right\}^2}\right]=\frac{q}{\pi}\ln\left[\frac{\left[\left\{1-\cos^2\left(\frac{\pi d_1}{2D}\right)\right\}^2\right]^{1/2}}{\left\{1-\cos\left(\frac{\pi d_1}{2D}\right)\right\}^2}\right]=\frac{q}{\pi}\ln\left[\frac{\left\{1-\cos^2\left(\frac{\pi d_1}{2D}\right)\right\}}{\left\{1-\cos\left(\frac{\pi d_1}{2D}\right)\right\}^2}\right]$$

Making use of equations (3.16) and (3.17), velocity potential $\phi(x,y)$ and stream function $\psi(x,y)$ can be computed at locations on a rectangular grid pattern in the flow domain and a flow net can be drawn.

Determination of q:

Let at $z=i\left(d_1+\frac{d_p}{2}\right)$, the piezometric head be equal to p^*/γ_w.

Hence, $\phi^*=-k\left(p^*/\gamma_w+d_1+d_p/2\right)+k\left(h_R+D\right)=kD_w$ and $\psi=0$.

Incorporating these in equation (3.14):

$$kD_w=\frac{q}{\pi}\ln\left[\frac{\cos\left(\frac{\pi d_1}{2D}\right)+\cos\left\{\frac{\pi i^2}{2D}\left(d_1+0.5d_p\right)\right\}}{\cos\left(\frac{\pi d_1}{2D}\right)-\cos\left\{\frac{\pi i^2}{2D}\left(d_1+0.5d_p\right)\right\}}\right]=\frac{q}{\pi}\ln\left[\frac{\cos\left(\frac{\pi d_1}{2D}\right)+\cos\left\{\frac{\pi}{2D}\left(d_1+0.5d_p\right)\right\}}{\cos\left(\frac{\pi d_1}{2D}\right)-\cos\left\{\frac{\pi}{2D}\left(d_1+0.5d_p\right)\right\}}\right]$$

(3.18)

Solving for q

(3.19)

$$q=\frac{\pi\,kD_w}{\ln\left[\frac{\cos\left(\frac{\pi d_1}{2D}\right)+\cos\left\{\frac{\pi}{2D}\left(d_1+0.5d_p\right)\right\}}{\cos\left(\frac{\pi d_1}{2D}\right)-\cos\left\{\frac{\pi}{2D}\left(d_1+0.5d_p\right)\right\}}\right]}$$

The dimensionless total flow from both sides, $Q/(kD_w)$, to the collector pipe is

$$Q/(kD_w)=\frac{2\pi}{\ln\left[\frac{\cos\left(\frac{\pi d_1}{2D}\right)+\cos\left\{\frac{\pi}{2D}\left(d_1+0.5d_p\right)\right\}}{\cos\left(\frac{\pi d_1}{2D}\right)-\cos\left\{\frac{\pi}{2D}\left(d_1+0.5d_p\right)\right\}}\right]}$$

(3.20)

Entrance velocity

Depending upon the type of soil an aquifer medium is comprised of, the entrance velocity to a collector pipe laid in the aquifer is to be maintained so as to restrict the movement

27

of fine particles into the collector pipe. The entrance velocity to a collector pipe is linearly proportional to the drawdown D_w in the well caisson, and hydraulic conductivity of the aquifer medium and inversely proportional to the open area fraction in the collector pipe. The expression for entrance velocity is derived as follows:

An average entrance velocity is determined with ease using the expression for flow to the collector pipe. Magnitude of average Darcy velocity at the periphery of the collector pipe is equal to $2q/(\pi d_p)$. The average entrance velocity is given by:

$$\bar{v}_e = 2q/(\pi d_p f_a) = \frac{2kD_w}{d_p f_a \ln\left[\dfrac{\cos\left(\dfrac{\pi d_1}{2D}\right) + \cos\left\{\dfrac{\pi}{2D}(d_1 + 0.5d_p)\right\}}{\cos\left(\dfrac{\pi d_1}{2D}\right) - \cos\left\{\dfrac{\pi}{2D}(d_1 + 0.5d_p)\right\}}\right]} \tag{3.21}$$

Dimensionless an average entrance velocity factor $\bar{v}_{ef}$ is defined as:

$$\bar{v}_{ef} = \frac{\bar{v}_e d_p f_a}{kD_w} = \frac{2}{\ln\left[\dfrac{\cos\left(\dfrac{\pi d_1}{2D}\right) + \cos\left\{\dfrac{\pi}{2D}(d_1 + 0.5d_p)\right\}}{\cos\left(\dfrac{\pi d_1}{2D}\right) - \cos\left\{\dfrac{\pi}{2D}(d_1 + 0.5d_p)\right\}}\right]} \tag{3.22}$$

The maximum and the minimum entrance velocities

The streamline BC_1 is the shortest flow path from the river bed to the collector pipe and the streamline $A_\infty E C_2$ is the longest flow path. Therefore, magnitude of the entrance velocity at point C_1 is the maximum, and the entrance velocity at location C_2 is the minimum. We derive expressions of the maximum and the minimum entrance velocities as follows:

Incorporating constant M in equation (3.2),

$$\frac{dt}{dz} = \frac{\pi}{-iD}\sqrt{(t+1)(1-t)} = \frac{i\pi}{D}\sqrt{(t+1)(1-t)} \tag{3.23}$$

Incorporating constant M_1 in equation (3.9)

$$\frac{dw}{dt} = \frac{q}{\pi}\sqrt{c+1}\frac{1}{(c-t)\sqrt{(t+1)}} \tag{3.24}$$

Multiplying $\dfrac{dw}{dt}$ with $\dfrac{dt}{dz}$

28

$$\frac{dw}{dt}\frac{dt}{dz} = \frac{dw}{dz} = \frac{iq}{D}\sqrt{c+1}\frac{\sqrt{(1-t)}}{(c-t)}$$ (3.25)

Incorporating the relation between t and z as given in equation (3.7) in equation (3.25)

$$\frac{dw}{dz} = u - iv = \frac{iq}{D}\sqrt{c+1}\frac{\sqrt{\left[1-\cos\left(i\frac{\pi z}{D}\right)\right]}}{\left[c-\cos\left(i\frac{\pi z}{D}\right)\right]}$$ (3.26)

The Darcy flow velocity at $z = i\left(d_1 + \frac{d_p}{2}\right)$ is given by

$$u - iv = \frac{iq}{D}\sqrt{1+c}\frac{\sqrt{\left[1-\cos\left\{\frac{\pi}{D}\left(d_1 + \frac{d_p}{2}\right)\right\}\right]}}{\left[\cos\left(\frac{\pi d_1}{D}\right) - \cos\left\{\frac{\pi}{D}\left(d_1 + \frac{d_p}{2}\right)\right\}\right]}$$ (3.27)

Equating the real parts on either sides of equation (3.27), we obtain $u = 0$. equating the imaginary parts and replacing q by equation (3.19), we obtain the Darcy velocity at $z = 0, i\left(d_1 + \frac{d_p}{2}\right)$ as

$$v_1 = \frac{-\pi\sqrt{1+c}}{D\ln\left[\frac{\cos\left(\frac{\pi d_1}{2D}\right) + \cos\left\{\frac{\pi}{2D}(d_1 + 0.5d_p)\right\}}{\cos\left(\frac{\pi d_1}{2D}\right) - \cos\left\{\frac{\pi}{2D}(d_1 + 0.5d_p)\right\}}\right]} \frac{\sqrt{\left[1-\cos\left\{\frac{\pi}{D}\left(d_1 + \frac{d_p}{2}\right)\right\}\right]}}{\left[\cos\left(\frac{\pi d_1}{D}\right) - \cos\left\{\frac{\pi}{D}\left(d_1 + \frac{d_p}{2}\right)\right\}\right]} kD_w$$ (3.28)

The negative sign indicates that the velocity at $z = 0, i\left(d_1 + \frac{d_p}{2}\right)$ is in the opposite direction of y. The absolute value of v_1 is the maximum on the periphery of the collector pipe. Performing a mass balance considering an elemental area $0.5d_p d\theta$ on the periphery of the collector pipe at $z = 0, i\left(d_1 + \frac{d_p}{2}\right)$

$$0.5d_p d\theta f_a v_{em} = 0.5d_p d\theta |v_1|$$ (3.29)

where, v_{em} is the maximum entrance velocity; f_a = fraction of the peripheral area of the collector pipe perforated in unit length of collector pipe. The maximum entrance velocity is obtained as

$$v_{em} = \frac{|v_1|}{f_a} \tag{3.30}$$

The maximum entrance velocity factor v_{emf} is defined as

$$v_{emf} = \frac{|v_1| D f_a}{k D_w} = \frac{\pi\sqrt{1+c}}{\ln\left[\dfrac{\cos\left(\dfrac{\pi d_1}{2D}\right) + \cos\left\{\dfrac{\pi}{2D}(d_1 + 0.5 d_p)\right\}}{\cos\left(\dfrac{\pi d_1}{2D}\right) - \cos\left\{\dfrac{\pi}{2D}(d_1 + 0.5 d_p)\right\}}\right]} \frac{\sqrt{\left[1 - \cos\left\{\dfrac{\pi}{D}\left(d_1 + \dfrac{d_p}{2}\right)\right\}\right]}}{\left[\cos\left(\dfrac{\pi d_1}{D}\right) - \cos\left\{\dfrac{\pi}{D}\left(d_1 + \dfrac{d_p}{2}\right)\right\}\right]} \tag{3.31}$$

The Darcy velocity at $z = i\left(d_1 - \dfrac{d_p}{2}\right)$ is given by

$$v_2 = \frac{-\pi\sqrt{1+c}}{D\ln\left[\dfrac{\cos\left(\dfrac{\pi d_1}{2D}\right) + \cos\left\{\dfrac{\pi}{2D}(d_1 + 0.5 d_p)\right\}}{\cos\left(\dfrac{\pi d_1}{2D}\right) - \cos\left\{\dfrac{\pi}{2D}(d_1 + 0.5 d_p)\right\}}\right]} \frac{\sqrt{\left[1 - \cos\left\{\dfrac{\pi}{D}\left(d_1 - \dfrac{d_p}{2}\right)\right\}\right]}}{\left[\cos\left(\dfrac{\pi d_1}{D}\right) - \cos\left\{\dfrac{\pi}{D}\left(d_1 - \dfrac{d_p}{2}\right)\right\}\right]} k D_w \tag{3.32}$$

Following similar procedure as above, the dimensionless minimum entrance velocity factor is derived as:

$$v_{2ef} = \frac{v_2 D f_a}{k D_w} = \frac{-\pi\sqrt{1+c}}{\ln\left[\dfrac{\cos\left(\dfrac{\pi d_1}{2D}\right) + \cos\left\{\dfrac{\pi}{2D}(d_1 + 0.5 d_p)\right\}}{\cos\left(\dfrac{\pi d_1}{2D}\right) - \cos\left\{\dfrac{\pi}{2D}(d_1 + 0.5 d_p)\right\}}\right]} \frac{\sqrt{\left[1 - \cos\left\{\dfrac{\pi}{D}\left(d_1 - \dfrac{d_p}{2}\right)\right\}\right]}}{\left[\cos\left(\dfrac{\pi d_1}{D}\right) - \cos\left\{\dfrac{\pi}{D}\left(d_1 - \dfrac{d_p}{2}\right)\right\}\right]} \tag{3.33}$$

The minimum travel time of a parcel of water from the stream bed to the collector pipe

Computation of the minimum travel time of a parcel of water from the stream to the collector pipe is of use to predict the log cycle reduction in bacteria concentration while a parcel of water moves from a stream to a collector pipe. For the present case, along y-axis $z = i\,y$, and $u = 0$. From equation (3.26), the Darcy velocity along y-axis is

$$v(y) = -\frac{q}{D}\sqrt{1+c} - \sqrt{\left[1 - \cos\left(\frac{\pi y}{D}\right)\right]} \bigg/ \left[c - \cos\left(\frac{\pi y}{D}\right)\right] \tag{3.34}$$

The travel time t, of a parcel of water from stream bed to the collector pipe is given by:

$$t_r = \int\limits_{d_1+0.5d_p}^{D} \frac{dy}{v(y)/\eta} = -\eta \frac{D}{q\sqrt{1+c}} \int\limits_{(d_1+0.5d_p)}^{D} \frac{c-\cos\left(\dfrac{\pi y}{D}\right)}{\sqrt{\left[1-\cos\left(\dfrac{\pi y}{D}\right)\right]}} dy$$

$$= -\eta \frac{D}{q\sqrt{1+c}} \int\limits_{(d_1+0.5d_p)}^{D} \frac{1-\cos\left(\dfrac{\pi y}{D}\right)+c-1}{\sqrt{\left[1-\cos\left(\dfrac{\pi y}{D}\right)\right]}} dy$$

$$= -\eta \frac{D}{q\sqrt{1+c}} \int\limits_{(d_1+0.5d_p)}^{D} \frac{c-1}{\sqrt{\left[1-\cos\left(\dfrac{\pi y}{D}\right)\right]}} dy - \eta \frac{D}{q\sqrt{1+c}} \int\limits_{(d_1+0.5d_p)}^{D} \sqrt{\left[1-\cos\left(\dfrac{\pi y}{D}\right)\right]} dy \qquad (3.35)$$

where, η is the volumetric porosity of the aquifer medium. Substituting, $\dfrac{\pi y}{D}=Y$, $dy=\dfrac{D}{\pi}dY$ in (3.35) and simplifying

$$t_r = \eta \frac{D^2(1-c)}{\pi q\sqrt{1+c}} \int\limits_{\frac{\pi}{D}(d_1+0.5d_p)}^{\pi} \frac{dY}{\sqrt{[1-\cos(Y)]}} - \eta \frac{D^2}{\pi q\sqrt{1+c}} \int\limits_{\frac{\pi}{D}(d_1+0.5d_p)}^{\pi} \left\{\sqrt{1-\cos(Y)}\right\} dY \qquad (3.36)$$

$$= I_1 - I_2$$

Substituting $\cos Y = 1 - 2\sin^2\left(\dfrac{Y}{2}\right)$

$$I_1 = \frac{\eta D^2(1-c)}{\pi q\sqrt{1+c}} \int\limits_{\frac{\pi}{D}(d_1+0.5d_p)}^{\pi} \frac{dY}{\sqrt{2}\sin\dfrac{Y}{2}}$$

Further substituting $Y/2 = \xi; dY = 2d\xi$

$$I_1 = \eta\sqrt{2}\frac{D^2(1-c)}{\pi q\sqrt{1+c}} \int\limits_{\frac{\pi}{2D}(d_1+0.5d_p)}^{\pi/2} \cos ec(\xi)d\xi = \eta\sqrt{2}\frac{D^2(1-c)}{\pi q\sqrt{1+c}} \ln\left(\tan\frac{\xi}{2}\right)\Bigg|_{\frac{\pi}{2D}(d_1+0.5d_p)}^{\pi/2}$$

$$= -\eta\sqrt{2}\frac{D^2(1-c)}{\pi q\sqrt{1+c}} \ln\left\{\tan\frac{\pi}{4D}(d_1+0.5d_p)\right\}$$

$$I_2 = \frac{\eta D^2}{\pi q\sqrt{1+c}} \int\limits_{\frac{\pi}{D}(d_1+0.5d_p)}^{\pi} \left\{\sqrt{1-\cos(Y)}\right\} dY = \frac{\eta D^2}{\pi q\sqrt{1+c}} \int\limits_{\frac{\pi}{D}(d_1+0.5d_p)}^{\pi} \sqrt{2}\sin\frac{Y}{2} dY$$

$$= 2\sqrt{2}\frac{\eta D^2}{\pi q\sqrt{1+c}} \cos\frac{\pi}{2D}(d_1+0.5d_p)$$

Incorporating I_1 and I_2 in (3.36)

$$t_r = -\sqrt{2}\frac{\eta D^2(1-c)}{\pi q\sqrt{1+c}} \ln\left\{\tan\frac{\pi}{4D}(d_1+0.5d_p)\right\} - 2\sqrt{2}\frac{\eta D^2}{\pi q\sqrt{1+c}} \cos\frac{\pi}{2D}\left(d_1+\frac{d_p}{2}\right)$$

31

$$= -\eta \sqrt{2} \, \frac{D^2}{\pi q \sqrt{1+c}} \left[(1-c) \ln \left\{ \tan \frac{\pi}{4D} \left(d_1 + \frac{d_p}{2} \right) \right\} + 2 \cos \left\{ \frac{\pi}{2D} \left(d_1 + \frac{d_p}{2} \right) \right\} \right] \tag{3.37}$$

For given d_1 / D, d_p / D, we define a dimensionless travel time factor t_{rf} as

$$t_{rf} = \frac{t_r k D_w}{\eta D^2} \tag{3.38}$$

Knowing the travel time of a parcel of river water to the collector pipe, the log cycle reduction in bacteria concentration in the parcel of water is computed using logistic function. The derivation of log cycle reduction in bacteria concentration using known travel time is given in Appendix B.

3.5 STATEMENT OF THE PROBLEM FOR VERTICAL SLIT

Plan and section of a typical collector pipe are shown in Fig.3.1 (a) and (b).The collector pipe is laid horizontally and is connected to a reinforced concrete caisson, which has been constructed on the river bank. The collector pipe runs perpendicular to the river axis in an aquifer of finite thickness. It is required to estimate the flow characteristics, such as yield, entrance velocity, travel time, and number of log cycle reduction of bacterial concentration through this collector pipe.

The difference in water level in the caisson and piezometric level in the collector pipe is D_w. The collector pipe is laid at a depth D_s below the river bed. The depth D_s needs to be more than the scour depth. The scour depth is estimated by using the expression as suggested by Lacey (1929). The collector pipe should be below the scour depth accounting the minimum filter thickness above the collector pipe required for natural filtration through the layer above the pipe. For rapid sand filter, the minimum filtration thickness is taken as 0.8 m (IS: 3955-1967). The detailed analysis of scour depth is shown in Appendix – A.

3.6 SOLUTION METHODOLOGY FOR VERTICAL SLIT

Schwartz-Cristoffel conformal mapping technique, explained in Appendix B, is applied to the idealized flow domain shown in Fig. 3.2 (b).Accordingly ψ values are assigned as shown in Fig. 3.2 (b) and the complex potential $w(= \phi + i\psi)$ for vertical slit is shown in Fig. (3.5).

The complex potential $w(= \phi + i\psi)$ pertaining to the flow domain for each case is shown in Fig. (3.5).
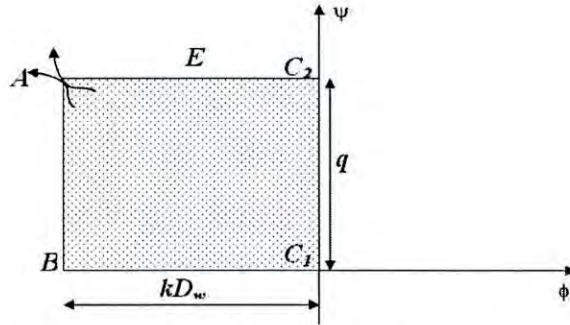
Fig. (3.5) Complex Potential $w(=\phi+i\psi)$ **Plane of Fig. 3.2 (B)**

Mapping of physical flow domain to upper half auxiliary t-plane

The vertices A, B, C_1, C_2, E, and A of the flow domain for vertical narrow slit are mapped onto $-\infty, -1, b, a, 1$ and ∞ respectively on the real axis of the auxiliary t $(=r+is)$ plane as shown in Fig. (3.6).The flow domain is mapped onto the upper half of auxiliary plane.
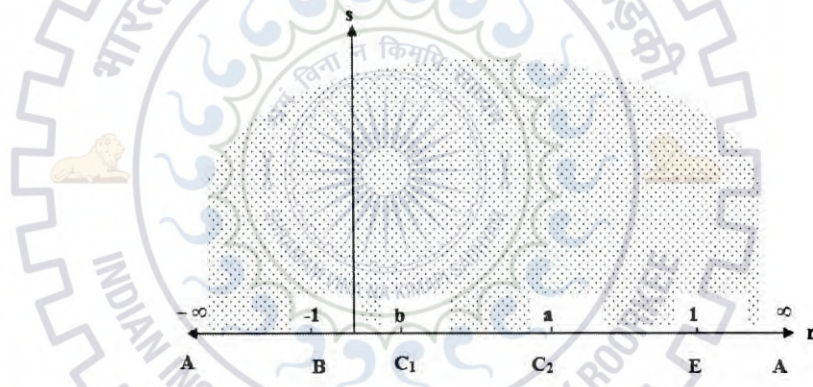
Fig. 3.6 Auxiliary $t(=r+is)$ **Plane of Fig. 3.2 (B)**

Accordingly, the conformal mapping of the flow domain in $z(=x+iy)$ plane onto upper half of the auxilliary $t(=r+is)$ plane is given by:

$$\frac{dz}{dt} = \frac{M}{\sqrt{(1+t)(1-t)}} \tag{3.39}$$

Integrating equation (3.39)

$$z = M\int \frac{dt}{\sqrt{(1+t)(1-t)}} + N \tag{3.40}$$

$$= M\sin^{-1}t + N \tag{3.41}$$

where, M and N are complex constants, which depend upon the geometry of flow domain. For vertex E, t=1, and $z = 0$. Hence,

33

$$0 = M\sin^{-1}(1) + N \tag{3.42a}$$

or

$$0 = M\frac{\pi}{2} + N \tag{3.42b}$$

For vertex B, $t = -1$, and $z = iD$. Therefore,

$$iD = M\sin^{-1}(-1) + N \tag{3.43a}$$

or

$$iD = -M\frac{\pi}{2} + N \tag{3.43b}$$

Solving M and N from equations (3.42b) and (3.43b), $N = \dfrac{iD}{2}$ and $M = -\dfrac{iD}{\pi}$. The transformation of z-plane onto the auxiliary t-plane is given by:

$$z = -\frac{iD}{\pi}\sin^{-1}t + \frac{iD}{2} \tag{3.44}$$

For point $C_2, t = a$ and $z = i\left(d_1 - \dfrac{d_p}{2}\right)$; hence,

$$i\left(d_1 - \frac{d_p}{2}\right) = -\frac{iD}{\pi}\sin^{-1}a + \frac{iD}{2} \tag{3.45}$$

Simplifying

$$a = \cos\left(\frac{\pi d_p}{2D} - \frac{\pi d_1}{D}\right) \tag{3.46}$$

For point $C_1, t = b$, and $z = i\left(d_1 + \dfrac{d_p}{2}\right)$; therefore,

$$i\left(d_1 + \frac{d_p}{2}\right) = -\frac{iD}{\pi}\sin^{-1}b + \frac{iD}{2} \tag{3.47}$$

Simplifying

$$b = \cos\left(\frac{\pi d_p}{2D} + \frac{\pi d_1}{D}\right) \tag{3.48}$$

The parameters a and b are dimensionless conformal mapping parameters, which depend upon the dimensions d_p, d_1 and D of the physical flow domain.

34

3.7 MAPPING OF THE *w* - PLANE ONTO THE UPPER HALF AUXILIARY t-PLANE

A, B, C_1, C_2 are the vertices in the complex potential plane. The complex potential plane is opened at vertex A, which has been mapped onto ∞. The relationship between w and t plane is given by:

$$\frac{dw}{dt} = \frac{M_1}{\sqrt{(a-t)(b-t)(-1-t)}}$$

(3.49a)

or

$$w(t) = M_1 \int \frac{dt}{\sqrt{(a-t)(b-t)(-1-t)}} + N_1$$

(3.49b)

The constant N_1 is governed by the lower limit of integration. Assuming the lower limit of integration to be $-\infty$, for which, $w = -kD_w + iq$, we obtain

$$w(t) = M_1 \int_{-\infty}^{t} \frac{dt}{\sqrt{(a-t)(b-t)(-1-t)}} - kD_w + iq$$

(3.50)

For $-\infty < t < -1$, performing the integration in equation (3.50) (Byrd and Friedman, 1954, p.72)

$$w(t) = M_1 \, g \, F\left(\sin^{-1}\sqrt{\frac{a+1}{a-t}}, \sqrt{\frac{a-b}{a+1}} \right) - kD_w + iq$$

(3.51)

where, $F(\varphi, k^*)$ is incomplete elliptic integral of first kind with amplitude φ and modulus k^* $g = \dfrac{2}{\sqrt{a+1}}$.

For $t = -1$, $w = -kD_w$. Applying this in equation (3.51)

$$-kD_w = \frac{2}{\sqrt{a+1}} M_1 \, F\left(\frac{\pi}{2}, \sqrt{\frac{a-b}{a+1}} \right) - kD_w + iq.$$

(3.52a)

or

$$iq = \frac{-2M_1}{\sqrt{a+1}} F(\frac{\pi}{2}, \sqrt{\frac{a-b}{a+1}})$$

(3.52b)

For $-1 < t < b$

$$w(t) = M_1 \int_{-1}^{t} \frac{dt}{\sqrt{(a-t)(b-t)(-1-t)}} - kD_w$$

(3.53a)

$$= \frac{M_1}{\sqrt{-1}} \int_{-1}^{t} \frac{dt}{\sqrt{(a-t)(b-t)(t+1)}} - kD_w \qquad (3.53b)$$

Performing the integration (Byrd and Friedman, 1954, p.72)

$$w(t) = \frac{M_1}{\sqrt{-1}} \frac{2}{\sqrt{a+1}} F\left(\sin^{-1}\sqrt{\frac{t+1}{b+1}}, \sqrt{\frac{b+1}{a+1}} \right) - kD_w \qquad (3.54)$$

For $t = b$ and $w = 0$. Applying this relation in equation (3.54)

$$0 = \frac{M_1}{\sqrt{-1}} \frac{2}{\sqrt{a+1}} F\left(\frac{\pi}{2}, \sqrt{\frac{b+1}{a+1}} \right) - kD_w \qquad (3.55a)$$

Considering $\sqrt{-1} = -i$, and solving for constant M_1

$$M_1 = -i \frac{\sqrt{a+1}}{2} \frac{kD_w}{F\left(\frac{\pi}{2}, \sqrt{\frac{b+1}{a+1}} \right)} \qquad (3.55b)$$

Substituting the constant M_1 in equation (3.52b) and solving for q

$$q = kD_w \left(\frac{F(\frac{\pi}{2}, \sqrt{\frac{a-b}{a+1}})}{F\left(\frac{\pi}{2}, \sqrt{\frac{b+1}{a+1}} \right)} \right) \qquad (3.56)$$

The total flow, Q, to the collector pipe per unit length is 2q. Thus total flow is:

$$Q = 2kD_w \frac{F(\frac{\pi}{2}, \sqrt{\frac{a-b}{a+1}})}{F\left(\frac{\pi}{2}, \sqrt{\frac{b+1}{a+1}} \right)} \qquad (3.57a)$$

or

$$\frac{Q}{kD_w} = 2 \frac{F(\frac{\pi}{2}, \sqrt{\frac{a-b}{a+1}})}{F\left(\frac{\pi}{2}, \sqrt{\frac{b+1}{a+1}} \right)} \qquad (3.57b)$$

Entrance velocity

The entrance velocity to the collector pipe is computed from Darcy velocity at the periphery of the collector pipe applying the principle of mass balance. From equations (3.49a) and (3.55b)

$$\frac{dw}{dt} = -i\frac{\sqrt{a+1}}{2}\frac{kD_w}{F\left(\frac{\pi}{2},\sqrt{\frac{b+1}{a+1}}\right)}\frac{1}{\sqrt{(a-t)(b-t)(-1-t)}}$$ (3.58)

From equation (3.39)

$$\frac{dz}{dt} = \frac{-iD}{\pi\sqrt{(1+t)(1-t)}}$$ (3.59)

$$\frac{dw}{dz} = \frac{dw}{dt}\frac{dt}{dz} = -i\frac{\sqrt{a+1}}{2}\frac{kD_w}{F\left(\frac{\pi}{2},\sqrt{\frac{b+1}{a+1}}\right)}\frac{1}{\sqrt{(a-t)(b-t)(-1-t)}}\frac{\pi\sqrt{(1+t)(1-t)}}{-iD}$$ (3.60a)

Simplifying

$$\frac{dw}{dz} = u - iv = \frac{1}{\sqrt{-1}}\frac{kD_w}{D}\frac{\pi}{2}\frac{\sqrt{a+1}}{F\left(\frac{\pi}{2},\sqrt{\frac{b+1}{a+1}}\right)}\frac{\sqrt{(1-t)}}{\sqrt{(a-t)(b-t)}}$$ (3.60b)

Considering, $\sqrt{-1} = -i$

$$\frac{dw}{dz} = u - iv = i\frac{kD_w}{D}\frac{\pi}{2}\frac{\sqrt{a+1}}{F\left(\frac{\pi}{2},\sqrt{\frac{b+1}{a+1}}\right)}\frac{\sqrt{(1-t)}}{\sqrt{(a-t)(b-t)}}$$ (3.60c)

Thus, for $t < b$, $u = 0$ and

$$v = -\frac{kD_w}{D}\frac{\pi}{2}\frac{\sqrt{a+1}}{F\left(\frac{\pi}{2},\sqrt{\frac{b+1}{a+1}}\right)}\frac{\sqrt{(1-t)}}{\sqrt{(a-t)(t-b)}}$$ (3.60d)

For $t = b$, at vertex C_1, $v = -\infty$ and for $b < t < a$, $v = 0$ and

$$u = -\frac{kD_w}{D}\frac{\pi}{2}\frac{\sqrt{a+1}}{F\left(\frac{\pi}{2},\sqrt{\frac{b+1}{a+1}}\right)}\frac{\sqrt{(1-t)}}{\sqrt{(a-t)(b-t)}}$$ (3.60e)

Thus, the flow velocity at points $C_1(t = b)$ and $C_2(t = a)$ are infinite. In reality, the flow velocity to a circular collector pipe is finite. This limitation is arising due to the idealizing the circular pipe as a slit.

At the middle of the pipe, $z = id_1$. From equation (3.44), $t = \cos\left(\frac{\pi d_1}{D}\right) = t_{d_1}$ (say)

Therefore, the horizontal flow velocity at the center of slit is:

$$u_{d_1} = -\frac{kD_w}{D}\frac{\pi}{2}\frac{\sqrt{a+1}}{F\left(\frac{\pi}{2},\sqrt{\frac{b+1}{a+1}}\right)}\frac{\sqrt{(1-t_{d_1})}}{\sqrt{(a-t_{d_1})(t_{d_1}-b)}}$$

(3.60f)

37

The entrance velocity is computed considering the actual flow area that is the slot area of a collector pipe. Mass balance is applied at the periphery of the collector i.e.

$$v_r \times \pi d_p = v_e \left(f_a \times \pi d_p \right) \tag{3.61a}$$

or

$$v_e = v_r / f_a \tag{3.61b}$$

here, f_a is equal to the ratio of area of opening to the peripheral area of the collector pipe per unit length of the collector pipe.

Darcy radial velocity is taken approximately to be

$$v_r = \frac{Q}{\pi d_p} = \frac{2 k D_w}{\pi d_p} \frac{F\left(\frac{\pi}{2}, \sqrt{\frac{a-b}{a+1}}\right)}{F\left(\frac{\pi}{2}, \sqrt{\frac{b+1}{a+1}}\right)} \tag{3.62}$$

The entrance velocity is given by:

$$v_e = \frac{v_r}{f_a} = \frac{2 k D_w}{\pi d_p f_a} \frac{F\left(\frac{\pi}{2}, \sqrt{\frac{a-b}{a+1}}\right)}{F\left(\frac{\pi}{2}, \sqrt{\frac{b+1}{a+1}}\right)} \tag{3.63}$$

Travel time of a parcel of water

The minimum travel time for a parcel of water is the time taken by it to reach from riverbed to collector pipe. The minimum travel time of a parcel of water is computed as follows:

Referring to equation (3.60c)

$$\frac{dw}{dz} = u - iv = i \frac{k D_w}{D} \frac{\pi}{2} \frac{\sqrt{a+1}}{F\left(\frac{\pi}{2}, \sqrt{\frac{b+1}{a+1}}\right)} \sqrt{\frac{(1-t)}{(a-t)(b-t)}} \tag{3.64}$$

Along the streamline BC_1, $u = 0$. Hence,

$$v = -\frac{k D_w}{D} \frac{\pi}{2} \frac{\sqrt{a+1}}{F\left(\frac{\pi}{2}, \sqrt{\frac{b+1}{a+1}}\right)} \sqrt{\frac{(1-t)}{(a-t)(b-t)}} \tag{3.65}$$

Referring to equation (3.44) the relation between z and t-planes is:

$$t = \cos\left(\pi \frac{iz}{D}\right) \tag{3.66}$$

Along the streamline BC_1, $z = iy$. Hence,

$$t = \cos\left(\pi\frac{y}{D}\right) \tag{3.67}$$

Incorporating equation (3.67) in equation (3.65)

$$v(y) = -\frac{kD_w}{D}\frac{\pi}{2}\frac{\sqrt{a+1}}{F\left(\frac{\pi}{2}, \sqrt{\frac{b+1}{a+1}}\right)}\sqrt{\frac{\left(1-\cos\left(\pi\frac{y}{D}\right)\right)}{\left(a-\cos\left(\pi\frac{y}{D}\right)\right)\left(b-\cos\left(\pi\frac{y}{D}\right)\right)}} \tag{3.68}$$

when the parcel of water is at y it will travel distance dy in duration dt which is given by:

$$dt = \frac{\eta\, dy}{v(y)} \tag{3.69}$$

in which, η is the volumetric effective porosity of the bed material.

Incorporating $v(y)$ in equation (3.69)

$$dt = -\frac{\eta D}{kD_w}\frac{2}{\pi}\frac{F\left(\frac{\pi}{2}, \sqrt{\frac{b+1}{a+1}}\right)}{\sqrt{a+1}}\sqrt{\frac{\left(a-\cos\left(\pi\frac{y}{D}\right)\right)\left(b-\cos\left(\pi\frac{y}{D}\right)\right)}{\left(1-\cos\left(\pi\frac{y}{D}\right)\right)}}\,dy \tag{3.70}$$

Integrating, the travel time t_r of the parcel of water along the stream line BC_1 is given by

$$t_r = -\frac{2\eta D}{\pi k D_w}\frac{F\left(\frac{\pi}{2}, \sqrt{\frac{b+1}{a+1}}\right)}{\sqrt{a+1}}\int_{\left(d_1+\frac{d_p}{2}\right)}^{D}\sqrt{\frac{\left(a-\cos\left(\pi\frac{y}{D}\right)\right)\left(b-\cos\left(\pi\frac{y}{D}\right)\right)}{\left(1-\cos\left(\pi\frac{y}{D}\right)\right)}}\,dy \tag{3.71}$$

The integration is carried out numerically applying Gauss-quadrature and adopting change of variable, $y = \frac{1}{2}\left\{\left(D-d_1-\frac{d_p}{2}\right)\xi + \left(D+d_1+\frac{d_p}{2}\right)\right\}$; $dy = \frac{1}{2}\left(D-d_1-\frac{d_p}{2}\right)d\xi$

$$t_r = \frac{\eta D}{\pi k d_w}\left(D-d_1-\frac{d_p}{2}\right)\frac{F\left(\frac{\pi}{2}, \sqrt{\frac{b+1}{a+1}}\right)}{\sqrt{a+1}}\int_{-1}^{1}\sqrt{\frac{\left(a-\cos\left(\pi\frac{y^*}{D}\right)\right)\left(b-\cos\left(\pi\frac{y^*}{D}\right)\right)}{\left(1-\cos\left(\pi\frac{y^*}{D}\right)\right)}}\,d\xi \tag{3.72}$$

where, $y^* = \frac{1}{2}\left\{\left(D-d_1-\frac{d_p}{2}\right)\xi + \left(D+d_1+\frac{d_p}{2}\right)\right\}$

Knowing the travel time, t_r, the number of log cycles of the bacteria concentration in a parcel of river water by the time the parcel travels from the riverbed to the collector pipe using logistic equation.

3.8 RESULTS AND DISCUSSIONS

Dimensionless flow parameter per unit length of collector pipe $Q/(kD_w)$, dimensionless average entrance velocity factor $\bar{v}_{ef}\left(=\dfrac{\bar{v}_e d_p f_a}{kD_w}\right)$, the maximum entrance velocity factor $v_{emf}\left(=\dfrac{|v_1|Df_a}{kD_w}\right)$, and travel time factor $t_{rf}\left(=\dfrac{t_r kD_w}{\eta D^2}\right)$ are shown in Table-3.1 through Table 3.3 for specific values of D, d_p/D and d_1/D. Using the dimensionless factors given in these tables, Q, $\bar{v}_e$, $|v_1|$ and t_r for any known values of D_w, k, f_a, η for the specified values of D, d_p/D, and d_1/D have been computed.

Table 3.1 Dimensionless Flow $Q/(kD_w)$ **, Entrance Velocity Factors** $\bar{v}_{ef}\left(=\dfrac{\bar{v}_e d_p f_a}{kD_w}\right)$

$v_{emf}\left(=\dfrac{|v_1|Df_a}{kD_w}\right)$**, and Travel Time Factor** $t_{rf}\left(=\dfrac{t_r kD_w}{\eta D^2}\right)$**, Travel Time** t_r **(day), and Number of**

Log Cycle Reduction, n **for** $d_p = 1m$, $d_1/D = \{0.25, 0.5, 0.75\}$, $D_w = 4m$, $k = 0.864(m/day)$, $\eta = 0.3$

$D(m)$	d_p/D	d_1/D	$Q/(kD_w)$	$\bar{v}_{ef}$	v_{emf}	t_{rf}	t_r	n
5	0.2	0.25	1.954	0.622	3.726	0.471	10.2158	0.8016
		0.5	2.635	0.839	4.878	0.171	3.7168	0.3712
		0.75	4.431	1.411	8.966	0.023	0.4961	0.0617
10	0.1	0.25	1.566	0.499	5.506	0.600	52.0895	2.7378
		0.5	1.990	0.633	6.838	0.237	20.6056	1.3335
		0.75	2.805	0.893	10.019	0.043	3.7413	0.3731
15	0.067	0.25	1.411	0.449	7.217	0.669	130.6291	6.1503
		0.5	1.75	0.557	8.798	0.272	53.1607	2.7844
		0.75	2.34	0.745	12.052	0.053	10.4229	0.8134
20	0.05	0.25	1.321	0.420	8.860	0.716	248.5443	11.2713
		0.5	1.615	0.514	10.687	0.296	102.7423	4.9392
		0.75	2.1	0.668	14.145	0.06	20.8859	1.3468

Table 3.2 Dimensionless Flow $Q/(kDw)$ **, Entrance Velocity Factors** $\bar{v}_{ef}\left(=\dfrac{\bar{v}_e d_p f_a}{kD_w}\right)$

$v_{emf}\left(=\dfrac{|v_1|Df_a}{kD_w}\right)$, **and Travel Time Factor** $t_{rf}\left(=\dfrac{t_r kD_w}{\eta D^2}\right)$, **Travel Time** t_r **(day),and Number of**

Log Cycle Reduction , n **for** $d_p = 0.5m$, $d_1/D = \{0.25, 0.5, 0.75\}$, $D_w = 4m$, $k = 0.864(m/day)$, $\eta = 0.3$

$D(m)$	d_p/D	d_1/D	$Q/(kD_w)$	$\bar{v}_{ef}$	v_{emf}	t_{rf}	t_r	n
5	0.1	0.25	1.566	0.997	5.506	0.6	13.0224	0.9558
		0.5	1.99	1.267	6.838	0.237	5.1514	0.4802
		0.75	2.805	1.786	10.019	0.043	0.9353	0.112
10	0.05	0.25	1.321	0.841	8.86	0.716	62.1361	3.1751
		0.5	1.615	1.028	10.687	0.296	25.6856	1.5699
		0.75	2.1	1.337	14.145	0.06	5.2215	0.4853
15	0.033	0.25	1.213	0.772	12.001	0.78	152.4193	7.0966
		0.5	1.458	0.928	14.288	0.328	64.1518	3.2627
		0.75	1.839	1.171	18.229	0.069	13.5262	0.9824
20	0.025	0.25	1.147	0.73	15.004	0.825	286.6011	12.9241
		0.5	1.365	0.869	17.719	0.351	121.9295	5.7724
		0.75	1.692	1.077	22.151	0.075	26.2138	1.594

Table 3.3 Dimensionless Flow $Q/(kDw)$ **, Entrance Velocity Factors** $\bar{v}_{ef}\left(=\dfrac{\bar{v}_e d_p f_a}{kD_w}\right)$

$v_{emf}\left(=\dfrac{|v_1|Df_a}{kD_w}\right)$, **and Travel Time Factor** $t_{rf}\left(=\dfrac{t_r kD_w}{\eta D^2}\right)$, **Travel Time** t_r **(day),and Number of**

Log Cycle Reduction , n **for** $d_p = 0.3m$, $d_1/D = \{0.25, 0.5, 0.75\}$, $D_w = 4m$, $k = 0.864(m/day)$, $\eta = 0.3$

$D(m)$	d_p/D	d_1/D	$Q/(kD_w)$	$\bar{v}_{ef}$	v_{emf}	t_{rf}	t_r	n
5	0.06	0.25	1.377	1.461	7.771	0.686	14.8908	1.053
		0.5	1.698	1.801	9.435	0.281	6.0969	0.5465
		0.75	2.245	2.382	12.751	0.056	1.2129	0.142
10	0.03	0.25	1.188	1.260	13.015	0.797	69.1787	3.4812
		0.5	1.422	1.509	15.448	0.337	29.2362	1.731
		0.75	1.782	1.891	19.554	0.072	6.2115	0.5543
15	0.02	0.25	1.101	1.168	17.909	0.860	167.9723	7.7721
		0.5	1.301	1.380	21.026	0.369	71.9943	3.6036
		0.75	1.594	1.691	25.935	0.080	15.6748	1.0928
20	0.015	0.25	1.047	1.111	22.592	0.904	314.0047	14.1142
		0.5	1.227	1.301	26.336	0.391	135.7542	6.3729
		0.75	1.483	1.574	32.006	0.086	29.9708	1.764

As seen from these tables, less the thickness of the porous medium below the riverbed more the flow to the collector pipe as the pipe is nearer to the riverbed. There is marginal increase in the yield of the collector pipe with larger value of collector pipe diameter.

The complete elliptic integral of the first kind $F\left(\dfrac{\pi}{2},k^*\right)$ is computed using the following polynomial approximation (Abramowitz and Stegun, 1964, p591):

$$F\left(\frac{\pi}{2},k^*\right)=\left[a_0+a_1 m_1+a_2 m_1^2+a_3 m_1^3+a_4 m_1^4\right]+\left[b_0+b_1 m_1+b_2 m_1^2+b_3 m_1^3+b_4 m_1^4\right]\ln\left(\frac{1}{m_1}\right)+\varepsilon(m)$$

$\varepsilon|m|\geq 2\times 10^{-8}$, where, $m_1=\left(1-k^{*2}\right)$, and $m=k^{*2}$. The coefficients a_i, and b_i are:

$a_0=1.3862943611$, $a_1=0.0966634425$, $a_2=0.0359009238$, $a_3=0.0374256371$, $a_4=0..0145119621$

$b_0=0.5$, $b_1=0.1249859359$, $b_2=0.0688024857$, $b_3=0.0332835534$, $b_4=0.0044178701$

Flow to the collector pipe for vertical slit:

Variations of $Q/(kD_w)$ with d_1/D for various values of d_p/D are presented in Fig. (3.7), through (3.11) for dimensionless pipe diameter $\dfrac{d_p}{D}=0.001, 0.01, 0.1, 0.2, 0.3$ respectively. The lower limit of $\dfrac{d_1}{D}=0.5\dfrac{d_p}{D}$ and the upper limit is less than $\left(1-0.5\dfrac{d_p}{D}\right)$. For $\dfrac{d_1}{D}=1-0.5\dfrac{d_p}{D}$, the flow to the collector pipe, $Q/(k\,D_w)$, tends to infinite. Accordingly, variations of $Q/(k\,D_w)$ with d_1/D are presented in these Figures.
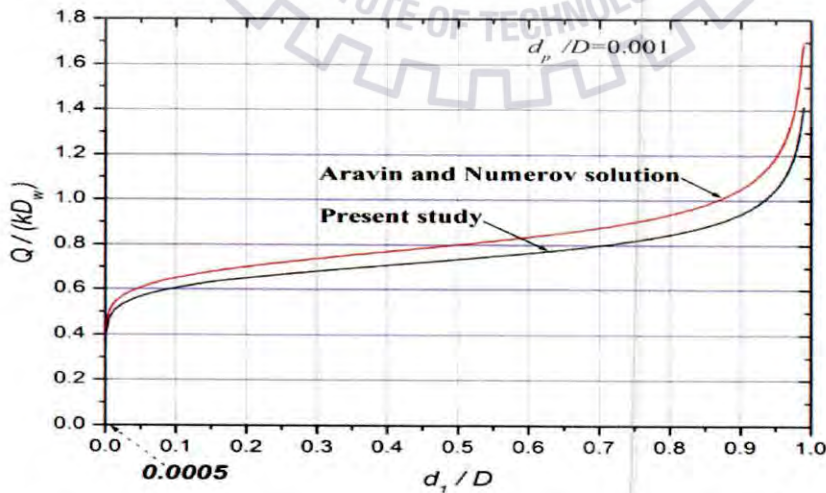
Fig. (3.7) Variation of $Q/(kD_w)$ with d_1/D for $d_p/D=0.001$ $0.0005 \leq \dfrac{d_1}{D} < 0.9995$
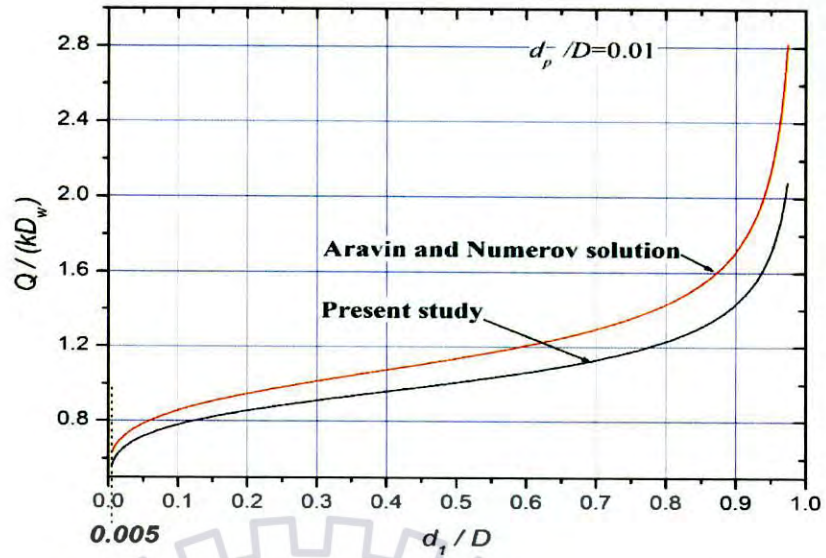
Fig. (3.8) Variation of $Q/(kD_w)$ with d_1/D for $d_p/D=0.01$ $0.005 \leq \dfrac{d_1}{D} < 0.995$
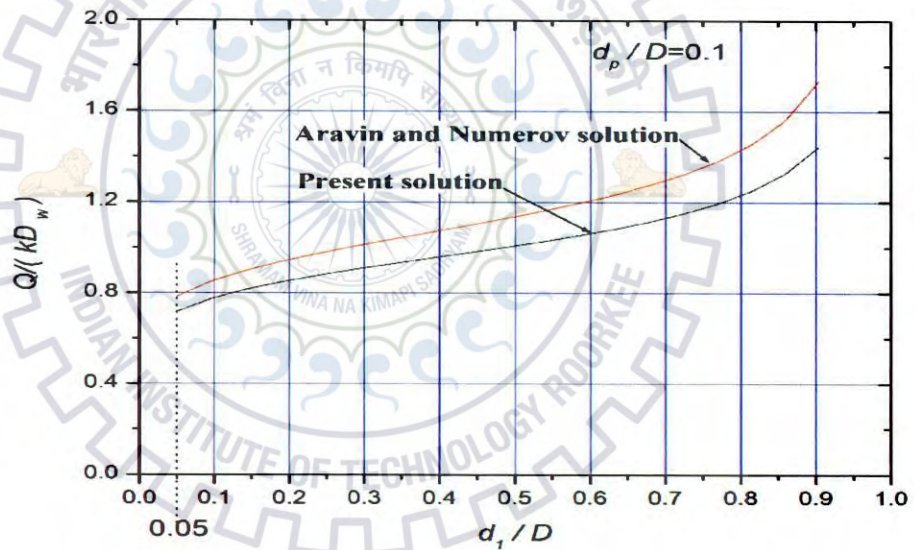
Fig. (3.9) Variation of $Q/(kD_w)$ with d_1/D for $d_p/D=0.1$ $0.05 \leq \dfrac{d_1}{D} < 0.95$

43
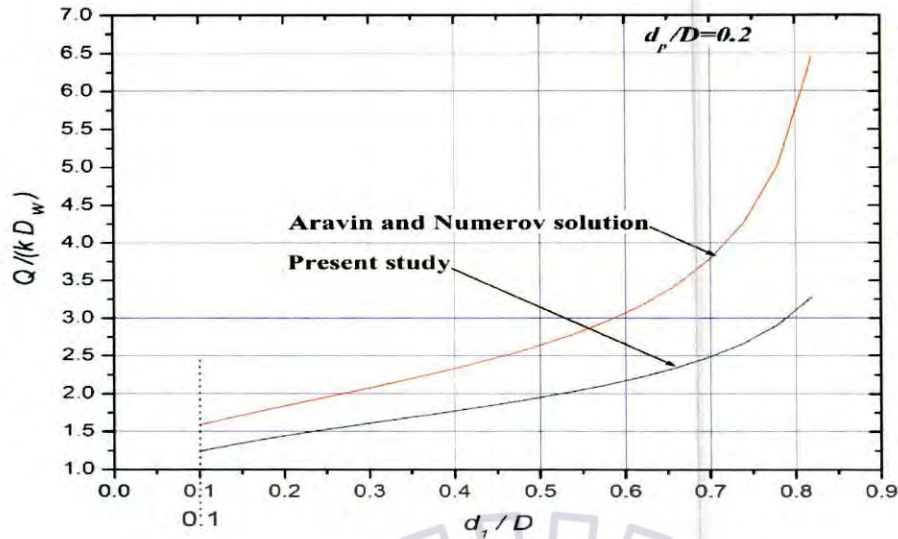
Fig. (3.10) Variation of $Q/(kD_w)$ with d_1/D for d_p/D=0.2 $0.1 \le \dfrac{d_1}{D} < 0.9$
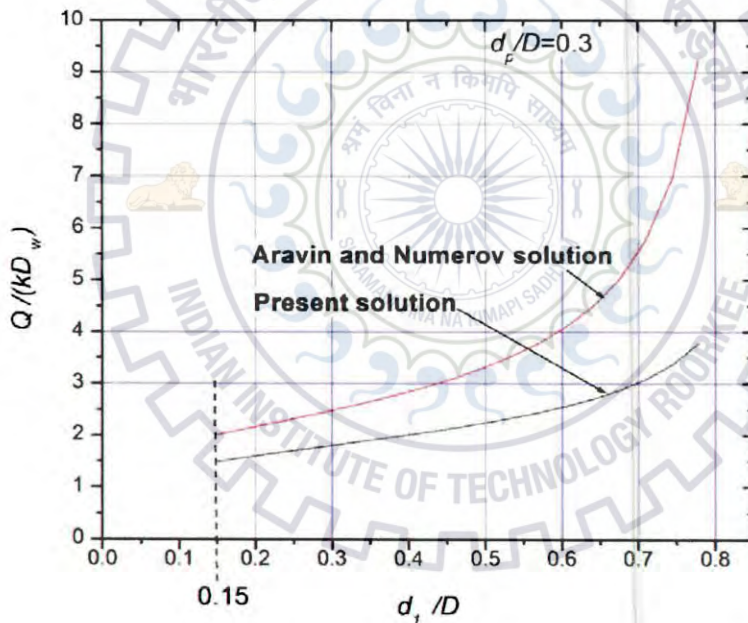
Fig. (3.11) Variation of $Q/(kD_w)$ with d_1/D for d_p/D=0.3 $0.15 \le \dfrac{d_1}{D} < 0.85$

As seen from these Figures, the flow to the collector pipe increases as the collector pipe is laid nearer to the riverbed. For $\dfrac{d_1}{D} = \left(1 - 0.5\dfrac{d_p}{D}\right)$, the flow to the collector pipe is infinite.

For $\dfrac{d_1}{D} \cong \left(0.5\dfrac{d_p}{D}\right)$, meaning thereby, the collector pipe is laid on the bottom impervious boundary, the flow to collector pipe is the minimum. The collector pipe is to be laid at a depth

44

such that $\left(D - d_1 - \dfrac{d_p}{2}\right) > D_s$, where, D_s, is scour depth minus depth of flow during the high flood for which the scour depth is computed. For different type of soils, silt factor and procedure for calculation of scour depth are presented in appendix A.

The flow to the collector pipe increases with increase in pipe diameter $\dfrac{d_p}{D}$ ratio. The diameter of d_p of the collector varies from 0.2 to 0.3m, Huisman and and Olsthoorn (1983).

Entrance velocity:

The entrance velocity to the collector pipe depends on
  i) Area of slot openings of the collector pipe,
  ii) The hydraulic conductivity (k) of the bed materials,
  iii) Drawdown (D_w) in the caisson,
  iv) Diameter (d_p) of the collector pipe,
  v) Depth to impervious bottom layer (d_1) below the collector pipe, and
  vi) Thickness (D) of the riverbed materials.

  While installing a collector pipe, one has to check the entrance velocity. The maximum entrance velocity is 3cm/s Blair(1970). Huisman(1972) has recommended the maximum entrance velocity to be 4 cm/s. The dimensionless Darcy velocities, obtained using equation (3.25) are presented in tables 3.4 through 3.8. Using the tabulated values and known f_a, the entrance velocity can be computed.

Table 3.4 Radial Flow Velocity $\dfrac{v_r}{k}\left(=\dfrac{Q}{\pi d_p k}\right)$ **for various d_1/D For $d_p/D=0.001$ and $D_w=1m$**

$\dfrac{d_1}{D}$	$\dfrac{Q}{kD_w}$ (Conformal mapping)	$\dfrac{Q}{kD_w}$ (Aravin)	$\dfrac{u_{d_1}}{k}$	$\dfrac{v_r}{k}=\dfrac{Q}{\pi d_p k}$ (Conformal mapping)	$\dfrac{v_r}{k}=\dfrac{Q_1}{\pi d_p k}$ (Aravin)
0.0005	0.40096	0.43076	-0.14713	0.12763	0.13711
0.0255	0.53462	0.56863	-0.17021	0.17017	0.18100
0.0505	0.56771	0.60592	-0.18072	0.18071	0.19287
0.0755	0.58926	0.63043	-0.18756	0.18757	0.20067
0.1005	0.60571	0.64925	-0.19280	0.19280	0.20666
0.1255	0.61926	0.66480	-0.19711	0.19712	0.21161
0.1505	0.63091	0.67823	-0.20083	0.20083	0.21589
0.1755	0.64125	0.69018	-0.20412	0.20412	0.21969
0.2005	0.65062	0.70104	-0.20710	0.20710	0.22315
0.2255	0.65928	0.71109	-0.20986	0.20986	0.22635

$\frac{d_1}{D}$	$\frac{Q}{kD_w}$ (Conformal mapping)	$\frac{Q}{kD_w}$ (Aravin)	$\frac{u_{d_1}}{k}$	$\frac{v_r}{k} = \frac{Q}{\pi d_p k}$ (Conformal mapping)	$\frac{v_r}{k} = \frac{Q_1}{\pi d_p k}$ (Aravin)
0.2505	0.66738	0.72051	-0.21244	0.21243	0.22934
0.2755	0.67504	0.72944	-0.21487	0.21487	0.23219
0.3005	0.68236	0.73800	-0.21721	0.21720	0.23491
0.3255	0.68943	0.74627	-0.21945	0.21945	0.23754
0.3505	0.69631	0.75433	-0.22164	0.22164	0.24011
0.3755	0.70305	0.76223	-0.22379	0.22379	0.24263
0.4005	0.70969	0.77005	-0.22590	0.22590	0.24511
0.4255	0.71629	0.77783	-0.22800	0.22800	0.24759
0.4505	0.72289	0.78561	-0.23010	0.23010	0.25007
0.4755	0.72953	0.79346	-0.23222	0.23222	0.25257
0.5005	0.73625	0.80142	-0.23436	0.23436	0.2551
0.5255	0.74310	0.80953	-0.23654	0.23653	0.25768
0.5505	0.75012	0.81787	-0.23877	0.23877	0.26034
0.5755	0.75736	0.82649	-0.24108	0.24108	0.26308
0.6005	0.76489	0.83547	-0.24347	0.24347	0.26594
0.6255	0.77277	0.84489	-0.24598	0.24598	0.26894
0.6505	0.78109	0.85484	-0.24863	0.24863	0.27210
0.6755	0.78994	0.86546	-0.25144	0.25145	0.27548
0.7005	0.79945	0.87689	-0.25447	0.25447	0.27912
0.7255	0.80977	0.88934	-0.25776	0.25776	0.28308
0.7505	0.82112	0.90305	-0.26137	0.26137	0.28745
0.7755	0.83375	0.91837	-0.26540	0.26539	0.29233
0.8005	0.84808	0.9358	-0.26994	0.26995	0.29787
0.8255	0.86463	0.95602	-0.27523	0.27522	0.30431

Table 3.5 Radial Flow Velocity $\frac{v_r}{k}\left(=\frac{Q}{\pi d_p k}\right)$ for various d_1/D for $d_p/D=0.01$ and $D_w=1m$

$\frac{d_1}{D}$	$\frac{Q}{kD_w}$ (Conformal mapping)	$\frac{Q}{kD_w}$ (Aravin)	$\frac{u_{d_1}}{k}$	$\frac{v_r}{k} = \frac{Q}{\pi d_p k}$ (Conformal mapping)	$\frac{v_r}{k} = \frac{Q_1}{\pi d_p k}$ (Aravin)
0.005	0.56709	0.62951	-0.20843	0.18051	0.20038
0.03	0.67654	0.73799	-0.21610	0.21535	0.23491
0.055	0.72392	0.79118	-0.23067	0.23043	0.25184
0.08	0.75684	0.82918	-0.24103	0.24091	0.26393
0.105	0.78284	0.85965	-0.24925	0.24919	0.27364
0.13	0.80475	0.88559	-0.25621	0.25616	0.28189
0.155	0.82395	0.90851	-0.26230	0.26227	0.28919
0.18	0.84123	0.92928	-0.26779	0.26777	0.29580
0.205	0.85710	0.94846	-0.27284	0.27282	0.30191

46

$\dfrac{d_1}{D}$	$\dfrac{Q}{kD_w}$ (Conformal mapping)	$\dfrac{Q}{kD_w}$ (Aravin)	$\dfrac{u_{d_1}}{k}$	$\dfrac{v_r}{k} = \dfrac{Q}{\pi d_p k}$ (Conformal mapping)	$\dfrac{v_r}{k} = \dfrac{Q_1}{\pi d_p k}$ (Aravin)
0.23	0.87191	0.96646	-0.27755	0.27754	0.30763
0.255	0.88591	0.98354	-0.28200	0.28199	0.31307
0.28	0.89929	0.99994	-0.28626	0.28625	0.31829
0.305	0.91220	1.01583	-0.29037	0.29036	0.32335
0.33	0.92475	1.03135	-0.29436	0.29436	0.32829
0.355	0.93707	1.04662	-0.29828	0.29828	0.33315
0.38	0.94923	1.06176	-0.30215	0.30215	0.33797
0.405	0.96132	1.07687	-0.30600	0.30600	0.34278
0.43	0.97343	1.09206	-0.30985	0.30985	0.34761
0.455	0.98562	1.10740	-0.31373	0.31373	0.35250
0.48	0.99799	1.12302	-0.31767	0.31767	0.35747
0.505	1.01060	1.13902	-0.32168	0.32168	0.36256
0.53	1.02355	1.15551	-0.32580	0.32581	0.36781
0.555	1.03694	1.17262	-0.33007	0.33007	0.37326
0.58	1.05088	1.19051	-0.33450	0.33451	0.37895
0.605	1.06550	1.20934	-0.33915	0.33916	0.38495
0.63	1.08094	1.22933	-0.34407	0.34407	0.39131
0.655	1.09739	1.25074	-0.34930	0.34931	0.39812
0.68	1.11509	1.27389	-0.35493	0.35495	0.40549
0.705	1.13432	1.29919	-0.36105	0.36107	0.41355
0.73	1.15547	1.32718	-0.36778	0.36780	0.42246
0.755	1.17902	1.35859	-0.37528	0.37529	0.43245
0.78	1.20568	1.39443	-0.38376	0.38378	0.44386
0.805	1.23644	1.43617	-0.39354	0.39357	0.45715
0.83	1.27277	1.48604	-0.40509	0.40514	0.47302
0.855	1.31701	1.54760	-0.41916	0.41922	0.49262
0.88	1.37312	1.62710	-0.43698	0.43708	0.51792
0.905	1.44857	1.73665	-0.46094	0.46110	0.55279
0.93	1.55984	1.90423	-0.49619	0.49651	0.60614
0.955	1.75406	2.21652	-0.55747	0.55833	0.70554
0.98	2.27908	3.22847	-0.71954	0.72545	1.02765

Table 3.6 Radial flow velocity $\dfrac{v_r}{k}\left(=\dfrac{Q}{\pi d_p k}\right)$ for various d_1/D for $d_p/D=0.1$ and $D_w=1$

$\dfrac{d_1}{D}$	$\dfrac{Q}{kD_w}$ (Conformal mapping)	$\dfrac{Q}{kD_w}$ (Aravin)	$\dfrac{u_{d_1}}{k}$	$\dfrac{v_r}{k} = \dfrac{Q}{\pi d_p k}$ (Conformal mapping)	$\dfrac{v_r}{k} = \dfrac{Q_1}{\pi d_p k}$ (Aravin)
0.05	0.97106	1.16987	-0.35654	0.30910	0.37238
0.075	1.03642	1.23697	-0.34955	0.32990	0.39374
0.1	1.08874	1.29506	-0.35755	0.34656	0.41223
0.125	1.13349	1.34729	-0.36785	0.36081	0.42886
0.15	1.17331	1.39548	-0.37837	0.37348	0.44419

$\dfrac{d_1}{D}$	$\dfrac{Q}{kD_w}$ (Conformal mapping)	$\dfrac{Q}{kD_w}$ (Aravin)	$\dfrac{u_{d_1}}{k}$	$\dfrac{v_r}{k}=\dfrac{Q}{\pi d_p k}$ (Conformal mapping)	$\dfrac{v_r}{k}=\dfrac{Q_1}{\pi d_p k}$ (Aravin)
0.175	1.20971	1.44078	-0.38863	0.38506	0.45861
0.2	1.24361	1.4841	-0.39854	0.39585	0.47237
0.225	1.27568	1.52573	-0.40813	0.40606	0.48565
0.25	1.30641	1.56644	-0.41746	0.41584	0.49861
0.275	1.33617	1.60652	-0.42658	0.42531	0.51137
0.3	1.36524	1.64631	-0.43555	0.43457	0.52403
0.325	1.39389	1.68608	-0.44445	0.44369	0.53671
0.35	1.42233	1.72616	-0.45331	0.45274	0.54945
0.375	1.45078	1.76681	-0.46221	0.46182	0.56239
0.4	1.47943	1.80831	-0.47117	0.47092	0.57561
0.425	1.50848	1.85098	-0.48028	0.48016	0.58919
0.45	1.53812	1.89515	-0.48959	0.48961	0.60324
0.475	1.56857	1.94118	-0.49915	0.49929	0.6179
0.5	1.60006	1.98951	-0.50905	0.50932	0.63328
0.525	1.63287	2.04062	-0.51936	0.51976	0.64955
0.55	1.66728	2.09513	-0.53017	0.53071	0.66691
0.575	1.70366	2.15375	-0.54159	0.54229	0.68556
0.6	1.74244	2.21741	-0.55375	0.55463	0.70582
0.625	1.78414	2.28723	-0.56681	0.56791	0.72805
0.65	1.82942	2.36476	-0.58097	0.58232	0.75273
0.675	1.87915	2.45197	-0.59649	0.59815	0.78049
0.7	1.93443	2.55161	-0.61368	0.61575	0.81221
0.725	1.99677	2.66756	-0.63321	0.63559	0.84911
0.75	2.06831	2.80549	-0.65505	0.65836	0.89301
0.775	2.15206	2.97414	-0.68071	0.68502	0.94671
0.8	2.25271	3.18775	-0.71125	0.71706	1.01469
0.825	2.37772	3.47138	-0.74871	0.75685	1.10497
0.85	2.54022	3.87398	-0.79645	0.80858	1.23313
0.875	2.76596	4.50713	-0.86067	0.88043	1.43466
0.9	3.11566	5.69777	-0.95441	0.99174	1.81366
0.925	3.79330	9.04447	-1.11157	1.20744	2.87894

Table 3.7 Radial Flow Velocity $\dfrac{v_r}{k}\left(=\dfrac{Q}{\pi d_p k}\right)$ for various d_1/D for $d_p/D=0.2$ and $D_w=1$

$\dfrac{d_1}{D}$	$\dfrac{Q}{kD_w}$ (Conformal mapping)	$\dfrac{Q}{kD_w}$ (Aravin)	$\dfrac{u_{d_1}}{k}$	$\dfrac{v_r}{k}=\dfrac{Q}{\pi d_p k}$ (Conformal mapping)	$\dfrac{v_r}{k}=\dfrac{Q_1}{\pi d_p k}$ (Aravin)
0.125	1.29721	1.65007	-0.44861	0.41291	0.52523
0.15	1.34964	1.71378	-0.45370	0.42961	0.54551
0.175	1.39804	1.77528	-0.46233	0.44501	0.56509
0.2	1.44357	1.83533	-0.47245	0.45950	0.58420

48

$\dfrac{d_1}{D}$	$\dfrac{Q}{kD_w}$ (Conformal mapping)	$\dfrac{Q}{kD_w}$ (Aravin)	$\dfrac{u_{d_1}}{k}$	$\dfrac{v_r}{k}=\dfrac{Q}{\pi d_p k}$ (Conformal mapping)	$\dfrac{v_r}{k}=\dfrac{Q_1}{\pi d_p k}$ (Aravin)
0.225	1.48702	1.89456	-0.48326	0.47333	0.60306
0.25	1.52901	1.95351	-0.49442	0.48671	0.62182
0.275	1.57120	2.01264	-0.50579	0.49975	0.64064
0.3	1.61038	2.07242	-0.51731	0.51261	0.65967
0.325	1.65051	2.13330	-0.5290	0.52537	0.67905
0.35	1.69068	2.19573	-0.54087	0.53816	0.69892
0.375	1.73119	2.26020	-0.55296	0.55105	0.71944
0.4	1.77233	2.32726	-0.56534	0.56415	0.74079
0.425	1.81441	2.39751	-0.57807	0.57755	0.76315
0.45	1.85775	2.47166	-0.59123	0.59134	0.78675
0.475	1.90271	2.55054	-0.60491	0.60565	0.81186
0.5	1.94967	2.63517	-0.61922	0.62060	0.83880
0.525	1.99912	2.72677	-0.63428	0.63634	0.86796
0.55	2.05160	2.82691	-0.65024	0.65305	0.89983
0.575	2.10779	2.93759	-0.66729	0.67093	0.93506
0.6	2.16852	3.06142	-0.68566	0.69026	0.97448
0.625	2.23486	3.20192	-0.70562	0.71138	1.01921
0.65	2.30818	3.36392	-0.72753	0.73472	1.07077
0.675	2.39034	3.55435	-0.75188	0.76087	1.13138
0.7	2.48388	3.78342	-0.77929	0.79064	1.20431
0.725	2.59245	4.06701	-0.81064	0.82521	1.29457
0.75	2.72150	4.43129	-0.84717	0.86628	1.41052
0.775	2.87970	4.92279	-0.89073	0.91664	1.56697
0.8	3.08189	5.63361	-0.94421	0.98099	1.79323
0.825	3.35655	6.77651	-1.01246	1.06842	2.15703
0.85	3.76908	8.98415	-1.10438	1.19974	2.85974
0.875	4.53226	15.39803	-1.23867	1.44266	4.90134

Table 3.8 Radial Flow Velocity $\dfrac{v_r}{k}\left(=\dfrac{Q}{\pi d_p k}\right)$ for various d_1/D for $d_p/D=0.3$ and $D_w=1m$

$\dfrac{d_1}{D}$	$\dfrac{Q}{kD_w}$ (Conformal mapping)	$\dfrac{Q}{kD_w}$ (Aravin)	$\dfrac{u_{d_1}}{k}$	$\dfrac{v_r}{k}=\dfrac{Q}{\pi d_p k}$ (Conformal mapping)	$\dfrac{v_r}{k}=\dfrac{Q_1}{\pi d_p k}$ (Aravin)
0.15	1.48222	2.00663	-0.53944	0.4718	0.63873
0.175	1.54087	2.08369	-0.53744	0.49048	0.66326
0.2	1.59645	2.16037	-0.54259	0.50816	0.68767
0.225	1.64987	2.23735	-0.55125	0.52517	0.71217
0.25	1.70185	2.31526	-0.56184	0.54172	0.73697
0.275	1.75295	2.39473	-0.57364	0.55798	0.76227
0.3	1.80365	2.47638	-0.58628	0.57412	0.78826
0.325	1.85438	2.56091	-0.59958	0.59027	0.81516

$\dfrac{d_1}{D}$	$\dfrac{Q}{kD_w}$ (Conformal mapping)	$\dfrac{Q}{kD_w}$ (Aravin)	$\dfrac{u_{d_1}}{k}$	$\dfrac{v_r}{k} = \dfrac{Q}{\pi d_p k}$ (Conformal mapping)	$\dfrac{v_r}{k} = \dfrac{Q_1}{\pi d_p k}$ (Aravin)
0.35	1.90553	2.64904	-0.61347	0.60655	0.84322
0.375	1.95751	2.74163	-0.62793	0.62310	0.87269
0.4	2.01072	2.83965	-0.64299	0.64003	0.90389
0.425	2.06561	2.94426	-0.65871	0.65750	0.93719
0.45	2.12261	3.05688	-0.67517	0.67565	0.97304
0.475	2.18232	3.17925	-0.69248	0.69465	1.01199
0.5	2.24534	3.31355	-0.71078	0.71471	1.05473
0.525	2.31245	3.4626	-0.73026	0.73607	1.10218
0.55	2.38457	3.63013	-0.75112	0.75903	1.15551
0.575	2.46289	3.82113	-0.77364	0.78396	1.21632
0.6	2.54893	4.04252	-0.79817	0.81135	1.28678
0.625	2.64469	4.30424	-0.82515	0.84183	1.37008
0.65	2.75293	4.62101	-0.85515	0.87629	1.47091
0.675	2.87756	5.01583	-0.88896	0.91596	1.59659
0.7	3.02436	5.52676	-0.92766	0.96268	1.75922
0.725	3.20245	6.22182	-0.97278	1.01937	1.98046
0.75	3.42728	7.23620	-1.02661	1.09094	2.30335

A comparison between the velocities $\dfrac{v_r}{k}\left(=\dfrac{Q}{\pi d_p k}\right)$ obtained for a line slit and for a line sink given by Aravin and Numerov (1965) is also presented in Tables 3.4 through 3.8. The dimensionless velocities have been computed assuming drawdown D_w in the well caisson as one meter. The entrance velocity is linearly proportional to the drawdown in the caisson. Therefore, by multiplying the actual drawdown to the present entrance velocity value, the actual entrance velocity can be computed.

The exact horizontal velocity, $\dfrac{u_{d_1}}{k}$, at midpoint of the line slit is very close to the average velocity, $\dfrac{v_r}{k}$ for values of $\dfrac{d_1}{D} > 0.1005$. Therefore, entrance velocity computed using Aravin and Numerov (1965) solution can be used to assess the entrance velocity that prevails around a collector pipe.

The minimum travel time of a parcel of water from riverbed to collector pipe:

The travel time of a parcel of water from river bed to the collector pipe for different position of the pipe obtained using conformal mapping technique for various type of the river bed material
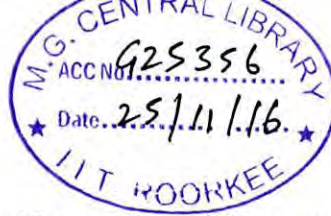
are presented in tables 3.9 through 3.11. The number of log cycles computed using logistic equation for the corresponding soils and collector pipe positions are also presented in the tables.

Table 3.9 Position of Collector pipe below the Riverbed and Number of Log Cycle Reduction for Fine Sand, k=0.35m/day, η =30%

Depth below riverbed $(D-d_1)$ (m)	Travel time (Days)	Number of Log cycle reduction (n)
1	0.268	<1
2	2.520	<1
3	7.243	<1
4	14.550	1.0
5	24.470	1.0

Table 3.10 Position of Collector Pipe below the Riverbed and Number of Log Cycle Reduction for silty sand, k=0.0864 m/day, η =30%

Depth below riverbed $(D-d_1)$ (m)	Travel time (days)	Number of log cycle reduction
1	1.086	<1
2	10.207	<1
3	29.34	1.75
4	58.96	3.0
5	99.15	4.78

Table 3.11 Position of Collector Pipe below the Riverbed and Number of Log Cycle Reduction For silt, k=0.00864m/day, η =30%

Depth below riverbed $(D-d_1)$ (m)	Travel time (Days)	Number of log cycle reduction
1	10.86	<1
2	102.07	5
3	293.40	13
4	589.577	26
5	991.51	44

An example for a line sink

A collector pipe is to be installed under the bed of a straight stream reach. The thickness of the aquifer under the stream bed is 10m. The hydraulic conductivity of the sandy silt deposit is 0.0864m/day, and porosity is 30%. The pipe is to be laid 5m below stream bed. The collector pipe has 16% opening area and its diameter is 0.5m. The allowable entrance velocity is 3cm/s.

If a drawdown of 4m is maintained in the well caisson compute the yield of a collector well having 25m collector length. Compute the entrance velocity.

Steps of computation:

Corresponding to $d_1/D = 0.5$, $d_p/D = 0.05$, from Table 3.2, the dimensionless flow $Q/(kD_w)$=1.615. Substituting k=0.0864m/day, $D_w = 4m$, the yield of the collector well having 25m length of collector is 1.615x0.0864x4x25=13.95 m^3 /day. In order to have respectable yield, several parallel collector pipes are to be laid and connected to the well caisson. From table 3.2, the maximum entrance velocity factor $\frac{v_{em} D f_a}{kD_w} = 10.687$ .The maximum entrance velocity $v_{em} = (10.687 \times 0.0864 \times 4)/(10 \times 0.16)$ m/day=0.002672cm/sec. The average entrance velocity factor $\bar{v}_{ef}\left(=\frac{\bar{v}_e d_p f_a}{kD_w}\right) = 1.028$. The average entrance velocity $\bar{v}_e = (1.028 \times 0.0864 \times 4)/(0.5 \times 0.16) m/day = 0.00257 cm/s$. Magnitude of the average entrance velocity is marginally less than the maximum entrance velocity. The dimensionless time factor $t_{rf}\left(=\frac{t_r kD_w}{\eta D^2}\right) = 0.296$ the travel time t_r corresponding to $\eta = 0.3$ is $t_r = 0.296 \times 0.3 \times 10^2 /(0.0864 \times 4) = 25.7 days$ .the log cycle reduction n is about 1.57 (B.7). This means the initial bacterial concentration in river water (C_o) will reduce to $C_o*10^{-1.57}$ during water travel from river bed to the collector pipe.

In case the aquifer material has a hydraulic conductivity of 1.0m/day, all other parameters remaining same as above, the well caisson will receive 161.5m^3/day of filtered water having a collector length of 25m. The travel time would be 2.22 days and log cycle reduction would be 0.242. The maximum entrance velocity will be 0.0309cm/sec. It is to be understood that irrespective of hydraulic conductivity, drawdown, fraction of opening of peripheral area of collector pipe f_a, and porosity η, the dimensionless factors remain unchanged for given values of d_1/D and d_p/D.

An illustrative example for vertical line slit
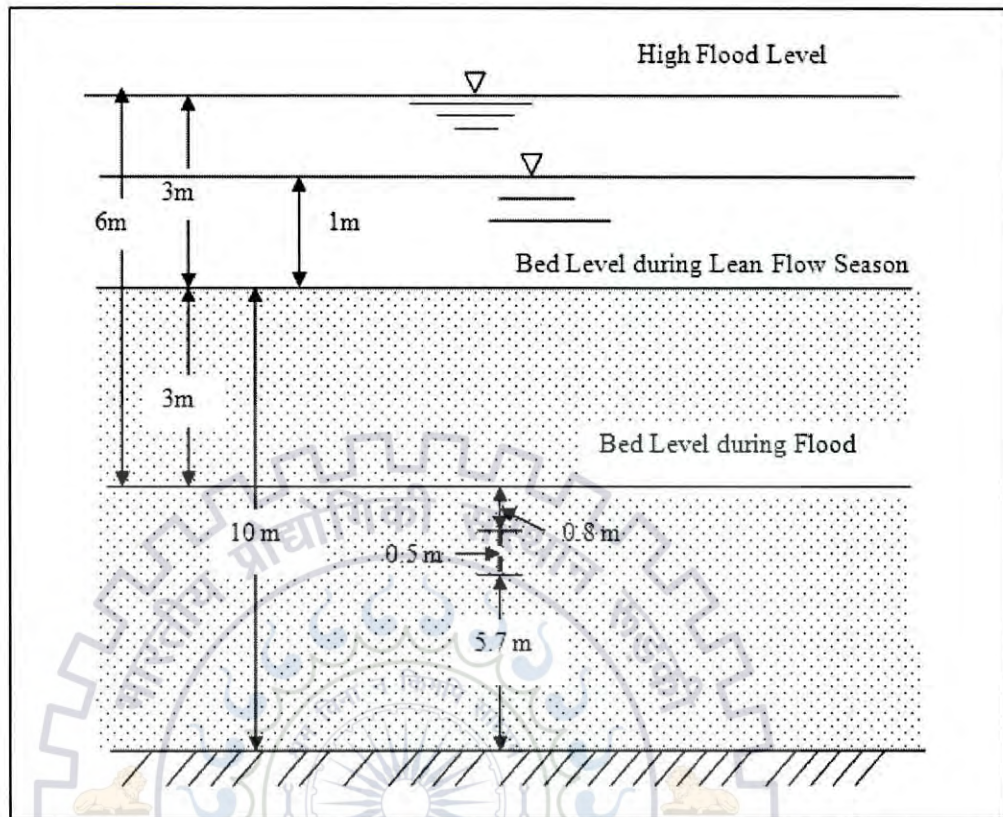
Fig. 3.12 Example of Collector Pipe Installed Under Riverbed

A collector pipe is to be installed below a riverbed at a site. The maximum flood discharge at the site is 1100 m³/s. The mean grain size of the bed material at the proposed collector well site is 0.149 mm, the bed material is considered as fine sand (Lancellotta, (2008)). Corresponding to the mean grain size of the bed material, the silt factor of riverbed material at the collector well site f_L is about 0.6 (Vellaisamy, (2007)). The thickness of the sediment layer at the section during lean flow period is 10m.The depth of water during lean flow period is 1 m. The d_{10} particle size is 0.02 mm. Corresponding to d_{10}=0.02 mm, applying Hazen's formula assuming C to be equal to 100(cm.s)$^{-1}$, (Fitts (2002)) the hydraulic conductivity of the sediments is 0.35 m/day. A minimum depth of 0.8 m sand medium is to be maintained above the collector pipe during passage of the maximum flood as per filtration requirement. Diameter of the collector pipe, d_p, is 1.0 m. Compute the specific capacity during lean flow period as well as during passage of the maximum flood.

Steps of computation:

(a)   During flood period:

Calculation of scour depth

   Using equation (A.1) the scour depth is found to be 5.75m. We have assumed the scour depth to be equal to 6.0m. The rise of water level during maximum flood is 2m above the water level prevailing during lean flow period. Therefore, the thickness of the bed material during high flood period is 7m. Considering a minimum filter thickness 0.8m to be required above the collector pipe and radius of collector to be 0.5m. the depth of placement of the collector pipe above the impervious base is found to be 5.7m. Accordingly, $\frac{d_p}{D} = 0.143$ and $\frac{d_1}{D} = 0.8143$.

Calculation of yield of the collector pipe using conformal mapping for D_w=5m. Corresponding to $\frac{d_p}{D} = 0.143$ and $\frac{d_1}{D} = 0.8143$, from equation (3.57b) the dimensionless flow $\frac{Q}{kD_w} = 2.697636$. During high flood period a drawdown less than 6m can be maintained at the well caisson. Assuming that a drawdown of 5m is maintained, length of the collector pipe is 50m, and hydraulic conductivity k=0.35 m/day, the yield of the collector pipe is estimated as 236.0 m³/day.

Calculation of entrance velocity:

   The entrance velocity is calculated considering $f_a = 0.3$ and $D_w = 5\,m$. The dimensionless Darcy velocity at middle of the slit, $\frac{u_{d_1}D}{kD_w}$ is obtained from conformal mapping using equation (3.60f) is -5.8876. The negative sign indicates that the flow is in the opposite direction of abscissa that is the flow is entering to the collector pipe. The entrance velocity is found to be -4.906408 m/day =0.0057 cm/s which is <4.0cm/s. The average entrance velocity calculated using equation (3.26) is found to be 5.0089 m/day (=0.0058 cm/s<4cm/s).

(b) During lean flow period:

Calculation of yield of the collector pipe using conformal mapping for D_w =1m

The thickness of the bed material during lean flow period D=10.0m. Corresponding to $\frac{d_p}{D} = 0.1$ and $\frac{d_1}{D} = 0.57$, from equation (3.20b) the dimensionless flow $\frac{Q}{kD_w} = 1.696207$. Assuming

Calculation of entrance velocity:

The entrance velocity is calculated considering $f_a = 0.3$ and $D_w = 1\,m$. The dimensionless Darcy velocity at middle of the slit $\frac{u_{d_1}D}{kD_w}$ obtained from conformal mapping using equation (3.60f) is -5.392504. The negative sign indicates that the flow is in the opposite direction of abscissa that is the flow is entering to the collector pipe. The entrance velocity computed using conformal mapping is found to be -0.62912 m/day (=0.0007cm/s<4.0cm/s). The average entrance velocity calculated using equation (3.26) is found to be 0.6299 m/day (=0.00073 cm/sec<4cm/s).

Travel time and number of log cycles reduction:

The Darcy velocity along the streamline BC_1 from riverbed to a near point of the collector pipe, assumed as a line slit, is shown in Fig. (3.12) corresponding to $D_W = 5\,m$ and k=0.35 *m/day* during flood period. The velocity (true velocity) of the parcel of water will be Darcy velocity divided by effective porosity. The effective porosity of the river bed material is assumed to be 30%. During flood period the travel time of parcel of water from riverbed to collector pipe is found to be 0.139 days corresponding to D_W=5m and number of log cycle reduction is found to be less than one. The reduction in number of log cycles in bacterial concentration in the parcel of water has been calculated assuming the parameters r =0.2 day^{-1} as reproduction rate and λ_L =0.3 day^{-1} as the decay rate.

The Darcy velocity distribution during the lean flow period corresponding to D_w =1m shown in Fig. (3.13). Travel time of a parcel of water from riverbed to the collector pipe is found to be 17.26 day and the number of log cycle reduction is found to be one.
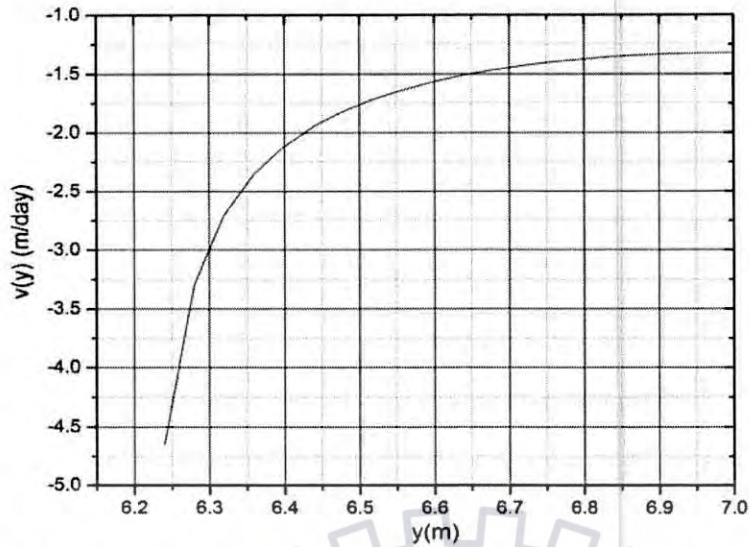
Fig. 3.13 Darcy Velocities along Streamline BC_1 during Flood Period,
D_w=5m, d_I=5.7m, and D=7.0m
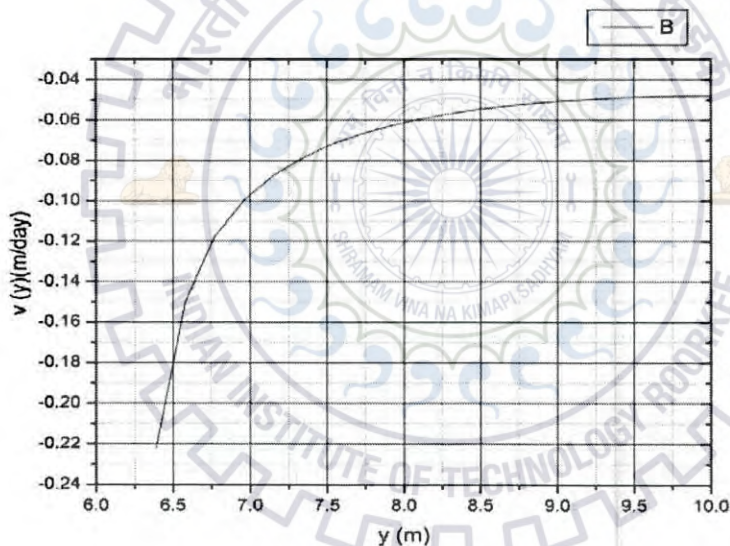
Fig. 3.14 Darcy Velocities along Stream Line BC_1 during Lean Flow Period
D_w=1m, d_I=5.7m, and D=10.0m

3.9   CONCLUSIONS

Based on the derivation of flow characteristics and dimensionless factors in riverbed filtration study, the following conclusions are drawn: Yield of a collector pipe is linearly proportional to (i) hydraulic conductivity of the river bed material, (ii) drawdown in the well caisson, (iii) length of the collector pipe, and nonlinearly dependent on (i) the diameter of the collector, (ii) thickness of the riverbed, (iii) height above the impervious base at which the collector pipe laid. A collector pipe of 25 m length and 0.5m diameter placed at a height of 5m

above the impervious base in a riverbed of 10m thick yields 40m³/day filtered water corresponding to 1m drawdown in well caisson, and 1.0 m/day hydraulic conductivity of riverbed material. For sandy silt soil riverbed material that has hydraulic conductivity of 0.1 m/day, the yield would be 4m³/day. Therefore, in such medium, several parallel collector pipes are to be laid and to be connected to a well caisson to provide good quality and quantity of water. If the soil medium below the river bed is comprised of soil with hydraulic conductivity 1m/day, a single pipe of 25m length can supply 160 m³ / day filtered water for a drawdown of 4m in well caisson.

The entrance velocity is linearly proportional to (i) hydraulic conductivity of the riverbed material, (ii) drawdown in the well caisson, and nonlinearly dependent on (i) the diameter of the collector, (ii) thickness of the riverbed, (iii) height above the impervious base at which the collector pipe laid, and inversely proportional to the fraction of peripheral area perforated. For both aquifer materials with high and low hydraulic conductivity, the maximum entrance velocity is much within safe limit.

The minimum travel time is directly proportional to porosity of the bed material, square of the riverbed thickness and inversely proportional to hydraulic conductivity of the porous medium in the riverbed and drawdown in the well caisson. Therefore, achieving respectable quantity of filtered water with improved quality simultaneously is a conflicting issue as quality and quantity depend mainly on the aquifer material, and allowable drawdown in the well caisson.

Aravin and Numerov have idealized the collector pipe as a line sink. In this chapter, the collector pipe has been idealized as a line slit with constant head boundary. Comparing the results for the dimensionless flow to collector pipe in both the cases, it is found that the Arvin and Numerov (1965) solution overestimates the flow to collector pipe. The entrance velocities computed by both the methods are found to be nearly equal. The scour depth is the main consideration while deciding the placement of the collector pipe. As indicated by an example, the entrance velocity is much less than the allowable entrance velocity. The utility of the study has been shown through an example. The bacteria concentration in the river water gets reduced by about 1.22 log cycle calculated through equation (B.7) during lean flow period. Thus the position of the collector pipe (4.3 m from the riverbed) is not sufficient to reduce the bacterial concentration.

It is aimed to determine (*i*) flow to the square collector pipe (*ii*) average entrance velocity and (*iii*) the minimum travel time of a parcel of water from the riverbed to the collector pipe. Equivalent square section is shown in Fig.4.1. Taking the advantage of symmetry, half of the flow domain is considered to apply the conformal mapping technique to find the flow characteristics.
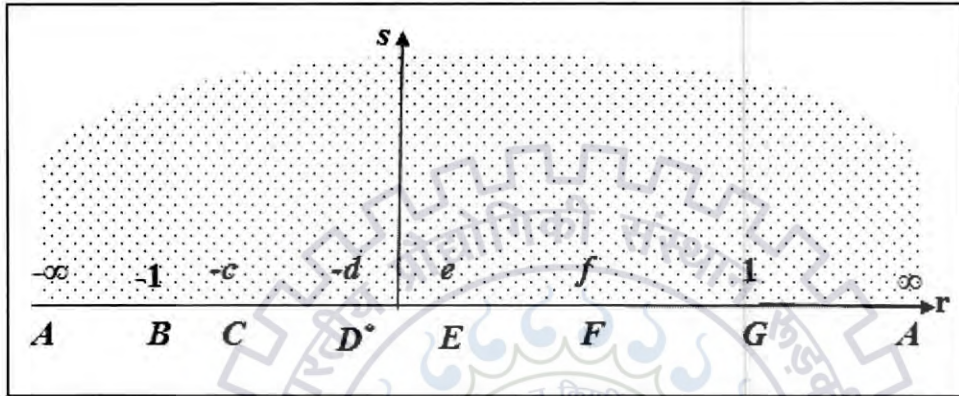
Fig. 4.2 Upper Half of Auxiliary $t(=r+is)$ **Plane**

4.3   MAPPING OF THE *z*-PLANE ONTO THE UPPER HALF OF AUXILIARY *t*-PLANE

The vertices A, B, C, D^*, E, F, G, and A being mapped onto $-\infty$, -1, -*c*, -*d*, *e*, *f*, 1, and ∞ respectively in the *t*-plane, the conformal mapping of the physical flow domain in *z*-plane onto the upper half of the auxiliary t-plane is given by (Harr 1965):

$$\frac{dz}{dt} = M \frac{(t+d)^{\frac{1}{2}}(t-e)^{\frac{1}{2}}}{(t+1)^{\frac{1}{2}}(t+c)^{\frac{1}{2}}(t-f)^{\frac{1}{2}}(t-1)^{\frac{1}{2}}} \tag{4.1}$$

Integrating equation (4.1)

$$z = M \int \frac{(t+d)^{\frac{1}{2}}(t-e)^{\frac{1}{2}}}{(t+1)^{\frac{1}{2}}(t+c)^{\frac{1}{2}}(t-f)^{\frac{1}{2}}(t-1)^{\frac{1}{2}}} dt + N \tag{4.2}$$

where, M and N are complex constants to be determined. The constants and all the mapping parameters, *c, d, e,* and *f* are determined from the geometry of the flow domain.

Estimation of constant M:

Substituting, $t = Re^{i\theta}$; $dt = Re^{i\theta}id\theta$ and applying the condition that when, one transverses in t-plane along a semi-circle of radius R, $R \to \infty$ from $\theta = 0$ to $\theta = \pi$, the jump in z-plane is iD, the constant M is found as follows:

$$iD = M\int_0^\pi \frac{\left(Re^{i\theta} + d\right)^{1/2}\left(Re^{i\theta} - e\right)^{1/2}}{\left(Re^{i\theta} + 1\right)^{1/2}\left(Re^{i\theta} + c\right)^{1/2}\left(Re^{i\theta} - f\right)^{1/2}\left(Re^{i\theta} - 1\right)^{1/2}}Re^{i\theta}id\theta\Bigg|_{R\to\infty} = M\int_0^\pi id\theta = Mi\pi$$

Hence,

$$M = \frac{D}{\pi} \tag{4.3}$$

Estimation of mapping parameters

Integration between vertices B and C $(-1 \le t \le -c)$:

At vertex $B, t = -1$, and $z = iD$; and at vertex C, $t = -c$, and $z = i(d_1 + 0.5d_s)$. Applying these conditions in equation (4.2), we obtain

$$i(d_1 + 0.5d_s) = \frac{D}{\pi}\int_{-1}^{-C} \frac{(-1)^{1/2}(-1)^{1/2}(-1)^{1/2}(-t-d)^{1/2}(-t+e)^{1/2}}{(-1)^{1/2}(-1)^{1/2}(t+1)^{1/2}(-t-c)^{1/2}(-t+f)^{1/2}(-t+1)^{1/2}}dt + iD \tag{4.4}$$

$\sqrt{-1} = \pm i$. In the interval $(-1 \le t \le -c)$, $\frac{dz}{dt} = -idy$. In order to satisfy this, we select $\sqrt{-1} = -i$.

Hence,

$$i(d_1 + 0.5d_s) = \frac{-Di}{\pi}\int_{-1}^{-C} \frac{(-t-d)^{1/2}(-t+e)^{1/2}}{(t+1)^{1/2}(-t-c)^{1/2}(-t+f)^{1/2}(-t+1)^{1/2}}dt + iD \tag{4.5}$$

or

$$0 = -i\frac{D}{\pi}\int_{-1}^{-c} \frac{(-d-t)^{1/2}(e-t)^{1/2}}{(t+1)^{1/2}(-c-t)^{1/2}(f-t)^{1/2}(1-t)^{1/2}}dt + i(D - d_1 - 0.5d_s) \tag{4.6}$$

or

$$\pi\left(1 - \frac{d_1}{D} - 0.5\frac{d_s}{D}\right) = \int_{-1}^{-c} \frac{(-d-t)^{1/2}(e-t)^{1/2}}{(t+1)^{1/2}(-c-t)^{1/2}(f-t)^{1/2}(1-t)^{1/2}}dt = I_1 \tag{4.7}$$

Hence,

$$F_1(c,d,e,f) = 1 - \frac{d_1}{D} - 0.5\frac{d_s}{D} - \frac{I_1}{\pi} \tag{4.8}$$

61

If all parameters are chosen correctly, then, $F_1(c,d,e,f) = 0$, otherwise not.

Integration between vertices C and D*: $(-c \leq t \leq -d)$

At point $C, t = -c$, and $z = i(d_1 + 0.5d_s)$; and at point $D^*, t = -d$, and $z = 0.5d_s + i(d_1 + 0.5d_s)$

Applying these conditions

$$0.5d_s + i(d_1 + 0.5d_s) = \frac{D}{\pi} \int_{-c}^{-d} \frac{(-1)^{1/2}(-1)^{1/2}(-d-t)^{1/2}(e-t)^{1/2}}{(-1)^{1/2}(-1)^{1/2}(t+1)^{1/2}(t+c)^{1/2}(f-t)^{1/2}(1-t)^{1/2}} dt + i(d_1 + 0.5d_s) \quad (4.9)$$

or

$$0.5d_s = \frac{D}{\pi} \int_{-c}^{-d} \frac{(-d-t)^{1/2}(e-t)^{1/2}}{(t+1)^{1/2}(t+c)^{1/2}(f-t)^{1/2}(1-t)^{1/2}} dt \quad (4.10)$$

or

$$0.5\pi \frac{d_s}{D} = \int_{-c}^{-d} \frac{(-d-t)^{1/2}(e-t)^{1/2}}{(t+1)^{1/2}(t+c)^{1/2}(f-t)^{1/2}(1-t)^{1/2}} dt = I_2 \quad (4.11)$$

Integration between vertices D* and E: $(-d \leq t \leq e)$

At point $D^*, t = -d$, and $z = 0.5d_s + i(d_1 + 0.5d_s)$; and at point $E, t = e$, and $z = 0.5d_s + i(d_1 - 0.5d_s)$

Applying these conditions

$$0.5d_s + i(d_1 - 0.5d_s) = M \int_{-d}^{e} \frac{(-1)^{1/2}(-1)^{1/2}(t+d)^{1/2}(e-t)^{1/2}}{(-1)^{1/2}(t+1)^{1/2}(t+c)^{1/2}(f-t)^{1/2}(1-t)^{1/2}} dt + 0.5d_s + i(d_1 + 0.5d_s) \quad (4.12)$$

In the interval $(-d \leq t \leq e)$, $\frac{dz}{dt} = -idy$. This is satisfied when one select $\sqrt{-1} = -i$. Incorporating this and simplifying

$$\pi \frac{d_s}{D} = \int_{-d}^{e} \frac{(t+d)^{1/2}(e-t)^{1/2}}{(t+1)^{1/2}(t+c)^{1/2}(f-t)^{1/2}(1-t)^{1/2}} dt = I_3 \quad (4.13)$$

Making use of equation (4.11) and (4.13), one can write the function

$$F_2(c,d,e,f) = \frac{I_2}{\pi} - 0.5\frac{I_3}{\pi} \quad (4.14)$$

62

Integration between vertices E and F: $\left(e \le t \le f\right)$

At vertex $E, t = e$, and $z = 0.5d_s + i\left(d_1 - 0.5d_s\right)$; and at vertex $F, t = f$, and $z = i\left(d_1 - 0.5d_s\right)$

Applying these conditions

$$i\left(d_1 - 0.5d_s\right) = \frac{D}{\pi} \int_e^f \frac{(-1)^{1/2}(-1)^{1/2}(t+d)^{1/2}(t-e)^{1/2}}{(t+1)^{1/2}(t+c)^{1/2}(f-t)^{1/2}(1-t)^{1/2}} dt + 0.5\,d_s + i\left(d_1 - 0.5d_s\right) \quad (4.15)$$

Simplifying

$$0.5\,d_s = \frac{D}{\pi} \int_e^f \frac{(t+d)^{1/2}(t-e)^{1/2}}{(t+1)^{1/2}(t+c)^{1/2}(f-t)^{1/2}(1-t)^{1/2}} dt \quad (4.16)$$

or

$$\frac{\pi d_s}{2D} = \int_e^f \frac{(t+d)^{1/2}(t-e)^{1/2}}{(t+1)^{1/2}(t+c)^{1/2}(f-t)^{1/2}(1-t)^{1/2}} dt = I_4 \quad (4.17)$$

Making use of equation (4.11) and equation (4.17), one can write the function

$$F_3\left(c,d,e,f\right) = \frac{I_2}{\pi} - \frac{I_4}{\pi} \quad (4.18)$$

Integration between vertices F and G: $\left(f \le t \le 1\right)$

At point $F, t = f$, and $z = i\left(d_1 - 0.5d_s\right)$; and at point $G, t = 1$, and $z = 0$. Applying these conditions

$$0 = \frac{D}{\pi} \int_f^1 \frac{(-1)^{1/2}(t+d)^{1/2}(t-e)^{1/2}}{(t+1)^{1/2}(t+c)^{1/2}(t-f)^{1/2}(1-t)^{1/2}} dt + i\left(d_1 - 0.5d_s\right) \quad (4.19)$$

Considering $\sqrt{-1} = i$, to satisfy within interval $f \le t \le 1$, $\frac{dz}{dt} = -idy$, one obtains after simplification

$$\frac{\pi}{D}\left(d_1 - 0.5d_s\right) = \int_f^1 \frac{(t+d)^{1/2}(t-e)^{1/2}}{(t+1)^{1/2}(t+c)^{1/2}(t-f)^{1/2}(1-t)^{1/2}} dt = I_5 \quad (4.20)$$

One can formulate the function $F_4\left(c,d,e,f\right)$ as

$$F_4\left(c,d,e,f\right) = \frac{\left(d_1 - 0.5d_s\right)}{D} - \frac{I_5}{\pi} \quad (4.21)$$

If all parameters are chosen correctly, then, $F_4\left(c,d,e,f\right) = 0$, otherwise not.

The parameters c, d, e and f are to be found for known values of $\frac{d_1}{D}$, and $\frac{d_s}{D}$, from the four

non-linear equations 4.8, 4.14, 4.18, and 4.21 .

63

The mapping steps result in a set of non-linear equations, which require a suitable technique to compute the unknown parameters. The implicit nature of the non-linear equations restricts the range of its applicability. So such non-linear equations are solved by iterative method given by Newton Rapshon. Newton Rapshon technique has been used to find the solution. Using corresponding Jacobian matrix these nonlinear equations containing the four unknowns' c, d, e and f are expressed as:

$$
\begin{bmatrix}
\dfrac{\partial F_1}{\partial c} & \dfrac{\partial F_1}{\partial d} & \dfrac{\partial F_1}{\partial e} & \dfrac{\partial F_1}{\partial f} \\[2mm]
\dfrac{\partial F_2}{\partial c} & \dfrac{\partial F_2}{\partial d} & \dfrac{\partial F_2}{\partial e} & \dfrac{\partial F_2}{\partial f} \\[2mm]
\dfrac{\partial F_3}{\partial c} & \dfrac{\partial F_3}{\partial d} & \dfrac{\partial F_3}{\partial e} & \dfrac{\partial F_3}{\partial f} \\[2mm]
\dfrac{\partial F_4}{\partial c} & \dfrac{\partial F_4}{\partial d} & \dfrac{\partial F_4}{\partial e} & \dfrac{\partial F_4}{\partial f}
\end{bmatrix}
\begin{bmatrix} \nabla c \\ \nabla d \\ \nabla e \\ \nabla f \end{bmatrix}
= -
\begin{bmatrix}
F_1\!\left(c^*, d^*\ e^*\ f^*\right) \\
F_2\!\left(c^*, d^*\ e^*\ f^*\right) \\
F_3\!\left(c^*, d^*\ e^*\ f^*\right) \\
F_4\!\left(c^*, d^*\ e^*\ f^*\right)
\end{bmatrix}
\tag{4.22}
$$

In which c^*, d^*, e^* and f^* are initial guess of the parameters. Following matrix inversion method

$$
\begin{bmatrix} \nabla c \\ \nabla d \\ \nabla e \\ \nabla f \end{bmatrix}
= -
\begin{bmatrix}
\dfrac{\partial F_1}{\partial c} & \dfrac{\partial F_1}{\partial d} & \dfrac{\partial F_1}{\partial e} & \dfrac{\partial F_1}{\partial f} \\[2mm]
\dfrac{\partial F_2}{\partial c} & \dfrac{\partial F_2}{\partial d} & \dfrac{\partial F_2}{\partial e} & \dfrac{\partial F_2}{\partial f} \\[2mm]
\dfrac{\partial F_3}{\partial c} & \dfrac{\partial F_3}{\partial d} & \dfrac{\partial F_3}{\partial e} & \dfrac{\partial F_3}{\partial f} \\[2mm]
\dfrac{\partial F_4}{\partial c} & \dfrac{\partial F_4}{\partial d} & \dfrac{\partial F_4}{\partial e} & \dfrac{\partial F_4}{\partial f}
\end{bmatrix}^{-1}
\begin{bmatrix}
F_1\!\left(c^*, d^*\ e^*\ f^*\right) \\
F_2\!\left(c^*, d^*\ e^*\ f^*\right) \\
F_3\!\left(c^*, d^*\ e^*\ f^*\right) \\
F_4\!\left(c^*, d^*\ e^*\ f^*\right)
\end{bmatrix}
\tag{4.23}
$$

The improved values of c, d, e, f are: $c = c^* + \nabla c, d = d^* + \nabla d, e = e^* + \nabla e, f = f^* + \nabla f$. The process is repeated till the desired accuracy is achieved. The success of iteration depends on the initial guess of the parameters $c^*,\ d^*,\ e^*,\ f^*$.

4.4 Complex potential $w\,(= \phi + i\psi)$

The velocity potential function ϕ is defined as:

$$\phi = -k\left(p/\gamma_w + y\right) + C^* \tag{4.24}$$

where, k is the saturated hydraulic conductivity of the sediments deposit; p = water pressure; γ_w = unit weight of water; y = elevation head; C^* = a constant conveniently chosen for square

section as $C^* = k(h_w + d_1)$, where h_w is piezometric head above the collector pipe and d_1 is the depth above the lower impervious layer to center of a collector pipe. The complex potential plane is shown in Fig. 4.3. The vertices A, B, C, F having been mapped onto $-\infty$, -1, $-c$, f and ∞ respectively in the t-plane, the conformal mapping of the complex potential plane onto the upper half auxiliary t-plane is given by Harr (1962):
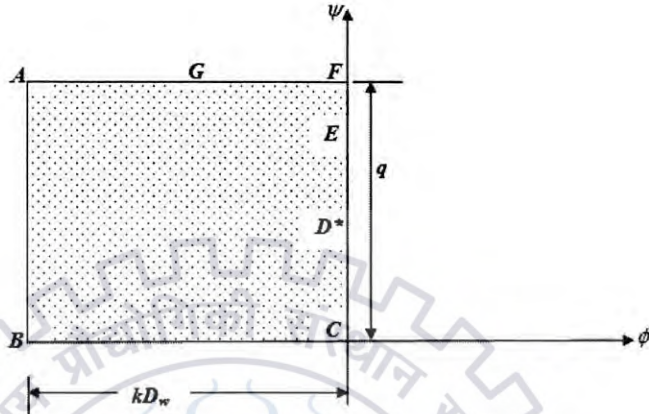
Fig. 4.3 Complex Potential w-Plane

4.5 MAPPING OF THE w-PLANE ONTO THE UPPER HALF AUXILIARY t-PLANE

$$\frac{dw}{dt} = \frac{M_1}{\sqrt{(-1-t)(-c-t)(f-t)}} \tag{4.25}$$

Integrating equation (4.25)

$$\frac{dw}{dt} = M_1 \int \frac{1}{\sqrt{(-1-t)(-c-t)(f-t)}} dt + N_1 \tag{4.26}$$

Where, M_1 and N_1 are complex constants which are to be determined. The constant N_1 is governed by the lower limit of integration. Hence,

$$w = M_1 \int_{-\infty}^{t'} \frac{1}{\sqrt{(-1-t)(-c-t)(f-t)}} dt - kD_w + iq \tag{4.27}$$

For $t' = -1$, $w = -kD_W$, hence,

$$-kD_w = M_1 \int_{-\infty}^{-1} \frac{1}{\sqrt{(-1-t)(-c-t)(f-t)}} dt - kD_w + iq \tag{4.28}$$

Performing the integration (Byrd and Fried man, 1954) and simplifying

$$-iq = M_1 \frac{2}{\sqrt{(1+f)}} F\left(\frac{\pi}{2}, \sqrt{\frac{(f+c)}{(1+f)}}\right) \tag{4.29}$$

65

At vertex B, $w = -kD_w$, and at vertex C, $w = 0$. Integrating between vertices B and C, considering $\sqrt{-1} = -i$ and simplifying

$$kD_w(-i) = M_1 \frac{2}{\sqrt{(1+f)}} F\left(\frac{\pi}{2}, \sqrt{\frac{(1-c)}{(1+f)}}\right) \tag{4.30}$$

Dividing equation (4.29) by equation (4.30)

$$\frac{q}{kD_w} = \frac{F\left(\dfrac{\pi}{2}, \sqrt{\dfrac{(f+c)}{(1+f)}}\right)}{F\left(\dfrac{\pi}{2}, \sqrt{\dfrac{(1-c)}{(1+f)}}\right)} \tag{4.31}$$

In which, $F\left(\dfrac{\pi}{2}, \sqrt{\dfrac{(f+c)}{(1+f)}}\right)$ and $F\left(\dfrac{\pi}{2}, \sqrt{\dfrac{(1-c)}{(1+f)}}\right)$ are complete elliptical integrals of the first kind

with moduli $\sqrt{\dfrac{(f+c)}{(1+f)}}$ and $\sqrt{\dfrac{(1-c)}{(1+f)}}$ respectively.

The total flow to a collector pipe that intercepts from an aquifer of unit thickness is 2q. The dimensionless flow to the collector pipe per unit length is expressed as:

$$\frac{Q}{kD_w} = \frac{2q}{kD_w} = 2\frac{F\left(\dfrac{\pi}{2}, \sqrt{\dfrac{(f+c)}{(1+f)}}\right)}{F\left(\dfrac{\pi}{2}, \sqrt{\dfrac{(1-c)}{(1+f)}}\right)} \tag{4.32}$$

Entrance velocity

Depending upon the type of soil an aquifer medium is comprised of, the entrance velocity to a collector pipe laid in the aquifer is to be maintained in order to restrict the movement of fine sediments to the collector pipe. The entrance velocity to a collector pipe is linearly proportional to the drawdown D_w in the well caisson, and hydraulic conductivity of the aquifer medium and inversely proportional to the open area fraction in the collector pipe. While designing a collector well, the magnitude of the entrance velocity is examined.

Average entrance velocity

An average entrance velocity is determined with ease using the expression for flow to the collector pipe. Magnitude of average Darcy velocity at the periphery of the collector pipe is equal to $2q/(4d_s)$. The average entrance velocity is given by:

66

$$\bar{v}_e = 2q / (4d_s f_a) = \frac{2kD_w}{4d_s f_a} \frac{F\left(\frac{\pi}{2}, \sqrt{\frac{(f+c)}{(1+f)}}\right)}{F\left(\frac{\pi}{2}, \sqrt{\frac{(1-c)}{(1+f)}}\right)} = Q / (4d_s f a) = Q / (\pi d_p f_a) \qquad (4.33)$$

The dimensionless average entrance velocity factor $\bar{v}_{ef.}$ can be written as:

$$\bar{v}_{ef} = \frac{\bar{v}_e d_s f_a}{kD_w} = 0.5 \frac{F\left(\frac{\pi}{2}, \sqrt{\frac{(f+c)}{(1+f)}}\right)}{F\left(\frac{\pi}{2}, \sqrt{\frac{(1-c)}{(1+f)}}\right)} \qquad (4.34)$$

The entrance velocity at point C:

For $-1 \le t \le -c$

$$\frac{dw}{dt} = (-i)kD_w \frac{\sqrt{(1+f)}}{2F\left(\frac{\pi}{2}, \sqrt{\frac{(1-c)}{(1+f)}}\right)\sqrt{(-1-t)(-c-t)(f-t)}} = kD_w \frac{\sqrt{(1+f)}}{2F\left(\frac{\pi}{2}, \sqrt{\frac{(1-c)}{(1+f)}}\right)\sqrt{(1+t)(-c-t)(f-t)}} \qquad (4.35)$$

$$\frac{dw}{dz} = \frac{dw}{dt}\frac{dt}{dz} \qquad (4.36)$$

$$= kD_w \frac{\sqrt{(1+f)}}{2F\left(\frac{\pi}{2}, \sqrt{\frac{(1-c)}{(1+f)}}\right)\sqrt{(1+t)(-c-t)(f-t)}} \frac{\pi}{D(-i)} \frac{(1+t)^{1/2}(-t-c)^{1/2}(-t+f)^{1/2}(-t+1)^{1/2}}{(-t-d)^{1/2}(-t+e)^{1/2}} \qquad (4.37)$$

$$= i k \pi \frac{D_w}{2D} \frac{\sqrt{(1+f)}}{F\left(\frac{\pi}{2}, \sqrt{\frac{(1-c)}{(1+f)}}\right)} \frac{(-t+1)^{1/2}}{(-t-d)^{1/2}(-t+e)^{1/2}} = u - iv \qquad (4.38)$$

Equating the imaginary parts

$$v(z) = -k \frac{D_w}{D} \frac{\pi\sqrt{f+1}}{2F\left(\frac{\pi}{2}, \sqrt{\frac{(1-c)}{(1+f)}}\right)} \sqrt{\frac{(1-t)}{(-d-t)(e-t)}} \qquad (4.39)$$

The real part is zero as u along y-axis is equal to zero. At point C, $t = -c$. Substituting the value of c in equation (4.39), the entrance velocity at $y = d_1 + 0.d_s$ is

$$v_C = -\frac{k D_w}{D} \frac{\pi\sqrt{f+1}}{2F\left(\frac{\pi}{2}, \sqrt{\frac{(f+c)}{(1+f)}}\right)} \sqrt{\frac{1+c}{(c-d)(e+c)}} \qquad (4.40)$$

Substituting $t = -1$ in equation (4.39), velocity at point B is obtained as

$$v_B = -k \frac{D_w}{D} \frac{\pi\sqrt{f+1}}{2F\left(\frac{\pi}{2}, \sqrt{\frac{(1-c)}{(1+f)}}\right)} \sqrt{\frac{2}{(1-d)(1+e)}} \qquad (4.41)$$

The negative sign appears as the direction of velocity is in the negative direction of y-axis.

67

The travel time of a parcel of water along streamline BC:

Computation of the minimum travel time of a parcel of water from the riverbed to the collector pipe is of use to predict the log cycle reduction in bacteria concentration while a parcel of water moves from a river to a collector pipe.

Darcy velocities have been computed at several points between vertices B and C, at least at 10 intermediate points and find an average arithmetic mean Darcy velocity $\bar{v}$ and compute an approximate travel time dividing $(D - d_1 - 0.5 d_s)$ by $\bar{v}/\eta$. Alternately one can compute the values of dz, and average velocity along each dz. The travel time for each dz is obtained dividing dz by the corresponding average true velocity. The total travel time is obtained by adding the travel time between two successive points.

Thus, the travel time t_r of a parcel of water to move from riverbed to collector along stream line BC is given by:

$$t_r = \frac{D - d_1 - 0.5 d_s}{\bar{v}/\eta} \tag{4.42}$$

where, η is volumetric porosity of the aquifer medium. For given d_1/D, d_s/D, one can define a dimensionless travel time factor t_{rf} as:

$$t_{rf} = \frac{t_r k D_w}{\eta D^2} \tag{4.43}$$

Knowing the travel time of a parcel of river water to the collector pipe, the log cycle reduction n in bacteria concentration in the parcel of water is computed using logistic function.

$$n = \log_{10} \frac{r/\lambda_L - e^{-(r-\lambda_L)t_r}}{(r/\lambda_L) - 1} \tag{4.44}$$

4.6   RESULTS AND DISCUSSIONS

Evaluation of the Integrals

The integrals I_1, I_2, I_3, I_4 appearing in equations (4.8), (4.14), (4.18), and (4.21) are improper integrals. Method of substitution and then Gaussian-quadrature have been used to evaluate the integrals. One can describe evaluation of the improper integrals below.

$$I_1 = \int_{-1}^{-c} \frac{(-d-t)^{1/2}(e-t)^{1/2}}{(t+1)^{1/2}(-c-t)^{1/2}(f-t)^{1/2}(1-t)^{1/2}} dt \tag{4.45}$$

$$= \int_{-1}^{-(1+c)/2} \frac{(-d-t)^{1/2}(e-t)^{1/2}}{(t+1)^{1/2}(-c-t)^{1/2}(f-t)^{1/2}(1-t)^{1/2}} dt + \int_{-(1+c)/2}^{-c} \frac{(-d-t)^{1/2}(e-t)^{1/2}}{(t+1)^{1/2}(-c-t)^{1/2}(f-t)^{1/2}(1-t)^{1/2}} dt = I_{11} + I_{12} \tag{4.46}$$

68

The integral I_{11} is improper because at the lower limit its integrand is infinite. For evaluation of the improper integral I_{11}, singularity can be removed by substituting, $t+1 = v^2; dt = 2vdv$ where v is a dummy variable. After substitution and simplification I_{11} reduces to:

$$I_{11} = \int_0^{\sqrt{(1-c)/2}} 2 \frac{\left(1-d-v^2\right)^{1/2}\left(1+e-v^2\right)^{1/2}}{\left(1-c-v^2\right)^{1/2}\left(1+f-v^2\right)^{1/2}\left(2-v^2\right)^{1/2}} dv \tag{4.47}$$

Further making a substitution $v = 0.5\sqrt{(1-c)/2}\,(1+X), dv = 0.5\sqrt{(1-c)/2}\,dX$, I_{11} reduces to

$$I_{11} = \int_{-1}^{1} \sqrt{(1-c)/2}\left[\frac{\left(1-d-v^2\right)^{1/2}\left(1+e-v^2\right)^{1/2}}{\left(1-c-v^2\right)^{1/2}\left(1+f-v^2\right)^{1/2}\left(2-v^2\right)^{1/2}}\right] dX; v = 0.5\sqrt{(1-c)/2}\,(1+X) \tag{4.48}$$

Gauss quadrature is applied to evaluate the integral I_{11}.

The integral I_{12} is improper, because at the upper limit, its integrand is infinite. For evaluation of the improper integral I_{12}, singularity can be removed by substituting $-c-t = v^2; dt = -2vdv$. After substitution and simplification I_{12} reduces to

$$I_{12} = \int_{-(1+c)/2}^{-c} \frac{\left(-d-t\right)^{1/2}\left(e-t\right)^{1/2}}{\left(t+1\right)^{1/2}\left(-c-t\right)^{1/2}\left(f-t\right)^{1/2}\left(1-t\right)^{1/2}} dt \tag{4.49}$$

$$= \int_0^{\sqrt{(1-c)/2}} 2\frac{\left(-d+c+v^2\right)^{1/2}\left(e+c+v^2\right)^{1/2}}{\left(1-c-v^2\right)^{1/2}\left(f+c+v^2\right)^{1/2}\left(1+c+v^2\right)^{1/2}} dv \tag{4.50}$$

Further making a substitution $v = 0.5\sqrt{(1-c)/2}\,(1+X); dv = 0.5\sqrt{(1-c)/2}\,dX$, I_{12} reduces to

$$I_{12} = \int_{-1}^{1} \sqrt{(1-c)/2}\left[\frac{\left(-d+c+v^2\right)^{1/2}\left(e+c+v^2\right)^{1/2}}{\left(1-c-v^2\right)^{1/2}\left(f+c+v^2\right)^{1/2}\left(1+c+v^2\right)^{1/2}}\right] dX; v = 0.5\sqrt{(1-c)/2}\,(1+X).$$

Gauss quadrature is applied to evaluate the integral I_{12}. The integral I_2 is improper because of its integrand is infinite at the lower limit. The integral is evaluated after removing its singularity by substituting $(t+c) = v^2$, $dt = 2vdv$. Thus

$$I_2 = \int_{-c}^{-d} \frac{\left(-d-t\right)^{1/2}\left(e-t\right)^{1/2}}{\left(t+1\right)^{1/2}\left(t+c\right)^{1/2}\left(f-t\right)^{1/2}\left(1-t\right)^{1/2}} dt = \int_0^{(c-d)^{1/2}} \frac{2\left(c-d-v^2\right)^{1/2}\left(c+e-v^2\right)^{1/2}}{\left(1-c+v^2\right)^{1/2}\left(f+c-v^2\right)^{1/2}\left(1+c-v^2\right)^{1/2}} dv \tag{4.51}$$

$$= \int_{-1}^{1} \frac{\left(c-d\right)^{1/2}\left(c-d-v^2\right)^{1/2}\left(c+e-v^2\right)^{1/2}}{\left(1-c+v^2\right)^{1/2}\left(f+c-v^2\right)^{1/2}\left(1+c-v^2\right)^{1/2}} dX; \quad v = 0.5(c-d)^{1/2}(1+X) \tag{4.52}$$

The integral I_3 is a proper integral. To apply Gauss quadrature, the lower and upper limits of the integral I_3 are changed to -1 and 1 by substituting $t = 0.5(e-d) + 0.5(e+d)X$; $dt = 0.5(e+d)dX$. Therefore,

$$I_3 = \int_{-d}^{e} \frac{(t+d)^{\frac{1}{2}} (e-t)^{\frac{1}{2}}}{(t+1)^{\frac{1}{2}} (t+c)^{\frac{1}{2}} (f-t)^{\frac{1}{2}} (1-t)^{\frac{1}{2}}} dt \tag{4.53}$$

$$= \int_{-1}^{1} 0.5(d+e) \frac{(t+d)^{\frac{1}{2}} (e-t)^{\frac{1}{2}}}{(t+1)^{\frac{1}{2}} (t+c)^{\frac{1}{2}} (f-t)^{\frac{1}{2}} (1-t)^{\frac{1}{2}}} dX; \quad t = 0.5(e-d) + 0.5(e+d)X \tag{4.54}$$

The integral I_4 is an improper integral as its integrand is infinite at its upper limit. Substituting $f - t = v^2$; $dt = -2v\,dv$ one can remove the singularity. Thus

$$I_4 = \int_{e}^{f} \frac{(t+d)^{\frac{1}{2}}(t-e)^{\frac{1}{2}}}{(t+1)^{\frac{1}{2}}(t+c)^{\frac{1}{2}} (f-t)^{\frac{1}{2}}(1-t)^{\frac{1}{2}}} dt = \int_{0}^{(f-e)^{1/2}} \frac{2(d+f-v^2)^{\frac{1}{2}}(f-e-v^2)^{\frac{1}{2}}}{(1+f-v^2)^{\frac{1}{2}}(c+f-v^2)^{\frac{1}{2}} (1-f+v^2)^{\frac{1}{2}}} dv \tag{4.55}$$

Further making a substitution $v = 0.5 (f-e)^{1/2} (1+X)$; $dv = 0.5 (f-e)^{1/2} dX$, I_4 reduces to

$$I_4 = \int_{-1}^{1} \frac{(f-e)^{1/2} (d+f-v^2)^{\frac{1}{2}} (f-e-v^2)^{\frac{1}{2}}}{(1+f-v^2)^{\frac{1}{2}} (c+f-v^2)^{\frac{1}{2}} (1-f+v^2)^{\frac{1}{2}}} dX; \quad v = 0.5 (f-e)^{1/2} (1+X) \tag{4.56}$$

The integral I_5 is an improper integral as its integrand is infinite at its lower as well as upper limit. Method of substitution has been adopted to remove the singularities. Dividing the range $f \le t \le 1$ into two parts

$$I_5 = \int_{f}^{1} \frac{(t+d)^{\frac{1}{2}} (t-e)^{\frac{1}{2}}}{(t+1)^{\frac{1}{2}} (t+c)^{\frac{1}{2}} (t-f)^{\frac{1}{2}} (1-t)^{\frac{1}{2}}} dt \tag{4.57}$$

$$= \int_{f}^{(1+f)/2} \frac{(t+d)^{\frac{1}{2}}(t-e)^{\frac{1}{2}}}{(t+1)^{\frac{1}{2}}(t+c)^{\frac{1}{2}}(t-f)^{\frac{1}{2}}(1-t)^{\frac{1}{2}}} dt + \int_{(1+f)/2}^{1} \frac{(t+d)^{\frac{1}{2}}(t-e)^{\frac{1}{2}}}{(t+1)^{\frac{1}{2}}(t+c)^{\frac{1}{2}}(t-f)^{\frac{1}{2}}(1-t)^{\frac{1}{2}}} dt \tag{4.58}$$

$$= I_{51} + I_{52} \tag{4.59}$$

The singularity in I_{51} is removed substituting $(t-f) = v^2$; $dt = 2v\,dv$. Accordingly I_{51} reduces to

$$I_{51} = \int_{0}^{\sqrt{(1-f)/2}} \frac{2(f+d+v^2)^{\frac{1}{2}}(f-e+v^2)^{\frac{1}{2}}}{(1+f+v^2)^{\frac{1}{2}}(f+c+v^2)^{\frac{1}{2}} (1-f-v^2)^{\frac{1}{2}}} dv \tag{4.60}$$

Further making a substitution $v = 0.5 \sqrt{(1-f)/2} (1+X)$, $dv = 0.5 \sqrt{(1-f)/2} \, dX$, I_{51} reduces to

$$I_{51} = \int_{-1}^{1} \sqrt{0.5(1-f)} \frac{(f+d+v^2)^{\frac{1}{2}}(f-e+v^2)^{\frac{1}{2}}}{(1+f+v^2)^{\frac{1}{2}}(f+c+v^2)^{\frac{1}{2}}(1-f-v^2)^{\frac{1}{2}}} dX ; v = 0.5\sqrt{0.5(1-f)}(1+X) \quad (4.61)$$

The singularity in I_{52} is removed substituting $(1-t)=v^2$; $dt = -2vdv$. Accordingly I_{52} reduces to

$$I_{52} = \int_{0}^{\sqrt{0.5(1-f)}} 2\frac{(1+d-v^2)^{\frac{1}{2}}(1-e-v^2)^{\frac{1}{2}}}{(2-v^2)^{\frac{1}{2}}(1+c-v^2)^{\frac{1}{2}}(1-f-v^2)^{\frac{1}{2}}} dv \quad (4.62)$$

Further making a substitution $v = 0.5\sqrt{(1-f)/2}(1+X), dv = 0.5\sqrt{(1-f)/2}\, dX$, I_{52} reduces to

$$I_{52} = \int_{-1}^{1} \sqrt{0.5(1-f)} \frac{(1+d-v^2)^{\frac{1}{2}}(1-e-v^2)^{\frac{1}{2}}}{(2-v^2)^{\frac{1}{2}}(1+c-v^2)^{\frac{1}{2}}(1-f-v^2)^{\frac{1}{2}}} dX ; v = 0.5\sqrt{0.5(1-f)}(1+X) \quad (4.63)$$

4.7 THE DIMENSIONLESS FLOW CHARACTERISTICS

Dimensionless flow to the collector pipe per unit length of the collector pipe $Q/(kD_w)$, dimensionless average entrance velocity factor $\bar{v}_{ef}\left(=\dfrac{\bar{v}_e d_p f_a}{kD_w}\right)$, and the dimensionless travel time factor $t_{rf} = \dfrac{t_r k D_w}{\eta D^2}$ have been presented in tables 4.1 (b), 4.2 (b), and 4.3(b). Besides this, average entrance velocity, $\bar{v}_e$, travel time of a parcel of water from the river bed to the collector pipe along the shortest path and the corresponding log cycle reduction in log cycle concentration of the bacteria has been presented in Table 4.1 through Table 4.3 for various conditions of hydraulic conductivity ($k = 0.0864 m/day$), porosity ($\eta = 30\%$) of the aquifer medium, drawdown $D_w = 4.0m$, pipe diameter $d_p = \{0.3, 0.5, 1.0\}m$ and area fraction opening $f_a = 0.16$ in the collector pipe, $d_1/D = \{0.25, 0.5, 0.75\}$, $D = \{5, 10, 15, 20\}m$. Using the dimensionless factors given in these tables, one can compute Q, $\bar{v}_e$, and t_r for any known values of D_w, k, f_a, and η for the specified values of D, d_p/D, and d_1/D.

Table 4.1(a) Mapping Parameters for d_p=1 m

d_1/D	c	d	e	f
0.25	-0.5952	-0.6289	0.7742	0.8004
0.5	0.1448	0.1026	0.1026	0.1448
0.75	0.8004	0.7742	-0.6289	-0.5952

Table 4.1(b) Dimensionless Flow $\dfrac{Q}{kD_w}$ **, entrance velocity factors** $\bar{v}_{ef}\left(=\dfrac{\bar{v}_e d_s f_a}{kD_w}\right)$ **and**

Travel Time Factor $t_{rf}\left(=\dfrac{t_r kD_w}{\eta D^2}\right)$ **, Corresponding to** $D_w = 4m$, $k = 0.0864\ m/day$ **,**

$f_a = 0.16$, $\eta = 30\%$, $d_1/D = \{0.25, 0.5, 0.75\}$, **and** $d_p = 1m$

d_p/D	d_1/D	$Q/(kD_w)$	$\bar{v}_{ef}$	t_{rf}	t_r	n
0.2	0.25	1.8159	0.454	0.4477	10.9613	0.8437
	0.5	2.4177	0.6044	0.2207	4.0933	0.401
	0.75	3.7058	0.9265	0.0504	0.6378	0.0783
0.1	0.25	1.5018	0.3754	0.3268	53.8767	2.8156
	0.5	1.8995	0.4749	0.1741	21.5557	1.3784
	0.75	2.5952	0.6488	0.0545	4.1031	0.4017
0.067	0.25	1.3673	0.3418	0.2569	133.0358	6.2548
	0.5	1.6908	0.4227	0.1402	54.7997	2.8558
	0.75	2.2183	0.5546	0.0484	11.032	0.8477
0.05	0.25	1.2862	0.3216	0.2127	250.8874	11.373
	0.5	1.5689	0.3922	0.1175	105.1592	5.0441
	0.75	2.0124	0.5031	0.0426	21.772	1.3885

Table 4.2(a) Mapping Parameters for d_p=0. 5m

d_1/D	c	d	e	f
0.25	-0.6533	-0.6693	0.7421	0.7562
0.5	0.0727	0.0514	0.0514	0.0727
0.75	0.7562	0.7421	-0.6693	-0.6533

Table 4.2 (b) Dimensionless flow $\dfrac{Q}{kD_w}$ **, entrance velocity factors** $\bar{v}_{ef}\left(=\dfrac{\bar{v}_e d_s f_a}{kD_w}\right)$ **and travel**

Time factor $t_{rf}\left(=\dfrac{t_r kD_w}{\eta D^2}\right)$ **, Corresponding to** $D_w = 4m$, $k = 0.0864\ m/day$, $f_a = 0.16$, $\eta = 30\%$,

$d_1/D = \{0.25, 0.5, 0.75\}$, **and** $d_p = 0.5m$

d_p/D	d_1/D	$Q/(kD_w)$	$\bar{v}_{ef}$	t_{rf}	t_r	n
0.1	0.25	1.5018	0.3754	0.3268	13.4692	0.9794
	0.50	1.8995	0.4749	0.1741	5.3889	0.4973
	0.75	2.5952	0.6488	0.0545	1.0258	0.1219
0.05	0.25	1.2862	0.3216	0.2127	62.7219	3.2006
	0.50	1.5689	0.3922	0.1175	26.2898	1.5975
	0.75	2.0124	0.5031	0.0426	5.4430	0.5011
0.033	0.25	1.1873	0.2968	0.1597	152.3182	7.0922
	0.50	1.4244	0.3561	0.0895	65.1946	3.3081
	0.75	1.7804	0.4451	0.0341	13.906	1.0022

d_p/D	d_1/D	$Q/(kD_w)$	$\bar{v}_{ef}$	t_{rf}	t_r	n
0.025	0.25	1.126	0.2815	0.1288	284.7857	12.8452
	0.5	1.3371	0.3343	0.0728	123.4577	5.8388
	0.75	1.646	0.4115	0.0285	26.7737	1.6195

Table 4.3 (a) Mapping Parameters for d_p=0. 3m

d_l/D	c	d	e	f
0.25	-0.6754	-0.6848	0.7284	0.7371
0.5	0.0437	0.0309	0.0309	0.0437
0.75	0.7371	0.7284	-0.6848	-0.6754

Table 4.3 (b) Dimensionless flow $\dfrac{Q}{kD_w}$, **entrance velocity factors** $\bar{v}_{ef}\left(=\dfrac{\bar{v}_e d_s f_a}{kD_w}\right)$ **and travel time factor** $t_{rf}\left(=\dfrac{t_r kD_w}{\eta D^2}\right)$, **corresponding to** $D_w=4m$, $k=0.0864$ m/day, $f_a=0.16$, $\eta=30\%$, $d_1/D=\{0.25,0.5,0.75\}$, **and** $d_p=0.3m$

d_p/D	d_1/D	$Q/(kD_w)$	$\bar{v}_{ef}$	t_{rf}	t_r	n
0.06	0.25	1.3364	0.3341	0.2401	15.1131	1.0644
	0.5	1.644	0.411	0.1316	6.2669	0.558
	0.75	2.1381	0.5345	0.0463	1.2757	0.1487
0.03	0.25	1.1641	0.291	0.1478	68.9804	3.4726
	0.5	1.3911	0.3478	0.0831	29.6683	1.7504
	0.75	1.7287	0.4322	0.032	6.3691	0.5649
0.02	0.25	1.0827	0.2707	0.1085	166.2861	7.6988
	0.5	1.2765	0.3191	0.0617	72.7302	3.6356
	0.75	1.555	0.3887	0.0246	15.9474	1.1066
0.015	0.25	1.0315	0.2579	0.0865	309.5876	13.9223
	0.5	1.206	0.3015	0.0495	136.8127	6.4188
	0.75	1.4516	0.3629	0.0201	30.3728	1.7821

Flow to a pipe with square cross-section having a finite potential at its periphery with that of the flow for a circular pipe treated as a line sink has been compared. For $d_1/D=0.5$, $d_p=1.0m$, $d_p/D=0.1$ from table 4.1 (b), $Q/(kD_w)=1.8995$. From table 3.1, $Q/(kD_w)=1.9990$. For $d_p=0.3m$ and $d_1/D=0.25$ $d_p/D=0.06$ from table 4.3 (b) $Q/(kD_w)=1.3364$. From table 3.3 $Q/(kD_w)=1.3771$. Thus, when the pipe is treated as a line sink, as the potential at a line sink is $+\infty$, the flow to the collector pipe is more the flow to a pipe with an equivalent square section having finite potential at its boundary.

In case of a pipe with square cross section, the entrance velocity factor is defined as $\bar{v}_{ef}\left(=\dfrac{\bar{v}_e d_s f_a}{kD_w}\right)$. In case of a pipe with circular cross section, the entrance velocity factor is defined as $\bar{v}_{ef}\left(=\dfrac{\bar{v}_e d_p f_a}{kD_w}\right)$. For $d_p/D=0.05$, $d_1/D=0.5$, and D=10m entrance velocity factor for a square cross section $\bar{v}_{ef}=0.3922$. For a circular pipe the corresponding value is $\bar{v}_{ef}=0.5140$. So the entrance velocity factor in case of circular pipe is more as it is treated as a line sink as well as the diameter d_p is more than the side of the equivalent square section with same perimeter.

It is seen from Tables 3.1 and 4.1(b) that, the travel time in case of a pipe with square cross section having perimeter equal to that of the circular pipe is more as the velocity of a parcel of water from the river bed to the collector is less and the travel path from the river bed to the collector pipe is more. In case of circular pipe as the distance is less and the velocity is more, because of the effect of line sink, the travel time is less.

When the pipe is treated as a line sink the solution is easy as compared to the solution for a pipe with square cross section. The results of flow characteristics obtained from this study with square cross section match with the solution obtained using the Aravin and Numerov (1965) line sink concept.

4.8 CONCLUSIONS

Based on the study, the following conclusions are drawn:

Solution for a square pipe is complex and involves solution of four implicit non-linear equations. The solution involves evaluation of improper integrals. The solution for a circular pipe when it is treated as a line sink is much more simple and tractable. However, there is no much difference between the flows and entrance velocity factors obtained weather the pipe is treated as a line sink or it is treated as a square pipe with finite potential boundary. Therefore, Aravin and Numerov (1965) line sink concept can be used conveniently to evaluate the flow characteristics for a collector with circular cross section.

74

FLOW CHARACTERISTICS OF MULTI-COLLECTOR
PIPES PLACED ADJACENT TO THE RIVER

5.1   INTRODUCTION

Riverbank Filtration is a process of attenuating the contaminants in the soil medium through percolating water and equilibrating the temperature of water. It acts as a cost effective and efficient alternative slow sand filter for water treatment processes. The filtrated water is provided for consumption with marginal treatment. A radial collector well is a part of riverbank filtration.

In some sedimentary ground water basin, aquifer thickness may not be sufficient to supply the required volume of water to a vertical well, even though the aquifer is hydraulically connected to a nearby surface-water body. The hydraulic conductivity of the sediments may be excellent, but the transmissivity is severely limited because the deposits are thin. A typical example occurs in a river valley where thin alluvial deposits overlie bedrock. In such hydro-geologic condition, a collector system, called a radial collector, which uses multiple screens extended horizontally outward from a caisson, can supply water at the desired rate. A radial collector is more commonly called as "Ranney Well". The radial collector wells are often set near streams, where aquifer storage is supplemented by an induced recharge of river water through the banks. The sustained capacity of the radial collector well is of the order of 0.2 to 0.4 m^3/ sec (1728 to 3456 m^3/day), Huisman, *et. al.* (1983), Driscoll (1987).

Plan and elevation of a typical radial collector well are shown in Fig.5.1. The caisson is made of reinforced concrete and is sunk vertically to the desired depth by excavating the earth material within. The bottom is subsequently sealed by a concrete plug. A typical caisson is about 4 m in diameter and 25 to 40m deep. It may be extended up to the shallow bed rock or clay layer. Portholes are provided about 1 m above the bottom of the caisson to accommodate radial collector pipes. A part of the radial near the caisson is kept blind as in case of a several radial collector system, the zone near the caisson happens to be a dead flow zone due to interference of flow to the radials. Depending upon the local conditions, the number of laterals varies from 4 to 20, their diameter between 0.15 and 0.5m and the individual length between 15 and 60m.
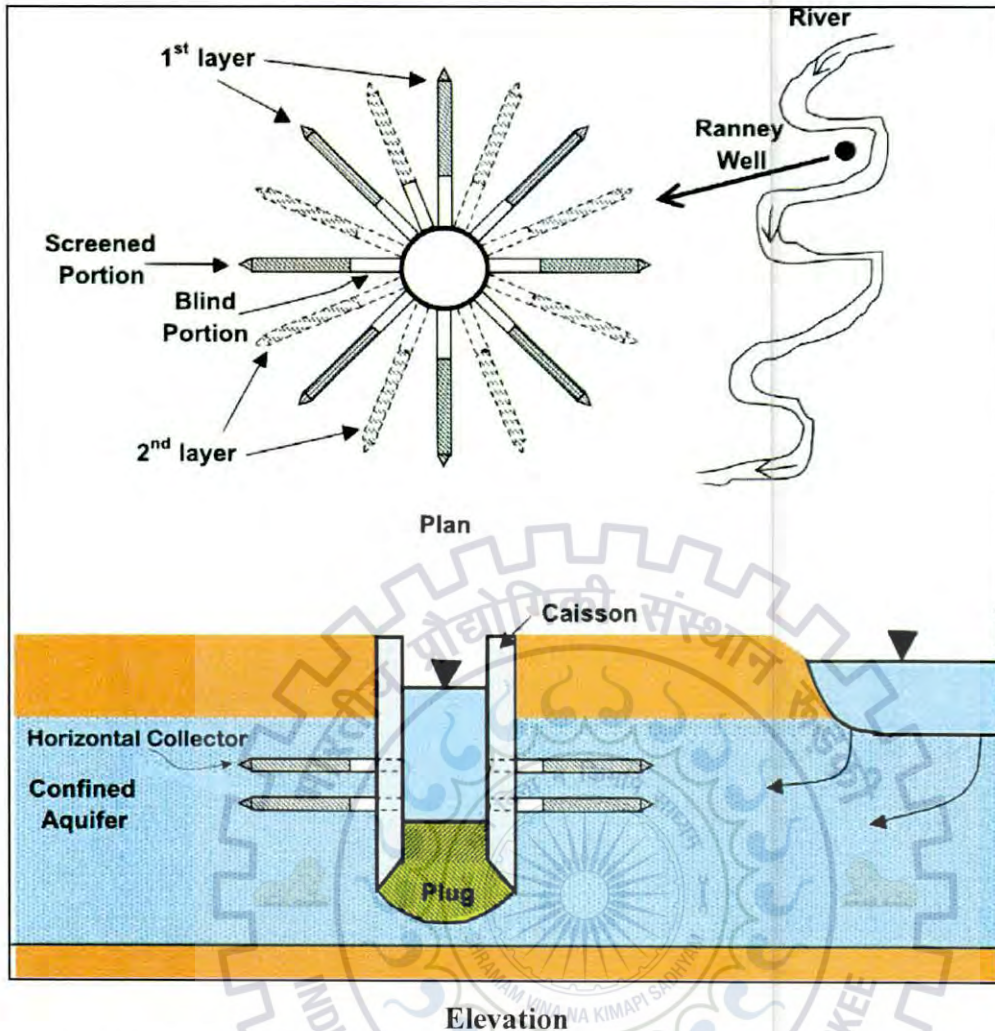
Fig.5.1 Plan and Elevation of a typical Two-Tier Radial Collector Well

Screen slot size is predicated based on the grain-size distribution of the filter pack; and should always retain 100 per cent of the filter pack. The yield of a collector well can be determined solving Boussinesq's equation for three-dimensional flow satisfying the existing initial and boundary conditions applying numerical method. For a given layout of radials and for a prescribed drawdown in the well caisson, the entrance velocity to the radials is computed and compared with the limiting entrance velocity (3cm/s). Varying the drawdown and simultaneously computing the entrance velocity and comparing with the permissible axial and entrance velocities, the maximum flow rate for a given layout and length of radials is determined, which is the capacity supply rate of the collector well. The base of the well-caisson is designed to counterbalance the uplift pressure. Alternately, the design of the collector well can be based on solution of Laplace equation for steady state flow condition satisfying the pertinent boundary conditions. Zhan and Cao (2000) put forward that at late pumping stage,

horizontal pseudo-radial flow takes place towards a horizontal collector pipe. This postulation supports the assumption of sheet flow condition in a thin aquifer and horizontal collector well system. Bruce Hunt (1983) has defined the potential ϕ at a collector gallery as the product of hydraulic conductivity, thickness of aquifer and head difference between the river and the gallery. This alternate definition of ϕ implies that flow to a collector pipe is linearly proportional to thickness of aquifer. Accuracy of this postulation remains yet to be verified. Idealizing the flow domain, and assuming condition of sheet flow for applying Schwartz-Christoffel conformal mapping technique, specific capacity of a radial collector well having several coplanar laterals in a thin aquifer located near a river reach has been quantified for different lengths of laterals, orientation of laterals and distance of the collector well from the river. In this chapter, one has to solve the case; the multi-collector pipes are located near a fully penetrating straight river reach. A correction factor to the flow, computed assuming sheet flow, has been derived to account for thickness of aquifer in which the collector pipes are laid.

5.2   STATEMENT OF THE PROBLEM

A radial collector well has four co-linear laterals located near a straight river reach. The lengths of the first, second, and third laterals are l_1, l_2, l_3 respectively. The length of the fourth lateral is l_2. Such assumption has been made to take advantage of symmetry and obtain tractable solution. The caisson of the collector well is located at a distance R from the river reach. The thickness (D) of the aquifer is small and the flow domain is conceptualized as a sheet flow domain.
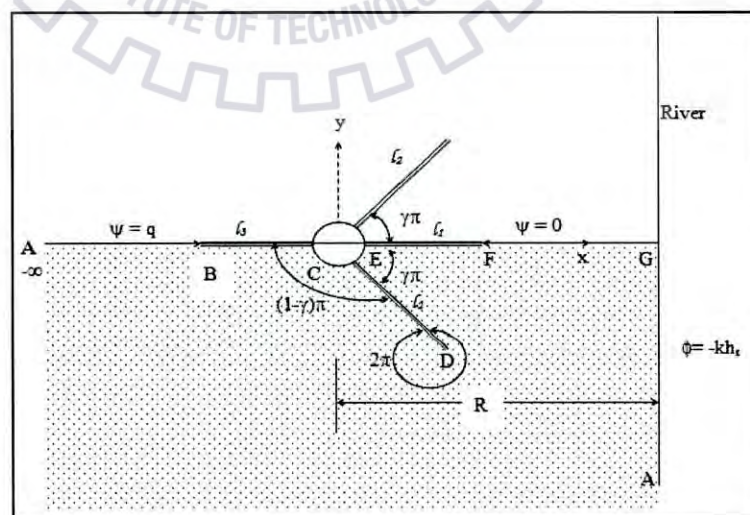
Fig.5.2 (a) Idealized Flow Domain or $z(=x+iy)$ Plane

77

Thus, the flow is occurring in a horizontal x-y plane. Layout plan of the laterals is shown in Fig.5.2 (a). It is required to solve Laplace equation in the horizontal x-y plane. The flow domain is symmetrical about the x-axis. Therefore, half of the flow domain is considered for solving Laplace equation. It is required to find the flow characteristics of multi-collector pipes placed adjacent to the river and river is only in one side.

5.3   CONFORMAL MAPPING OF z-PLANE ONTO AUXILIARY LOWER HALF t-PLANE

The vertices A, C, D, E, G, A in z plane are mapped onto $-\infty, 0, d, 1, g, \infty$ on real axis of an auxiliary $t (= r + is)$ plane shown in Fig. 5.2(b).

Fig.5.2 (b) Lower Half Auxuliary t (=r+is) Plane

According to Schwarz-Christoffel transformation, the conformal mapping of the flow domain to the lower half of the auxiliary t plane is given by (Harr, 1962):

$$z = M \int_0^{t'} \frac{(d-t)}{t^\gamma (1-t)^{1-\gamma} (g-t)^{1/2}} dt + N \tag{5.1a}$$

$$= Md \int_0^{t'} \frac{dt}{t^\gamma (1-t)^{1-\gamma} (g-t)^{1/2}} - M \int_0^{t'} \frac{t^{1-\gamma} dt}{(1-t)^{1-\gamma} (g-t)^{1/2}} + N \tag{5.1b}$$

M and N are constants. The constant N is governed by the lower limit of integration. Corresponding to vertex C, $t' = 0$ and $z = 0$; hence, the constant $N=0$. For point E, $z = 0$ and $t' = 1$; therefore,

78

$$d = \frac{\displaystyle\int_0^1 \frac{t^{1-\gamma}\,dt}{(1-t)^{1-\gamma}(g-t)^{1/2}}}{\displaystyle\int_0^1 \frac{dt}{t^{\gamma}(1-t)^{1-\gamma}(g-t)^{1/2}}} = \frac{I_1}{I_2} \tag{5.2}$$

Substituting $t = 1 - v^{1/\gamma}$, $dt = -\frac{1}{\gamma}v^{(1-\gamma)/\gamma}\,dv$ in the integrand appearing in I_1, we convert the improper integral I_1 to a proper one and obtain

$$I_1 = \int_0^1 \frac{t^{1-\gamma}\,dt}{(1-t)^{1-\gamma}(g-t)^{1/2}} = \frac{1}{\gamma}\int_0^1 \frac{\left(1-v^{1/\gamma}\right)^{1-\gamma}}{\left(g-1+v^{1/\gamma}\right)^{1/2}}\,dv$$

Integrating from limits 0 to ½ and ½ to 1, the integral I_2 is split into two parts and expressed as:

$$I_2 = \int_0^1 \frac{dt}{t^{\gamma}(1-t)^{1-\gamma}(g-t)^{1/2}} = \int_0^{1/2} \frac{dt}{t^{\gamma}(1-t)^{1-\gamma}(g-t)^{1/2}} + \int_{1/2}^1 \frac{dt}{t^{\gamma}(1-t)^{1-\gamma}(g-t)^{1/2}} = I_3 + I_4$$

The improper integrals I_3, and I_4 are converted to proper integrals through substitutions as described below. Substituting $t = v^{1/(1-\gamma)}$, $dt = \frac{1}{1-\gamma}v^{\gamma/(1-\gamma)}\,dv$

$$I_3 = \int_0^{1/2} \frac{dt}{t^{\gamma}(1-t)^{1-\gamma}(g-t)^{1/2}} = \frac{1}{1-\gamma}\int_0^{(1/2)^{1-\gamma}} \frac{dv}{\left(1-v^{1/(1-\gamma)}\right)^{1-\gamma}\left(g-v^{1/(1-\gamma)}\right)^{1/2}}$$

Substituting $1 - t = v^{1/\gamma}$, $dt = -\frac{1}{\gamma}v^{(1-\gamma)/\gamma}$

$$I_4 = \int_{1/2}^1 \frac{dt}{t^{\gamma}(1-t)^{1-\gamma}(g-t)^{1/2}} = \frac{1}{\gamma}\int_0^{1/2^{\gamma}} \frac{dv}{\left(1-v^{1/\gamma}\right)^{\gamma}\left(g-1+v^{1/\gamma}\right)^{1/2}}$$

The parameter d is given by:

$$d = \frac{\dfrac{1}{\gamma}\displaystyle\int_0^1 \frac{\left(1-v^{1/\gamma}\right)^{1-\gamma}}{\left(g-1+v^{1/\gamma}\right)^{1/2}}\,dv}{\dfrac{1}{1-\gamma}\displaystyle\int_0^{(1/2)^{1-\gamma}} \frac{dv}{\left(1-v^{1/(1-\gamma)}\right)^{1-\gamma}\left(g-v^{1/(1-\gamma)}\right)^{1/2}} + \dfrac{1}{\gamma}\displaystyle\int_0^{(1/2)^{\gamma}} \frac{dv}{\left(1-v^{1/\gamma}\right)^{\gamma}\left(g-1+v^{1/\gamma}\right)^{1/2}}} \tag{5.3}$$

Corresponding to vertex D, $t'= d$ and $z = z_D = l_2 e^{i(2-\gamma)\pi}$. Applying this condition in (5.1a), the constant M is found to be

$$M = \frac{l_2(1-\gamma)e^{i(2-\gamma)\pi}}{\displaystyle\int_0^{d^{(1-\gamma)}} \frac{\left(d-v^{1/(1-\gamma)}\right)dv}{\left(1-v^{1/(1-\gamma)}\right)^{1-\gamma}\left(g-v^{1/(1-\gamma)}\right)^{1/2}}}$$ (5.4)

For vertex G, $t' = g$, $z = z_G = R$. Applying this condition, from equation (5.1a) we obtain

$$R = M\int_1^g \frac{(d-t)}{t^\gamma(1-t)^{1-\gamma}(g-t)^{1/2}}dt$$

$$= M\left\{\int_1^{(1+g)/2} \frac{(d-t)}{t^\gamma(1-t)^{1-\gamma}(g-t)^{1/2}}dt + \int_{(1+g)/2}^g \frac{(d-t)}{t^\gamma(1-t)^{1-\gamma}(g-t)^{1/2}}dt\right\} = M(I_5+I_6)$$ (5.5)

Substituting $t=1+v^{1/\gamma}$ for converting the improper integral I_5 and $g-t=v^2$ for integrating I_6 and simplifying we obtain

$$R = -Me^{i\pi(\gamma-1)}\left[\frac{1}{\gamma}\int_0^{((g-1)/2)^\gamma} \frac{\left(1+v^{1/\gamma}-d\right)dv}{\left(1+v^{1/\gamma}\right)^\gamma\left(g-1-v^{1/\gamma}\right)^{1/2}} + 2\int_0^{((g-1)/2)^{1/2}} \frac{(g-d-v^2)dv}{(g-v^2)^\gamma(g-v^2-1)^{1-\gamma}}\right]$$ (5.6)

Incorporating the constant M in equation (5.6) we obtain

$$R/l_2 = \frac{(1-\gamma)\left[\dfrac{1}{\gamma}\displaystyle\int_0^{((g-1)/2)^\gamma} \dfrac{\left(1+v^{1/\gamma}-d\right)dv}{\left(1+v^{1/\gamma}\right)^\gamma\left(g-1-v^{1/\gamma}\right)^{1/2}} + 2\displaystyle\int_0^{((g-1)/2)^{1/2}} \dfrac{(g-d-v^2)dv}{(g-v^2)^\gamma(g-v^2-1)^{1-\gamma}}\right]}{\displaystyle\int_0^{d^{(1-\gamma)}} \dfrac{\left(d-v^{1/(1-\gamma)}\right)dv}{\left(1-v^{1/(1-\gamma)}\right)^{1-\gamma}\left(g-v^{1/(1-\gamma)}\right)^{1/2}}}$$ (5.7)

For an assumed value of parameter g, parameter d is obtained from (5.3). Required value of g for known value of R/l_2 is obtained through an iteration making use of equation (5.7).

Corresponding to point F, $t = f$ and $z = l_1$ using this relation we obtain

$$l_1 = M\int_1^f \frac{(d-t)}{t^\gamma(1-t)^{1-\gamma}(g-t)^{1/2}}dt$$ (5.8)

Substituting $t=1+v^{1/\gamma}$ for converting the improper integral into proper one

$$l_1 = Me^{i\pi(\gamma-1)}\frac{1}{\gamma}\int_0^{(f-1)^\gamma} \frac{(1+v^{1/\gamma}-d)dv}{\left(1+v^{1/\gamma}\right)^\gamma(g-1-v^{1/\gamma})^{1/2}}$$

80

Incorporating the constant M

$$l_1/l_2 = \frac{1-\gamma}{\gamma} \frac{\displaystyle\int_0^{(f-1)^\gamma} \frac{(1+v^{1/\gamma}-d)dv}{\left(1+v^{1/\gamma}\right)^\gamma (g-1-v^{1/\gamma})^{1/2}}}{\displaystyle\int_0^{d^{(1-\gamma)}} \frac{\left(d-v^{1/(1-\gamma)}\right)dv}{\left(1-v^{1/(1-\gamma)}\right)^{1-\gamma}\left(g-v^{1/(1-\gamma)}\right)^{1/2}}} \tag{5.9}$$

For known l_1/l_2, corresponding parameter f is found using Newton-Raphson technique.

Let a function $F_1(f)$ be defined as:

$$F_1(f) = \frac{1-\gamma}{\gamma} \frac{\displaystyle\int_0^{(f-1)^\gamma} \frac{(1+v^{1/\gamma}-d)dv}{\left(1+v^{1/\gamma}\right)^\gamma (g-1-v^{1/\gamma})^{1/2}}}{\displaystyle\int_0^{d^{(1-\gamma)}} \frac{\left(d-v^{1/(1-\gamma)}\right)dv}{\left(1-v^{1/(1-\gamma)}\right)^{1-\gamma}\left(g-v^{1/(1-\gamma)}\right)^{1/2}}} - l_1/l_2 \tag{5.10}$$

Let f^* be very near to the zero of the function $F_1(f)$. Applying Taylor series expansion to $F_1(f)$ near $f = f^*$, neglecting higher order terms we obtain

$$F_1(f) \cong F_1^*(f^*) + \left.\frac{dF_1}{df}\right|_{f^*} \Delta f = 0 \tag{5.11a}$$

$$\Delta f = -F_1^*(f^*) / \left.\frac{dF_1}{df}\right|_{f^*} \tag{5.11b}$$

Applying Leibniz rule and simplifying the derivative

$$\left.\frac{dF_1(f)}{df}\right|_{f^*} = \left\{ \frac{1}{\displaystyle\int_0^{d^{(1-\gamma)}} \frac{\left(d-v^{1/(1-\gamma)}\right)dv}{\left(1-v^{1/(1-\gamma)}\right)^{1-\gamma}\left(g-v^{1/(1-\gamma)}\right)^{1/2}}} \right\} \left\{ \frac{f^*-d}{f^{*\gamma}\left(g-f^*\right)^{1/2}} \right\} \left\{ \frac{1-\gamma}{\left(f^*-1\right)^{1-\gamma}} \right\} \tag{5.12}$$

The value of f is improved by

$$f = f^* + \Delta f \tag{5.13}$$

The procedure is repeated till Δf is negligible.

Corresponding to location B, $z = z_B = -l_3$, and $t' = -b$. Applying this relation in equation 5.1(a), we obtain

$$-l_3 = M \int_0^{-b'} \frac{(d-t)}{t^\gamma (1-t)^{1-\gamma}(g-t)^{1/2}} dt = M(-1)^\gamma \int_0^{-b'} \frac{(d-t)}{\left(-t^\gamma\right)(1-t)^{1-\gamma}(g-t)^{1/2}} dt \tag{5.14}$$

Substituting $t = -v^{1/(1-\gamma)}$, $dt = -\frac{1}{1-\gamma} v^{\gamma/(1-\gamma)} dv$ in (5.14)

$$l_3 = \frac{M(-1)^\gamma}{(1-\gamma)} \int_0^{b^{(1-\gamma)}} \frac{(d+v^{1/(1-\gamma)})dv}{(1+v^{1/(1-\gamma)})^{1-\gamma}(g+v^{1/(1-\gamma)})^{1/2}} \tag{5.15}$$

Incorporating the constant M in equation (5.15), we obtain

$$l_3/l_2 = \frac{\displaystyle\int_0^{b^{(1-\gamma)}} \frac{(d+v^{1/(1-\gamma)})dv}{(1+v^{1/(1-\gamma)})^{1-\gamma}(g+v^{1/(1-\gamma)})^{1/2}}}{\displaystyle\int_0^{d^{(1-\gamma)}} \frac{(d-v^{1/(1-\gamma)})dv}{(1-v^{1/(1-\gamma)})^{1-\gamma}(g-v^{1/(1-\gamma)})^{1/2}}} \tag{5.16}$$

For known l_3/l_2, corresponding parameter b is found using Newton-Raphson technique.

Let a function $F_2(b)$ be defined as:

$$F_2(b) = \frac{\displaystyle\int_0^{b^{(1-\gamma)}} \frac{(d+v^{1/(1-\gamma)})dv}{(1+v^{1/(1-\gamma)})^{1-\gamma}(g+v^{1/(1-\gamma)})^{1/2}}}{\displaystyle\int_0^{d^{(1-\gamma)}} \frac{(d-v^{1/(1-\gamma)})dv}{(1-v^{1/(1-\gamma)})^{1-\gamma}(g-v^{1/(1-\gamma)})^{1/2}}} - l_3/l_2 \tag{5.17}$$

Let b^* be very near to the zero of the function $F_2(b)$. Applying Taylor series expansion to $F_2(b)$ near $b = b^*$, neglecting higher order terms we obtain

$$F_2(b) \cong F_2^*(b^*) + \left.\frac{dF_2}{db}\right|_{b^*} \Delta b = 0 \tag{5.18a}$$

$$\Delta b = -F_2^*(b^*) / \left.\frac{dF_2}{db}\right|_{b^*} \tag{5.18b}$$

Applying Leibniz rule and simplifying the derivative

$$\left.\frac{dF_2}{db}\right|_{b^*} = \left\{ \frac{1}{\displaystyle\int_0^{d^{(1-\gamma)}} \frac{(d-v^{1/(1-\gamma)})dv}{(1-v^{1/(1-\gamma)})^{1-\gamma}(g-v^{1/(1-\gamma)})^{1/2}}} \right\} \left\{ \frac{d+b^*}{(1+b^*)^{1-\gamma}(g+b^*)^{1/2}} \right\} \left\{ \frac{1-\gamma}{b^{*\gamma}} \right\} \tag{5.19}$$

The value of b is improved by

$$b = b^* + \Delta b \tag{5.20}$$

The procedure is repeated till Δb is negligible.

All the proper integrals appearing above are computed using Gauss Quadrature. We adopt the following procedure before applying the Gauss Quadrature:

$$\int_{L_L}^{L_U} f(v)dv = B^* \int_{-1}^{1} f(X)dX; \quad v = A^* + B^*X; \quad dv = B^*dX; \quad A^* = (L_U+L_L)/2; \quad B^* = (L_U-L_L)/2$$

82

5.4 MAPPING OF *w*-PLANE ONTO *t*-PLANE

The complex potential $w = \phi + i\psi$ for half of the flow domain is shown in Fig.5.2(c). ψ = stream function and ϕ = velocity potential function defined as:

$$\phi = -k\left(p/\gamma_w + y\right) + C^*$$
(5.21)

k = hydraulic conductivity; p=water pressure at a point (x,y); γ_w = unit weight of water; y = elevation head which is equal to zero anywhere in the x-y plane; and C^* = a constant assumed to be equal to 0. The ψ values assumed are consistent with Cauchy-Riemann conditions. It is assumed that the axial flow in the laterals is not subjected to friction loss.
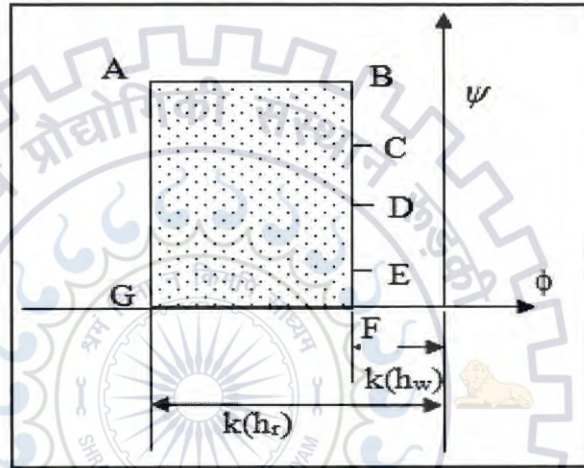
Fig.5.2(c) Complex Potential w-Plane

The conformal mapping of the complex potential plane shown in Fig.5.2 (c) onto the lower half of the 't' plane, the vertices A,B,F,G having been mapped onto $-\infty, -b, f, g$ respectively, for $-\infty < t < -b$ is given by:

$$w = M_1 \int_{-\infty}^{t'} \frac{dt}{(-b-t)^{1/2}(f-t)^{1/2}(g-t)^{1/2}} - kh_r + iq$$
(5.21a)

Integrating (Gradshteyn and Ryzhik, 1965)

$$w = M_1 \frac{2}{\sqrt{g+b}} F\left(\sin^{-1}\sqrt{(g+b)/(g-t')}, \sqrt{(g-f)/(g+b)}\right) - kh_r + iq$$
(5.21b)

For point B, $t' = -b$, and $w = -kh_w + iq$; hence, constant M_1 is

$$M_1 = \frac{\sqrt{g+b}}{2F\left(\pi/2, \sqrt{(g-f)/(g+b)}\right)} k(h_r - h_w)$$
(5.22)

where, $F\left(\pi/2, \sqrt{(g-f)/(g+b)}\right)$ is complete elliptic integral of the first kind with modulus $\sqrt{(g-f)/(g+b)}$.

83

For $-b \leq t \leq f$, the relation between w and t plane is given by:

$$w = \frac{M_1}{\sqrt{-1}} \int_{-b}^{t} \frac{dt}{(b+t)^{1/2}(f-t)^{1/2}(g-t)^{1/2}} - kh_w + iq \qquad (5.23)$$

Integrating (Gradshteyn and Ryzhik, 1965) and incorporating the constant M_1

$$w(t') = -i \frac{F\left\{\sin^{-1}\sqrt{(t'+b)/(f+b)}, \sqrt{(f+b)/(g+b)}\right\}}{F\left(\pi/2, \sqrt{(g-f)/(g+b)}\right)} k(h_r - h_w) - kh_w + iq; \quad -b \leq t' \leq f \qquad (5.24)$$

For point F, $t' = f$, and $w(t') = -kh_w$. Applying this condition in equation (5.24), q is found to be

$$q = k \frac{F\left\{\pi/2, \sqrt{(f+b)/(g+b)}\right\}}{F\left(\pi/2, \sqrt{(g-f)/(g+b)}\right)} (h_r - h_w) \qquad (5.25)$$

The total flow to the collector system is equal to $2q$.

Using equation (5.24), one can find flow to individual laterals. The vertex C has been mapped onto $t' = 0$. One half of the flow intercepted by the lateral BC, q_3, is given by:

$$q_3 = \psi(-b) - \psi(0) = \frac{w(-b) - w(0)}{i} = \frac{F\left\{\sin^{-1}\sqrt{(b)/(f+b)}, \sqrt{(f+b)/(g+b)}\right\}}{F\left(\pi/2, \sqrt{(g-f)/(g+b)}\right)} k (h_r - h_w) \qquad (5.26)$$

The flow q_2 intercepted by lateral CDE is given by

$$q_2 = \psi(0) - \psi(1) = \frac{w(0) - w(1)}{i}$$

$$= \left[\frac{F\left\{\sin^{-1}\sqrt{(1+b)/(f+b)}, \sqrt{(f+b)/(g+b)}\right\}}{F\left(\pi/2, \sqrt{(g-f)/(g+b)}\right)} - \frac{F\left\{\sin^{-1}\sqrt{(b)/(f+b)}, \sqrt{(f+b)/(g+b)}\right\}}{F\left(\pi/2, \sqrt{(g-f)/(g+b)}\right)}\right] k (h_r - h_w) \qquad (5.27)$$

One half of the flow intercepted by the lateral EF, q_1, is given by:

$$q_1 = \psi(1) - \psi(f) = \frac{w(1) - w(f)}{i}$$

$$= \left[\frac{F\left\{\pi/2, \sqrt{(f+b)/(g+b)}\right\}}{F\left(\pi/2, \sqrt{(g-f)/(g+b)}\right)} - \frac{F\left\{\sin^{-1}\sqrt{(1+b)/(f+b)}, \sqrt{(f+b)/(g+b)}\right\}}{F\left(\pi/2, \sqrt{(g-f)/(g+b)}\right)}\right] k (h_r - h_w) \qquad (5.28)$$

From equation (5.24)

$$\psi(0) = q - \frac{F\left\{\sin^{-1}\sqrt{b/(f+b)}, \sqrt{(f+b)/(g+b)}\right\}}{F\left(\pi/2, \sqrt{(g-f)/(g+b)}\right)} k(h_r - h_w) \qquad (5.29)$$

$$\psi(d) = q - \frac{F\left\{\sin^{-1}\sqrt{(d+b)/(f+b)}, \sqrt{(f+b)/(g+b)}\right\}}{F\left(\pi/2, \sqrt{(g-f)/(g+b)}\right)} k(h_r - h_w) \qquad (5.30)$$

84

The flow q_{2l}, entering to the second lateral through side CD is given by:

$$q_{2l} = \frac{w(0) - w(d)}{i} = \psi(0) - \psi(d)$$

$$= \left[\frac{F\left\{\sin^{-1}\sqrt{(d+b)/(f+b)}, \sqrt{(f+b)/(g+b)}\right\}}{F\left(\pi/2, \sqrt{(g-f)/(g+b)}\right)} - \frac{F\left\{\sin^{-1}\sqrt{b/(f+b)}, \sqrt{(f+b)/(g+b)}\right\}}{F\left(\pi/2, \sqrt{(g-f)/(g+b)}\right)} \right] k(h_r - h_w) \quad (5.31)$$

The flow q_{2r}, entering to the second lateral through side ED, is given by:

$$q_{2r} = \frac{w(d) - w(1)}{i} = \psi(d) - \psi(1)$$

$$= \left[\frac{F\left\{\sin^{-1}\sqrt{(1+b)/(f+b)}, \sqrt{(f+b)/(g+b)}\right\}}{F\left(\pi/2, \sqrt{(g-f)/(g+b)}\right)} - \frac{F\left\{\sin^{-1}\sqrt{(d+b)/(f+b)}, \sqrt{(f+b)/(g+b)}\right\}}{F\left(\pi/2, \sqrt{(g-f)/(g+b)}\right)} \right] k(h_r - h_w) \quad (5.32)$$

5.5   RESULTS AND DISCUSSIONS

Dimensionless flow per unit thickness of aquifer, $2q_1/\{k(h_r - h_w)\}$, $q_2/\{k(h_r - h_w)\}$, $2q_3/\{k(h_r - h_w)\}$ and $(2q_1 + q_2 + 2q_3 + q_4)/\{k(h_r - h_w)\}$ for different values of R/l_2 and γ for $l_1/l_2 = l_3/l_2 = 1$ are presented below. The flow $q_4 = q_2$

Table 5.1 Yield of a Collector with Four Radials of Equal Lengths

R/l_2	γ	$2q_1/\{k(h_r - h_w)\}$	$q_2/\{k(h_r - h_w)\}$	$2q_3/\{k(h_r - h_w)\}$	$(2q_1 + q_2 + 2q_3 + q_4)/\{k(h_r - h_w)\}$
2	0.1667	0.6091	0.9964	1.0709	3.6728
	0.2	0.6954	0.9979	1.0274	3.7186
	0.25	0.8157	0.9916	0.9625	3.7616
	0.3333	0.9929	0.9654	0.8565	3.7802
	0.5	1.2754	0.8854	0.656	3.7022
	0.6667	1.491	0.7972	0.4697	3.5551
	0.75	1.5823	0.7538	0.3789	3.4680
3	0.1667	0.4155	0.7569	0.9456	2.8748
	0.2	0.4741	0.7621	0.9093	2.9076
	0.25	0.5581	0.7653	0.8552	2.9439
	0.3333	0.6882	0.7606	0.7660	2.9754
	0.5	0.9133	0.7262	0.5930	2.9587
	0.6667	1.0997	0.6747	0.4271	2.8761
	0.75	1.1821	0.6458	0.3449	2.8185
4	0.1667	0.3421	0.6507	0.8699	2.5135
	0.2	0.3896	0.6561	0.8373	2.5392
	0.25	0.4583	0.6611	0.7888	2.5693
	0.3333	0.5665	0.662	0.7086	2.5991
	0.5	0.7607	0.6431	0.5517	2.5986
	0.6667	0.9287	0.6068	0.3987	2.5410
	0.75	1.005	0.5846	0.3222	2.4965

R/l_2	γ	$2q_1/\{k(h_r-h_w)\}$	$q_2/\{k(h_r-h_w)\}$	$2q_3/\{k(h_r-h_w)\}$	$(2q_1+q_2+2q_3+q_4)/\{k(h_r-h_w)\}$
5	0.1667	0.302	0.5882	0.8174	2.2959
	0.2	0.3435	0.5934	0.7872	2.3176
	0.25	0.4037	0.5988	0.7422	2.3435
	0.3333	0.4992	0.6019	0.6679	2.3709
	0.5	0.6741	0.5903	0.5217	2.3763
	0.6667	0.8294	0.5622	0.3780	2.3318
	0.75	0.9013	0.5439	0.3057	2.2947
10	0.1667	0.2243	0.4562	0.6831	1.8198
	0.2	0.2544	0.4604	0.6582	1.8335
	0.25	0.2981	0.4655	0.6214	1.8505
	0.3333	0.3682	0.4706	0.5608	1.8701
	0.5	0.5009	0.4694	0.4409	1.8806
	0.6667	0.6254	0.4556	0.3212	1.8578
	0.75	0.6855	0.4446	0.2602	1.8351
15	0.1667	0.1963	0.4045	0.6206	1.6259
	0.2	0.2223	0.4082	0.598	1.6368
	0.25	0.2601	0.4128	0.5646	1.6505
	0.3333	0.321	0.4179	0.5099	1.6667
	0.5	0.4373	0.4189	0.4017	1.6768
	0.6667	0.5486	0.4092	0.2932	1.6601
	0.75	0.6031	0.4007	0.2378	1.6422
20	0.1667	0.1807	0.3747	0.5820	1.5121
	0.2	0.2045	0.3782	0.5607	1.5216
	0.25	0.2391	0.3825	0.5294	1.5334
	0.3333	0.2948	0.3873	0.4782	1.5476
	0.5	0.4018	0.3891	0.377	1.5571
	0.6667	0.5052	0.3813	0.2756	1.5434
	0.75	0.5564	0.3741	0.2236	1.5281

The analysis of flow to a collector well with four radials of equal length is valid for $R/l_2>1$. Therefore, results are presented for $R/l_2>1$. As seen from table 5.1, with increasing distance of the collector well from the river i.e., with increasing value of R/l_2, the flow to any radial of the collector well deceases. For lower value of γ, flow to the radial number 1, i.e., $2q_1/\{k(h_r-h_w)\}$ is less than $q_2/\{k(h_r-h_w)\}$ because of interference of the second and fourth laterals. In case of a collector well with 4 laterals of equal length, the maximum flow occurs when angle between the laterals oriented towards the river is $\pi/3$ for $R/l_2< 5$. For $R/l \geq 5$, flow to the collector well is the maximum for $\gamma =0.5$.

Yield of collector wells having three laterals of equal length, and $l_3 = 0$ is a particular case and is obtained from equation (5.25) by substituting $b = 0$ and is given by:

$$q = k \frac{F\left\{\pi/2, \sqrt{f/g}\right\}}{F\left(\pi/2, \sqrt{(g-f)/g}\right)}(h_r - h_w) \tag{5.33}$$

$2q_1/\{k(h_r-h_w)\}, q_2/\{k(h_r-h_w)\}$ and $(2q_1+q_2+q_4)/\{k(h_r-h_w)\}$ for different values of R/l_2 and γ for $l_1/l_2 = 1$ are presented below. The flow $q_4 = q_2$

Table 5.2(a) Yield of a Collector with Three Radials of Equal Lengths, $l_3 = 0$

R/l_2	γ	$2q_1/\{k(h_r-h_w)\}$	$q_2/\{k(h_r-h_w)\}$	$(2q_1+q_2+q_4)/\{k(h_r-h_w)\}$
2	0.1667	0.6171	1.3251	3.2672
	0.20	0.7035	1.3195	3.3425
	0.25	0.8238	1.3020	3.4279
	0.3333	1.0011	1.2552	3.5116
	0.50	1.2837	1.1283	3.5402
	0.6667	1.4983	0.9860	3.4704
	0.75	1.5886	0.9123	3.4133
3	0.1667	0.4291	1.0613	2.5518
	0.20	0.4878	1.0597	2.6071
	0.25	0.5717	1.0521	2.6759
	0.3333	0.7015	1.0281	2.7576
	0.50	0.9253	0.9500	2.8253
	0.6667	1.1092	0.8483	2.8058
	0.75	1.19	0.7912	2.7724
4	0.1667	0.3585	0.9391	2.2366
	0.20	0.4062	0.9376	2.2815
	0.25	0.4749	0.9320	2.3390
	0.3333	0.5826	0.9143	2.4113
	0.50	0.7747	0.8539	2.4826
	0.6667	0.9394	0.7701	2.4796
	0.75	1.0136	0.7212	2.4561
5	0.1667	0.3201	0.8647	2.0493
	0.20	0.3618	0.8631	2.0880
	0.25	0.4221	0.8581	2.1382
	0.3333	0.5171	0.8431	2.2031
	0.50	0.6893	0.7915	2.2723
	0.6667	0.8408	0.7178	2.2765
	0.75	0.9103	0.6740	2.2583
10	0.1667	0.2447	0.6996	1.6438
	0.20	0.2752	0.6972	1.6697
	0.25	0.3191	0.6925	1.7040
	0.3333	0.3886	0.6807	1.7501
	0.50	0.5182	0.6437	1.8056
	0.6667	0.638	0.5898	1.8177
	0.75	0.6953	0.5567	1.8086
	0.1667	0.2171	0.6311	1.4792
	0.20	0.2435	0.6284	1.5004

R/l_2	γ	$2q_1/\{k(h_r-h_w)\}$	$q_2/\{k(h_r-h_w)\}$	$(2q_1+q_2+q_4)/\{k(h_r-h_w)\}$
15	0.25	0.2816	0.6235	1.5285
	0.3333	0.3419	0.6124	1.5668
	0.50	0.4549	0.5797	1.6143
	0.6667	0.5612	0.5327	1.6266
	0.75	0.6129	0.5036	1.6202
20	0.1667	0.2014	0.5905	1.3824
	0.20	0.2257	0.5876	1.4009
	0.25	0.2606	0.5826	1.4257
	0.3333	0.3157	0.5718	1.4594
	0.50	0.4195	0.5412	1.5019
	0.6667	0.5178	0.498	1.5138
	0.75	0.5661	0.4712	1.5086

As seen from Table 5.2 (a), for the case of a radial collector well with three radials in which one of the collectors orients perpendicularly towards the river and $l_3 = 0$, the flow to the collector well is maximum, if the other two radials are oriented at an angle $\gamma = 0.5$ for $R/l_2 < 5$; for $R/l_2 \geq 5$, the flow to the collector well is maximum if $\gamma = 2/3$.

Yield of collector wells having three laterals of equal length, and $l_1 = 0$ is also a particular case and is obtained from equation (5.25) by substituting $f = 1$ and is given by:

$$q = k\frac{F\left\{\pi/2, \sqrt{(1+b)/(g+b)}\right\}}{F\left(\pi/2, \sqrt{(g-1)/(g+b)}\right)}(h_r - h_w) \qquad (5.34)$$

$q_2/\{k(h_r-h_w)\}, 2q_3/\{k(h_r-h_w)\}$ and $(q_2+2q_3+q_4)/\{k(h_r-h_w)\}$ for different values of R/l_2 and γ for $l_3/l_2 = 1$ and $l_4/l_2 = 1$ are presented in Table 5.2 (b). The flow $q_4 = q_2$.

Table 5.2 (b) Yield of a Collector with Three Radials of Equal Lengths, $l_1 = 0$

R/l_2	γ	$q_2/\{k(h_r-h_w)\}$	$2q_3/\{k(h_r-h_w)\}$	$(q_2+2q_3+q_4)/\{k(h_r-h_w)\}$
2	0.1667	1.2281	1.0761	3.5323
	0.20	1.2521	1.0334	3.5374
	0.25	1.2733	0.9697	3.5164
	0.3333	1.2807	0.8656	3.4269
	0.50	1.2395	0.6692	3.1482
	0.6667	1.1714	0.4867	2.8296
	0.75	1.1348	0.3972	2.6669
3	0.1667	0.9279	0.9525	2.8082
	0.2	0.9521	0.9173	2.8213
	0.25	0.9802	0.8648	2.8253
	0.3333	1.0098	0.7782	2.7978
	0.50	1.0229	0.6099	2.6558

R/l_2	γ	$q_2/\{k(h_r-h_w)\}$	$2q_3/\{k(h_r-h_w)\}$	$(q_2+2q_3+q_4)/\{k(h_r-h_w)\}$
	0.6667	1.0014	0.4476	2.4504
	0.75	0.9837	0.3662	2.3337
4	0.1667	0.7954	0.8772	2.468
	0.20	0.8173	0.8459	2.4805
	0.25	0.8446	0.7992	2.4885
	0.3333	0.8775	0.7219	2.4770
	0.50	0.9068	0.57	2.3835
	0.6667	0.9039	0.4206	2.2284
	0.75	0.8949	0.3448	2.1347
5	0.1667	0.7177	0.8249	2.2604
	0.20	0.7379	0.796	2.2718
	0.25	0.7638	0.753	2.2806
	0.3333	0.7968	0.6817	2.2754
	0.50	0.8324	0.5407	2.2055
	0.6667	0.839	0.4005	2.0785
	0.75	0.8349	0.3288	1.9986
10	0.1667	0.5548	0.6905	1.8001
	0.20	0.5706	0.667	1.8082
	0.25	0.5918	0.6322	1.8159
	0.3333	0.6214	0.5748	1.8176
	0.50	0.662	0.4603	1.7843
	0.6667	0.6827	0.3441	1.7095
	0.75	0.6872	0.2837	1.658
15	0.1667	0.4915	0.6277	1.6108
	0.20	0.5055	0.6065	1.6175
	0.25	0.5244	0.5751	1.624
	0.3333	0.5515	0.5235	1.6266
	0.50	0.5911	0.4207	1.6029
	0.6667	0.6146	0.3157	1.5448
	0.75	0.6214	0.2608	1.5036
20	0.1667	0.4552	0.5889	1.4994
	0.20	0.4681	0.569	1.5052
	0.25	0.4857	0.5397	1.5111
	0.3333	0.5111	0.4915	1.5137
	0.50	0.5494	0.3957	1.4945
	0.6667	0.5737	0.2977	1.4451
	0.75	0.5815	0.2462	1.4093

As seen from above table 5.2(b), in case of a collector well with three radials of equal length in which one of them oriented away from the river, the other two should be oriented at

an angle $0.2 \leq \gamma \leq 1/3$ for $R/l_2 \leq 5$ to obtain near maximum yield. For $R/l_2 > 5$ their orientation should be $1/3 \leq \gamma \leq 1/2$.

Yield of collector well having two laterals of equal length running parallel to a fully penetrating stream is also a particular case and is obtained from equation (5.25) by substituting $b = 0$, and $f = 1$ and given by:

$$q = k \frac{F\{\pi/2, \sqrt{1/g}\}}{F\left(\pi/2, \sqrt{(g-1)/g}\right)}(h_r - h_w) = q_2 \qquad (5.35)$$

For such case, there is no restriction on length of the radials. In Table 5.3, total flow to each collector and ratio of the components of flow entering from the right and left side are presented. It is to be noted that both the components of flow are river water only.

Table 5.3 Yield of a Collector with Two Radials of Equal Lengths, running parallel to a Stream, $l_1 = l_3 = 0$, $l_2 = l_4$

R/l_2	$q_2/\{k(h_r - h_w)\}$	$2q_2/\{k(h_r - h_w)\}$	q_{2l}/q_{2r}
0.5	3.2634	6.5268	0.3973
1	2.1158	4.2315	0.5713
1.5	1.7065	3.4129	0.6722
2	1.4899	2.9798	0.7365
2.5	1.3532	2.7063	0.7803
3	1.2575	2.5149	0.812
4	1.13	2.2599	0.8543
5	1.047	2.0939	0.8812
6	0.9875	1.9749	0.8998
7	0.9421	1.8842	0.9134
8	0.906	1.8119	0.9237
9	0.8763	1.7526	0.9318
10	0.8513	1.7027	0.9384
15	0.7672	1.5344	0.9585
20	0.7169	1.4338	0.9687

As seen from table 5.3, water entering to the collector pipe from right hand side is more than that from left side as the river is on the right hand side. Therefore, $q_{2r} > q_{2l}$ and the ratio $q_{2l}/q_{2r} < 1$.

5.6 CONCLUSIONS

Based on the study of this chapter the following conclusions are drawn:

1. The yield of collector well increases as it is located nearer to the water body; it also increases with increase in length and diameter of the collector pipe.

2. A collector well having two collinear laterals each of 25m length running parallel to the river axis in a confined aquifer of 10m thickness comprising of silt sand can yield $17.31m^3$ /day while located at a distance of 250m. In such geological situation, several parallel pipes are required to be installed to a common caisson to get desired quantity of filtered water.

3. The yield of collector well increases with increase diameters and numbers of collector pipes.

4. The yield from the laterals dependent upon the orientations of collector pipes.

5. In case of a collector well with 4 laterals of equal length, the maximum flow occurs when angle between the laterals oriented towards the river is $\pi/3$ for $R/l_2 < 5$. For $R/l \geq 5$, flow to the collector well is the maximum for $\gamma = 0.5$.

6. For the case of a radial collector well with three radials in which one of the collectors orients perpendicularly towards the river and $l_3 = 0$, the flow to the collector well is maximum, if the other two radials are oriented at an angle $\gamma = 0.5$ for $R/l_2 < 5$; for $R/l_2 \geq 5$, the flow to the collector well is maximum if $\gamma = 2/3$.

7. The water entering to the collector pipe from river side is more than that from left side as the river is on the right hand side. In steady state condition the water comes to the collector pipes only from river.

Chapter 6

FLOW CHARACTERISTICS OF A COLLECTOR PIPE USING SHEET FLOW CONCEPT LAID ADJACENT TO THE RIVER

6.1   INTRODUCTION

In order to check the degree of accuracy in the concept of sheet flow, an exact analytical solution for computing flow to a line sink in a confined aquifer laid parallel to a river considering the thickness of the aquifer needs to be solved. Applying conformal mapping technique, an exact analytical solution for two-dimensional flow in a vertical plane normal to a collector pipe laid parallel to a fully penetrating river in the middle of a confined aquifer is presented below.

6.2   STATEMENT OF THE PROBLEM

Two collector pipes each of diameter d_p and length l_2 are laid in the middle of a confined homogeneous aquifer parallel to a fully penetrating river one each on either side of a well caisson. Each collector pipe has long length more than twice the thickness of aquifer. Objective is to find the flow characteristics of the line sink placed in the middle of the confined aquifer adjacent to the river and suggest correction factor for the assumption of sheet flow, if any. The flow can be assumed as two dimensional in any vertical plane perpendicular to the collectors' axis in the middle parts of the collector pipes.

Aravin and Numerov (1965) have analysed steady flow to a collector pipe laid under a river bed treating the collector pipe as a line sink and considering half of the flow domain on one side of the axis of symmetry. Approach suggested by Aravin and Numerov (1965) is followed in this study for solving this problem. Under unsteady flow condition, water enters to the collector pipes from aquifer storage as well as from the river. When the flow attains steady state condition, water enter to the collector pipes from the left side as well as from right side is supplied by the river only. For steady flow condition, conformal mapping can be applied conveniently to solve the Laplace equation. The idealised flow domain is shown in figure 6.1 (a). The lines AB_L and CB_R are lines of symmetry and are therefore stream lines. Considering the lines of symmetry, one can consider the lower half flow domain ACD^*A.
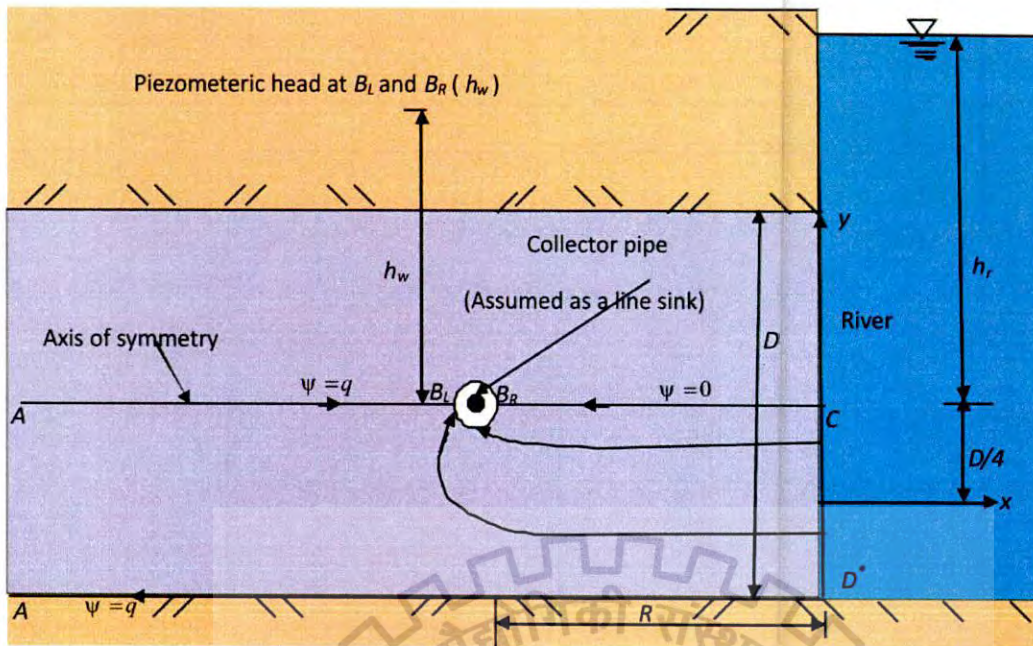
Fig. 6.1(a) Idealized Flow Domain

6.3 METHODOLOGY FOR ESTIMATION OF FLOW CHARACTERISTICS

The vertices A, C, D^*, A have been mapped onto $-\infty, -1, 1, \infty$ on the real axis of an auxiliary $t(=r+is)$ plane as shown in figure 6.1(b).
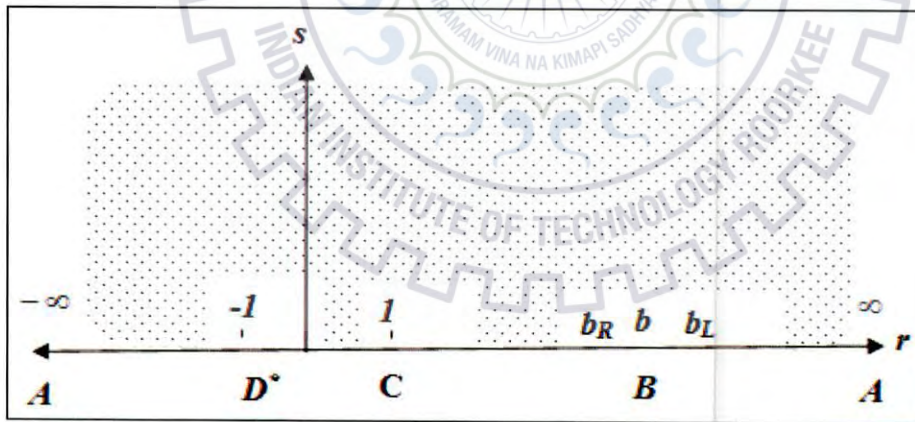
Fig. 6.1(b) Upper Half of the Auxiliary t-Plane

Mapping of the $z(=x+iy)$ plane to the upper half of the auxiliary t plane is given by:

$$\frac{dz}{dt} = \frac{M}{\sqrt{(1+t)(1-t)}} \qquad (6.1)$$

Integrating

$$z = M \int \frac{dt}{\sqrt{(1+t)(1-t)}} + N \qquad (6.2)$$

Substituting $t = \sin\theta$, $dt = \cos\theta\, d\theta$ and integrating

$$z = M\,\theta + N \qquad (6.3)$$

or

$$z = M \sin^{-1} t + N \qquad (6.4)$$

At $t = 0$, $z = 0$; hence, $N = 0$. At $t = 1$, $z = iD/4$. Applying this condition, the other constant is found to be $M = \dfrac{iD}{2\pi}$. Finally

$$z = \frac{iD}{2\pi} \sin^{-1} t \qquad (6.5)$$

or

$$t = \sin\left(\frac{2\pi z}{iD}\right) \qquad (6.6)$$

Let the line sink be located at $t = b$. Substituting $t = b$, and $z = -R + \dfrac{iD}{4}$ in (6.6),

$$b = \sin\left\{\frac{2\pi}{iD}\left(-R + \frac{iD}{4}\right)\right\} \qquad (6.7)$$

Simplifying

$$b = \cosh\left(\frac{2\pi\,R}{D}\right) \qquad (6.8)$$

Let the point B_R at a radial distance $d_p/2$ from the line sink on the right side be located at b_R on the t–plane. Substituting $z = -R + \dfrac{d_p}{2} + \dfrac{iD}{4}$ and $t = b_R$ in (6.6) and simplifying

$$b_R = \cosh\left\{\frac{2\pi}{D}\left(R - \frac{d_p}{2}\right)\right\} \qquad (6.9)$$

Let the point B_L at a radial distance $d_p/2$ from the line sink on the left side be located at b_L on the t–plane. Substituting $z = -R - \dfrac{d_p}{2} + \dfrac{iD}{4}$ and $t = b_L$ in (6.6) and simplifying

$$b_L = \cosh\left\{\frac{2\pi}{D}\left(R + \frac{d_p}{2}\right)\right\} \qquad (6.10)$$

Mapping of the $w(= \phi + i\psi)$ *plane to the upper half auxiliary* $t(= r + i s)$ *plane*

Considering the lines of symmetry, the complex potential corresponding to lower half of the flow domain is shown in figure 6.1(c). The velocity potential function has been defined as: $\phi = -k(p/\gamma_w + y) + c$; the constant c has been assumed to be equal to 0. The velocity potential ϕ at the line sink is ∞.
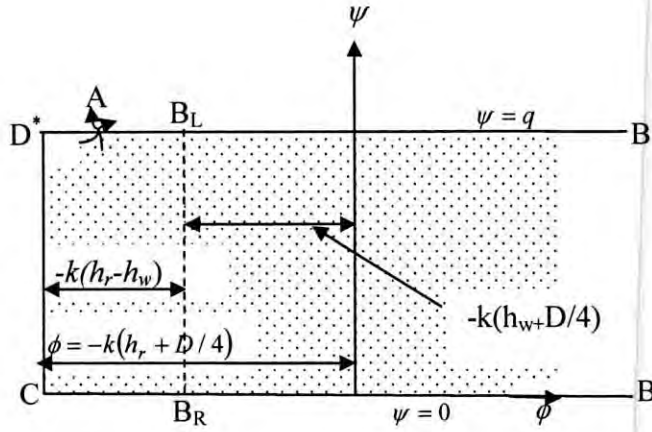
Fig. 6.1(c) Complex Potential Plane $w(=\phi+i\psi)$

The mapping of the complex potential w plane to the upper half of the auxiliary t plane is given by:

$$\frac{dw}{dt}=\frac{M_1}{(b-t)\sqrt{(1-t)(1+t)}} \tag{6.11}$$

$$w=M_1\int\frac{dt}{(b-t)\sqrt{(1-t)(1+t)}}+N_1, \quad \text{for } -1\le t\le 1 \tag{6.12}$$

Substituting $t=\sin\theta$, $dt=\cos\theta\, d\theta$ and integrating we obtain

$$w=M_1\int\frac{d\theta}{(b-\sin\theta)}+N_1 \tag{6.13}$$

Integrating (Abramowitz and Stegun, 1962, p78)

$$w=\frac{2M_1}{\sqrt{(b^2-1)}}\tan^{-1}\left\{\frac{b\tan\left(\frac{\theta}{2}\right)-1}{\sqrt{(b^2-1)}}\right\}+N_1=\frac{2M_1}{\sqrt{(b^2-1)}}\tan^{-1}\left\{\frac{b\tan\left(\frac{\sin^{-1}t}{2}\right)-1}{\sqrt{(b^2-1)}}\right\}+N_1 \tag{6.14}$$

At, $t=1$, $w=-k\left(h_r+\frac{D}{4}\right)$. Applying this condition in (6.14)

$$-k\left(h_r+\frac{D}{4}\right)=\frac{2M_1}{\sqrt{(b^2-1)}}\tan^{-1}\left\{\frac{b\tan\left(\frac{\sin^{-1}(1)}{2}\right)-1}{\sqrt{(b^2-1)}}\right\}+N_1=\frac{2M_1}{\sqrt{(b^2-1)}}\tan^{-1}\left(\sqrt{\frac{b-1}{b+1}}\right)+N_1$$

At $t=-1$, $w=-k\left(h_r+\frac{D}{4}\right)+iq$. Applying this condition in (6.14)

$$-k\left(h_r+\frac{D}{4}\right)+iq=\frac{2M_1}{\sqrt{(b^2-1)}}\tan^{-1}\left\{\frac{b\tan\left(\frac{\sin^{-1}(-1)}{2}\right)-1}{\sqrt{(b^2-1)}}\right\}+N_1$$

96

$$= -\frac{2M_1}{\sqrt{(b^2-1)}} \tan^{-1}\left(\sqrt{\frac{b+1}{b-1}}\right) + N_1 \tag{6.16}$$

Subtracting (6.15) from (6.16)

$$iq = \frac{-2M_1}{\sqrt{(b^2-1)}} \left\{ \tan^{-1}\left(\sqrt{\frac{b+1}{b-1}}\right) + \tan^{-1}\left(\sqrt{\frac{b-1}{b+1}}\right) \right\} \tag{6.17}$$

Applying the relationship $\left(\tan^{-1} A + \tan^{-1} B\right) = \tan^{-1}\left(\frac{A+B}{1-AB}\right)$ (Abramowitz and Stegun, 1970, p. 80) and simplifying

$$M_1 = -\frac{\sqrt{(b^2-1)}\,i\,q}{\pi} \tag{6.18}$$

Incorporating M_1 in (6.15) and solving for N_1

$$N_1 = \frac{2\,i\,q}{\pi} \tan^{-1}\left(\sqrt{\frac{b-1}{b+1}}\right) - k\left(h_r + \frac{D}{4}\right) \tag{6.19}$$

For $-1 \le t \le 1$, referring equation(6.14), and incorporating constants M_l and N_l, one can obtain

$$w = -\frac{i\,2q}{\pi} \tan^{-1}\left\{ \frac{b\tan\left(\dfrac{\sin^{-1}t}{2}\right) - 1}{\sqrt{(b^2-1)}} \right\} + \frac{2\,i\,q}{\pi} \tan^{-1}\left(\sqrt{\frac{b-1}{b+1}}\right) - k\left(h_r + \frac{D}{4}\right) \tag{6.20}$$

Derivation of flow per unit length (q) of the collector pipe

For $1 \le t < b$

$$\frac{dw}{dt} = -i\,\frac{\sqrt{(b^2-1)}\,q}{\pi} \cdot \frac{1}{\sqrt{-1}\,(b-t)(1+t)^{1/2}(t-1)^{1/2}} \tag{6.21}$$

$\frac{dw}{dt}$ is positive in the range $1 \le t < b$. We therefore consider $\sqrt{-1} = -i$ and obtain

$$\frac{dw}{dt} = \frac{\sqrt{(b^2-1)}\,q}{\pi} \cdot \frac{1}{(b-t)(t-1)^{1/2}(t+1)^{1/2}} \tag{6.22}$$

Integrating

$$w = \frac{\sqrt{(b^2-1)}\,q}{\pi} \int_1^{t'} \frac{dt}{(b-t)(t-1)^{1/2}(t+1)^{1/2}} - k(h_r + D/4) \tag{6.23}$$

At $t = b_R$, $w = -k(h_w + D/4)$. Hence,

97

$$-k(h_w + D/4) = \frac{\sqrt{(b^2-1)}\,q}{\pi}\int_1^{b_R}\frac{dt}{(b-t)(t-1)^{1/2}(t+1)^{1/2}} - k(h_r + D/4) \qquad (6.24)$$

$$k(h_r - h_w) = \frac{\sqrt{(b^2-1)}\,q}{\pi}\int_1^{b_R}\frac{dt}{(b-t)(t-1)^{1/2}(t+1)^{1/2}} \qquad (6.25)$$

Substituting $t = \cosh\theta$, $dt = \sinh\theta\, d\theta$, and integrating (Gradshteyn and Ryzhik,1965) the integral

$$\int_1^{b_R}\frac{dt}{(b-t)(t-1)^{1/2}(t+1)^{1/2}} = \int_0^{\cosh^{-1} b_R}\frac{d\theta}{(b-\cosh\theta)} = \frac{1}{\sqrt{(b^2-1)}}\ln\frac{b-1+\sqrt{(b^2-1)}\tanh\left(\dfrac{\cosh^{-1}b_R}{2}\right)}{b-1-\sqrt{(b^2-1)}\tanh\left(\dfrac{\cosh^{-1}b_R}{2}\right)} = I_1$$

Differentiating $\dfrac{1}{\sqrt{(b^2-1)}}\ln\dfrac{b-1+\sqrt{b^2-1}\,\tanh(\theta/2)}{b-1-\sqrt{b^2-1}\,\tanh(\theta/2)}$ we verify

that $\dfrac{d}{d\theta}\left\{\dfrac{1}{\sqrt{(b^2-1)}}\ln\dfrac{b-1+\sqrt{b^2-1}\,\tanh(\theta/2)}{b-1-\sqrt{a^2-b^2}\,\tanh(\theta/2)}\right\} = \dfrac{1}{(b-\cosh\theta)}$. Incorporating I_1 in (6.25), and

simplifying, the dimensionless total flow $\dfrac{2q}{k(h_r - h_w)}$ entering to the collector pipe both from top

and bottom sides through unit length of the pipe is given by:

$$\frac{2q}{k(h_r - h_w)} = \frac{2\pi}{\sqrt{(b^2-1)}\,I_1} = \frac{2\pi}{\ln\dfrac{b-1+\sqrt{(b^2-1)}\tanh\left(\dfrac{\cosh^{-1}b_R}{2}\right)}{b-1-\sqrt{(b^2-1)}\tanh\left(\dfrac{\cosh^{-1}b_R}{2}\right)}} \qquad (6.26)$$

The inverse $\cosh^{-1}b_R$ is computed using the logarithmic relation (Abramowitz and Stegun,

1970, p 87): $\cosh^{-1}b_R = \ln\left\{b_R + \left(b_R^2 - 1\right)^{1/2}\right\}$ $b_R \geq 1$.

Let us designate dimensionless flow per unit length of the collector pipe $\dfrac{2q}{k(h_r - h_w)}$

by Q_d. The total flow to a collector pipe of length l_2 will be $Q_d l_2$

Estimation of an entrance velocity

One has to check the entrance velocity at the periphery of the collector pipe while designing a collector well. An average entrance velocity factor, $\bar{v}_{ef}$, for the present case is given by

98

$$\bar{v}_e = 2q/(\pi \, d_p f_a) = \cfrac{2k(h_r - h_w)}{d_p f_a \ln \cfrac{b - 1 + \sqrt{(b^2 - 1)} \tanh\left(\cfrac{\cosh^{-1} b_R}{2}\right)}{b - 1 - \sqrt{(b^2 - 1)} \tanh\left(\cfrac{\cosh^{-1} b_R}{2}\right)}} \tag{6.27a}$$

in which f_a is the fraction of the peripheral area of the collector pipe perforated. A dimensionless average entrance velocity factor is given by:

$$\bar{v}_{ef} = \bar{v}_e f_a d_p / k(h_r - h_w) = \cfrac{2}{\ln \cfrac{b - 1 + \sqrt{(b^2 - 1)} \tanh\left(\cfrac{\cosh^{-1} b_R}{2}\right)}{b - 1 - \sqrt{(b^2 - 1)} \tanh\left(\cfrac{\cosh^{-1} b_R}{2}\right)}} \tag{6.27b}$$

It is also needed to check the maximum entrance velocity. Maximum entrance velocity is obtained as follows.

Dividing equation (6.11) by equation (6.1) and substituting the constants M and M_1 one can obtain

$$\frac{dw}{dt} \Big/ \frac{dz}{dt} = \frac{dw}{dt} \times \frac{dt}{dz} = \frac{dw}{dz} = \frac{-\sqrt{b^2 - 1} \, iq}{\pi \left(\dfrac{iD}{2\pi}\right)} \frac{1}{\{b - t\}} \tag{6.28a}$$

Replacing the parameter $t = \sin\left(\dfrac{2\pi z}{iD}\right)$ given in equation (6.6), and substituting $z = x + iD/4$ for $1 \leq t < b$ and further simplifying we obtain

$$\frac{dw}{dz} = u - iv = -\sqrt{b^2 - 1} \frac{2}{D} q \frac{1}{\left\{b - \cosh\left(\dfrac{2\pi x}{D}\right)\right\}} \tag{6.28b}$$

Along the horizontal stream line CB_R, the vertical component of velocity $v = 0$. Therefore, the horizontal Darcy velocity along the stream line CB_R is given by

$$u = -\sqrt{b^2 - 1} \frac{2}{D} q \frac{1}{\left\{b - \cosh\left(\dfrac{2\pi x}{D}\right)\right\}} \tag{6.29}$$

The negative sign indicates that direction of the velocity vector u is in the opposite direction of x ordinate. The modulus of entrance velocity at $x = -(R - d_p/2)$, which is the maximum entrance velocity, is

$$|u_{max}| = \frac{2q\sqrt{b^2-1}}{f_a D\left[b - \cosh\left\{-\dfrac{2\pi(R - d_p/2)}{D}\right\}\right]} = \frac{2q\sqrt{b^2-1}}{f_a D\left[b - \cosh\left\{\dfrac{2\pi(R - d_p/2)}{D}\right\}\right]}$$

$$= \frac{2\sqrt{b^2-1}}{f_a D\left[b - \cosh\left\{\dfrac{2\pi(R - d_P/2)}{D}\right\}\right]} \frac{\pi k(h_r - h_w)}{\ln\dfrac{b - 1 + \sqrt{(b^2-1)}\tanh\left(\dfrac{\cosh^{-1} b_R}{2}\right)}{b - 1 - \sqrt{(b^2-1)}\tanh\left(\dfrac{\cosh^{-1} b_R}{2}\right)}} \qquad (6.30)$$

Maximum dimensionless entrance velocity factor is defined as:

$$u_{mef} = \frac{|u_{max}| D f_a}{k(h_r - h_w)} = \frac{2\sqrt{b^2-1}}{\left[b - \cosh\left\{\dfrac{2\pi(R - d_p/2)}{D}\right\}\right]} \frac{\pi}{\ln\dfrac{b - 1 + \sqrt{(b^2-1)}\tanh\left(\dfrac{\cosh^{-1} b_R}{2}\right)}{b - 1 - \sqrt{(b^2-1)}\tanh\left(\dfrac{\cosh^{-1} b_R}{2}\right)}} \qquad (6.31)$$

Estimation of a travel time of a parcel of water

Having derived an expression for velocity, we derive next the minimum travel time of a parcel of water that moves along the shortest stream line CB_R. Using this travel time, the reduction in bacteria concentration of a parcel of water while it moves from the river to the collector well, can be ascertained with ease using production function. The true velocity is given by u/η, in which η is the porosity of the aquifer medium. The travel time dt to move along an elemental length dx is given by

$$dt = \eta \frac{dx}{u} = \eta \frac{\left(b - \cosh\dfrac{2\pi x}{D}\right)}{-\sqrt{b^2-1}\,\dfrac{2}{D}q}\, dx \qquad (6.32)$$

Integrating the travel time for a parcel of water from the river to the collector pipe is:

$$t_r = \frac{-\eta}{\sqrt{b^2-1}\,\frac{2}{D}q} \int_0^{\left(R-\frac{d_p}{2}\right)} \left(b - \cosh\frac{2\pi x}{D}\right) dx = \frac{-\eta}{\sqrt{b^2-1}} \frac{D}{2q}\left(\int_0^{\left(R-\frac{d_p}{2}\right)} b\,dx - \int_0^{\left(R-\frac{d_p}{2}\right)} \cosh\frac{2\pi x}{D}\,dx\right)$$

$$= \frac{-\eta}{\sqrt{b^2-1}} \frac{D}{2q}\left[-b\left(R-\frac{d_p}{2}\right) + \frac{D}{2\pi}\sinh\left\{\frac{2\pi}{D}\left(R-\frac{d_p}{2}\right)\right\}\right]$$

$$= \frac{\eta}{\sqrt{b^2-1}} \frac{D^2}{2q}\left[b\left(\frac{R}{D} - 0.5\frac{d_p}{D}\right) - \frac{1}{2\pi}\sinh\left\{2\pi\left(\frac{R}{D} - 0.5\frac{d_p}{D}\right)\right\}\right] \tag{6.33}$$

Incorporating q in (6.33), we derive the dimensionless time factor as t_{rf} as

$$t_{rf} = \frac{t_r k(h_r - h_w)}{\eta D^2} = \frac{1}{2\pi\sqrt{b^2-1}}\left[b\left(\frac{R}{D} - \frac{d_p}{2D}\right) - \frac{1}{2\pi}\sinh\left\{2\pi\left(\frac{R}{D} - \frac{d_p}{2D}\right)\right\}\right] \ln\frac{b-1+\sqrt{(b^2-1)}\tanh\left(\frac{\cosh^{-1}b_R}{2}\right)}{b-1-\sqrt{(b^2-1)}\tanh\left(\frac{\cosh^{-1}b_R}{2}\right)}$$

$$\tag{6.34}$$

Corresponding to the travel time t_r, the number of log cycle reduction is

$$n = \log_{10}\frac{r/\lambda_L - e^{-(r-\lambda_L)t_r}}{(r/\lambda_L)-1} \tag{6.35}$$

6.4 NEED OF A CORRECTION FACTOR

While deriving flow to a radial collector well assuming sheet flow, the thickness of aquifer, and diameter of the collector pipe are not considered. To account for the thickness of the aquifer, we multiply the flow to a collector pipe by D, the thickness of the aquifer. As the flow does not increase linearly with thickness of the aquifer, a correction factor needs to be applied. A correction factor for the specific case of two laterals, each of equal length l_2, running parallel to the river has been derived.

Let the thickness of aquifer be 1m; let us designate the flow to the collector pipe of length l_2, $q_2 / \{k(h_r - h_w)\}$, presented in Table 6.3 as Q_s.

Correction factor C_f

For deriving the correction factor C_f, considering we multiply the dimensionless flow to one of the collector pipes of length l_2, Q_s, by the thickness of the aquifer D and a correction factor C_f and equate it to the dimensionless flow Q_d multiplied by length l_2:

$$Q_s DC_f = Q_d l_2 \tag{6.36}$$

101

The correction factor is

$$C_f = \frac{Q_d l_2}{Q_S D} = \frac{Q_d}{Q_S} \frac{l_2}{R} \frac{R}{D}$$

(6.37)

For given $\dfrac{R}{l_2}$, Q_s values are derived. Further, for given $\dfrac{R}{D}$ and $\dfrac{d_p}{D}$, Q_d is obtained. Using these, the value of correction factor C_f is obtained.

6.5 RESULTS AND DISCUSSIONS

For obtaining result, the programme needs to adopt double precision. The parameter b is a function of R/D and b_R is a function of R/D and d_p/D. One has to present the flow characteristics for $D=10$m, and $d_p=1$m in Table 6.1. It is found that for $R/D > 5.5$, $b > 5.09 \times 10^{14}$ and $b_R > 3.72 \times 10^{14}$. For very large value of b_R, the term $\tanh\left(\dfrac{\cosh^{-1} b_R}{2}\right)$ appearing in equation (6.26) becomes very nearly equals to 1 and the term $b - 1 - \sqrt{(b^2 - 1)} \tanh\left(\dfrac{\cosh^{-1} b_R}{2}\right)$ becomes a negative quantity, thereby making the logarithmic term an imaginary number. In this study, a numerical method for evaluating the integral $I_1 = \displaystyle\int_0^{\cosh^{-1} b_R} \dfrac{d\theta}{(b - \cosh\theta)}$ and Gauss Quadrature technique are adopted. In Gauss Quadrature, since the integration is not carried up to the upper limit of integration exactly, it becomes feasible for evaluation of the integral for comparatively higher value of R/D.

The following procedure is adopted for evaluating I_1. Since $\cosh^{-1} b_R > 1$

$$\int_0^{\cosh^{-1} b_R} \frac{d\theta}{(b - \cosh\theta)} = \int_0^1 \frac{d\theta}{(b - \cosh\theta)} + \int_1^{\cosh^{-1} b_R} \frac{d\theta}{(b - \cosh\theta)};$$

$$\int_1^{\cosh^{-1} b_R} \frac{d\theta}{(b - \cosh\theta)} = \int_{1/\cosh^{-1} b_R}^1 \frac{d\varphi}{\varphi^2 (b - \cosh(1/\varphi))}$$

$$= \int_{1/\cosh^{-1} b_R}^{1/\cosh^{-1} b_R + 0.1} \frac{d\varphi}{\varphi^2 (b - \cosh(1/\varphi))} + \int_{1/\cosh^{-1} b_R + 0.1}^{1/\cosh^{-1} b_R + 0.2} \frac{d\varphi}{\varphi^2 (b - \cosh(1/\varphi))}$$

$$+ \int_{1/\cosh^{-1} b_R + 0.2}^{1/\cosh^{-1} b_R + 0.3} \frac{d\varphi}{\varphi^2 (b - \cosh(1/\varphi))} + \int_{1/\cosh^{-1} b_R + 0.3}^{1/\cosh^{-1} b_R + 0.4} \frac{d\varphi}{\varphi^2 (b - \cosh(1/\varphi))} + \int_{1/\cosh^{-1} b_R + 0.4}^{1/\cosh^{-1} b_R + 0.5} \frac{d\varphi}{\varphi^2 (b - \cosh(1/\varphi))}$$

$$+ \int_{1/\cosh^{-1} b_R + 0.5}^{1} \frac{d\varphi}{\varphi^2 \left(b - \cosh(1/\varphi)\right)}$$

Gauss Quadrature considering 96 weights for evaluating each integral after changing the lower and upper limits of each integral to -1 to 1 has been adopted in this study.

Table 6.1 Comparison of Analytical and Numerical Methods for evaluation of I_1 and Dimensionless Flow Characteristics computed for $D=10m$ and $d_p=1m$

R/l_2	R/D	B	b_R	Q_D	Q_S	$\bar{v}_{ef}$	u_{mef}	t_{rf}	C_f	Method
0.4	1	2.68E+02	1.96E+02	0.8631	3.8157	1.7171	3.2014	0.966	0.5655	A^*
				0.8631	3.8157	1.7171	3.2014	0.966	0.5655	N^*
0.8	2	1.43E+05	1.05E+05	0.4633	2.4108	0.9216	1.7183	3.9584	0.4804	A
				0.4633	2.4108	0.9216	1.7183	3.9584	0.4804	N
1.2	3	7.68E+07	5.61E+07	0.3166	1.914	0.6298	1.1743	8.9508	0.4135	A
				0.3166	1.914	0.6298	1.1743	8.9508	0.4135	N
1.6	4	4.11E+10	3.00E+10	0.2405	1.6533	0.4784	0.8919	15.9431	0.3636	A
				0.2405	1.6533	0.4784	0.8919	15.9431	0.3636	N
2	5	2.20E+13	1.61E+13	0.1938	1.4899	0.3856	0.7189	24.9395	0.3252	A
				0.1939	1.4899	0.3857	0.719	24.9355	0.3253	N
2.2	5.5	5.09E+14	3.72E+14	0.1768	1.4286	0.3517	0.6558	30.1683	0.3094	A
				0.1767	1.4286	0.3516	0.6555	30.1817	0.3093	N
2.4	6	1.18E+16	8.61E+15	—	—	—	—	—	—	A
				0.124	1.3765	0.3230	0.6023	35.9279	0.2949	N

A^*=Analytical method; N^*=Numerical method

Table 6.2 Dimensionless Flow Characteristics computed for $D=10m$ and $d_p=1m$ adopting Numerical Method for Integration

R/l_2	R/D	Q_D	Q_S	$\bar{v}_{ef}$	u_{mef}	t_{rf}	C_f
1	2.5	0.3761	2.1158	0.7483	1.3952	6.2046	0.4444
2	5	0.1939	1.4899	0.3857	0.719	24.9355	0.3253
3	7.5	0.1306	1.2575	0.2598	0.4843	56.1664	0.2596
4	10	0.0984	1.13	0.1958	0.3651	99.8974	0.2178
5	12.5	0.079	1.047	0.1572	0.293	156.1283	0.1886
6	15	0.066	0.9875	0.1312	0.2447	224.8594	0.167
7	17.5	0.0571	0.9421	0.1137	0.2119	303.3813	0.1516
8	20	0.05	0.906	0.0995	0.1854	396.7145	0.138
9	22.5	0.0444	0.8763	0.0884	0.1648	502.5476	0.1268
10	25	0.04	0.8514	0.0796	0.1484	620.8806	0.1175
11	27.5	0.0364	0.83	0.0723	0.1349	751.7135	0.1095
12	30	0.0333	0.8113	0.0663	0.1236	895.0467	0.1027
13	32.5	0.0308	0.7949	0.0612	0.1141	1050.879	0.0968
14	35	0.0286	0.7803	0.0568	0.106	1219.212	0.0915
15	37.5	0.0267	0.7672	0.0531	0.0989	1400.043	0.0869
16	40	0.025	0.7553	0.0497	0.0927	1593.372	0.0827
17	42.5	0.0235	0.7445	0.0468	0.0873	1799.201	0.079
18	45	0.0222	0.7345	0.0442	0.0824	2017.526	0.0756

R/l_2	R/D	Q_D	Q_S	$\bar{v}_{ef}$	u_{mef}	t_{rf}	C_f
19	47.5	0.0211	0.7254	0.0419	0.0781	2248.348	0.0726
20	50	0.02	0.7169	0.0398	0.0742	2491.666	0.0697

Table 6.3 Dimensionless Flow Characteristics computed for D=5m and d_p=1m adopting Numerical Method for Integration

R/l_2	R/D	Q_D	Q_S	$\bar{v}_{ef}$	u_{mef}	t_{rf}	C_f
1	5	0.1991	2.1158	0.3962	0.4269	24.1783	0.4706
2	10	0.0998	1.4899	0.1985	0.2139	98.3605	0.3349
3	15	0.0666	1.2575	0.1324	0.1427	222.5428	0.2647
4	20	0.0503	1.13	0.1001	0.1079	393.6213	0.2228
5	25	0.0402	1.047	0.08	0.0862	617.0079	0.1921
6	30	0.0335	0.9875	0.0666	0.0718	890.3945	0.1696
7	35	0.0287	0.9421	0.0571	0.0615	1213.781	0.1522
8	40	0.0251	0.906	0.0499	0.0538	1587.167	0.1384
9	45	0.0223	0.8763	0.0443	0.0478	2010.553	0.1272
10	50	0.0201	0.8514	0.0399	0.043	2483.937	0.1178

Table 6.4 Dimensionless Flow Characteristics computed for D=10m and d_p=0.5m adopting Numerical Method for Integration

R/l_2	R/D	Q_D	Q_S	$\bar{v}_{ef}$	u_{mef}	t_{rf}	C_f
1	2.5	0.3595	2.1158	1.4303	2.4728	6.5069	0.4247
2	5	0.1893	1.4899	0.7533	1.3024	25.5592	0.3177
3	7.5	0.1285	1.2575	0.5113	0.884	57.1114	0.2555
4	10	0.0973	1.13	0.387	0.6691	101.1637	0.2152
5	12.5	0.0782	1.047	0.3113	0.5382	157.716	0.1868
6	15	0.0654	0.9875	0.2604	0.4502	226.7684	0.1657
7	17.5	0.0567	0.9421	0.2257	0.3903	305.6109	0.1506
8	20	0.0497	0.906	0.1977	0.3418	399.265	0.1371
9	22.5	0.0442	0.8763	0.1759	0.3041	505.4194	0.1261
10	25	0.0398	0.8514	0.1584	0.2738	624.073	0.1169
11	27.5	0.0362	0.83	0.144	0.249	755.2249	0.109
12	30	0.0332	0.8113	0.1321	0.2284	898.875	0.1023
13	32.5	0.0307	0.7949	0.122	0.2109	1055.021	0.0964
14	35	0.0285	0.7803	0.1133	0.1959	1223.662	0.0912
15	37.5	0.0266	0.7672	0.1058	0.1828	1404.795	0.0866
16	40	0.0249	0.7553	0.0992	0.1715	1598.42	0.0825
17	42.5	0.0235	0.7445	0.0934	0.1614	1804.532	0.0788
18	45	0.0222	0.7345	0.0882	0.1525	2023.13	0.0754
19	47.5	0.021	0.7254	0.0836	0.1445	2254.215	0.0724
20	50	0.02	0.7169	0.0794	0.1373	2497.78	0.0696

Table 6.5 Dimensionless Flow Characteristics computed for *D*=5m and *d_p*=0.5m Adopting Numerical Method for Integration

R/l_2	R/D	Q_D	Q_S	$\bar{v}_{ef}$	u_{mef}	t_{rf}	C_f
1	5	0.1939	2.1158	0.7713	0.719	24.9355	0.4581
2	10	0.0984	1.4899	0.3917	0.3651	99.8974	0.3303
3	15	0.066	1.2575	0.2625	0.2447	224.8594	0.2623
4	20	0.05	1.13	0.1989	0.1854	396.7145	0.2212
5	25	0.04	1.047	0.1591	0.1484	620.8806	0.191
6	30	0.0333	0.9875	0.1326	0.1236	895.0467	0.1688
7	35	0.0286	0.9421	0.1137	0.106	1219.212	0.1516
8	40	0.025	0.906	0.0995	0.0927	1593.372	0.138
9	45	0.0222	0.8763	0.0884	0.0824	2017.526	0.1268
10	50	0.02	0.8514	0.0796	0.0742	2491.666	0.1175

Table 6.6 Dimensionless Flow Characteristics computed for D=10m and *d_p*=0.3m adopting Numerical Method for Integration

R/l_2	R/D	Q_D	Q_S	$\bar{v}_{ef}$	u_{mef}	t_{rf}	C_f
1	2.5	0.3486	2.1158	2.312	3.8762	6.7124	0.4119
2	5	0.1863	1.4899	1.2353	2.0711	25.9836	0.3126
3	7.5	0.1271	1.2575	0.8428	1.413	57.7549	0.2527
4	10	0.0964	1.13	0.6396	1.0723	102.0261	0.2134
5	12.5	0.0777	1.047	0.5153	0.864	158.7973	0.1856
6	15	0.0651	0.9875	0.4315	0.7234	228.0688	0.1647
7	17.5	0.0565	0.9421	0.3744	0.6277	307.1295	0.1498
8	20	0.0495	0.906	0.3281	0.5501	401.0016	0.1365
9	22.5	0.044	0.8763	0.292	0.4895	507.372	0.1256
10	25	0.0397	0.8514	0.263	0.441	626.2386	0.1165
11	27.5	0.0361	0.83	0.2393	0.4012	757.5982	0.1087
12	30	0.0331	0.8113	0.2195	0.368	901.447	0.102
13	32.5	0.0306	0.7949	0.2027	0.3399	1057.783	0.0962
14	35	0.0284	0.7803	0.1884	0.3158	1226.602	0.091
15	37.5	0.0265	0.7672	0.1759	0.2949	1407.9	0.0864
16	40	0.0249	0.7553	0.165	0.2766	1601.676	0.0823
17	42.5	0.0234	0.7445	0.1553	0.2604	1807.927	0.0786
18	45	0.0221	0.7345	0.1467	0.246	2026.648	0.0753
19	47.5	0.021	0.7254	0.139	0.2331	2257.842	0.0723
20	50	0.0199	0.7169	0.1321	0.2215	2501.505	0.0695

Table 6.7 Dimensionless Flow Characteristics computed for *D=5m* and *d$_p$=0.3m* adopting Numerical Method for Integration

R/l_2	R/D	Q_D	Q_S	$\bar{v}_{ef}$	u_{mef}	t_{rf}	C_f
1	5	0.1905	2.1158	1.2631	1.1087	25.4021	0.4501
2	10	0.0976	1.4899	0.6469	0.5679	100.8448	0.3274
3	15	0.0656	1.2575	0.4348	0.3817	226.2875	0.2607
4	20	0.0498	1.13	0.33	0.2897	398.6226	0.2202
5	25	0.0399	1.047	0.2643	0.232	623.2695	0.1903
6	30	0.0332	0.9875	0.2204	0.1934	897.9133	0.1683
7	35	0.0285	0.9421	0.189	0.1659	1222.548	0.1512
8	40	0.0249	0.906	0.1654	0.1452	1597.164	0.1377
9	45	0.0222	0.8763	0.1471	0.1291	2021.75	0.1265
10	50	0.02	0.8514	0.1324	0.1162	2496.291	0.1173

The dimensionless flow per unit length of collector, Q_D, is a function of d_p/D, R/D and the dimensionless flow Q_s is only a function of R/l_2. The dimensionless flow Q_D, and Q_s and other flow characteristics are presented in Tables 6.2 to 6.7 for various values of R/D and R/l_2 for $d_p = \{1, 0.5, 0.3\}$ m and $D = \{10,5\}$ m. As expected, flow to the collector pipe for given d_p/D decreases as the distance between river and the pipe laid parallel to the river increases. For a large value of R, the hydraulic gradient approaches $(h_r - h_w)/R$; hence, the dimensionless flow $Q_D \to (D/R)$. For $R/D = 50$, $d_p = 0.3m$, $Q_D = 0.0199 \cong (D/R)$. For other values of d_p, for $R/D = 50$, $Q_D = 0.02$. We, therefore, confirm that the solution presented is correct.

The correction factor increases marginally as the thickness of aquifer decreases. It decreases as the distance of the collector from the riverbank increases. As the correction factor is very much less than 1, Broom's postulation $\phi = -kD(p/\gamma_w + y) + C^*$ for computation of flow characteristics estimated using sheet flow concept overestimates the yield of collector pipe and needs a correction factor. The derived correction factors may be applied to the yield of collector wells with collector pipes more than 2, those are obtained using sheet flow concept.

An illustrative example:

Compute yield of a collector well having two radials each of 25m length running parallel to the river axis at a distance of 250m from the river bank? The diameter of the collector pipes is 1m, and the pipes are laid in the middle of the aquifer. The thickness of the aquifer is 10m.The hydraulic conductivity of the aquifer material comprising of silt sand is 1.73 m/day, Harr (1962). The effective porosity of the aquifer medium is 0.3. A drawdown of 5m is

106

maintained in the well caisson. Compute the yield of the collector well and the maximum entrance velocity. The collector pipe has 16% opening area. Also find the log cycle reduction in Bacteria concentration by the time a parcel of water moves from the river to the collector pipe.

Step of computation

Corresponding to $R/l_2 = 10$, $R/D = 25$ from Table 6.2, the dimensionless flow to the collector of 25m length, $Q_s = q_2/\{k(h_r - h_w)\} = 0.8514$, and the correction factor $C_f = 0.1175$. The total flow, Q, to both collectors is given by:

$$Q = 2 Q_s D C_f k(h_r - h_w) = 2 \times 0.8514 \times 10 \times 0.1175 \times 1.73 \times 5 = 17.31 \ \left(m^3/day\right)$$

For getting requisite quantity, several parallel collectors perpendicular to the river axis which can be connected to a common caisson on the river bank can be installed.

The maximum entrance velocity v_{em} is computed as follows: From Table 6.2 for $R/l_2 = 10, R/D = 25$, $u_{mef} = \dfrac{|u_{max}| D f_a}{k(h_r - h_w)} = 0.1484$. Hence, $|u_{max}| = \dfrac{u_{mef} k(h_r - h_w)}{D f_a}$

$= 0.1484 \times 1.73 \times 5/(10 \times 0.16) = 8.01 \ (m/day) = 0.01cm/\sec < 3cm/\sec$. The maximum entrance velocity is within safe limit.

The dimensionless travel time $t_{rf} = \dfrac{t_r k(h_r - h_w)}{\eta D^2} = 620.88$;

hence, $t_r = 620.88 \times 0.3 \times 10^2/(1.73 \times 5) = 2153.34 \, days$. Corresponding to the travel time the number of log cycle reduction is 94. This indicates that the water will be free from pathogenic bacteria when the collector pipe is laid 250m away from river bank.

6.6 CONCLUSIONS

Based on the study the following conclusions are drawn:

1. The yield of collector well increases as it is located nearer to the water body, it also increases with increase in length and diameter of the collector pipe.

2. A collector well having two collinear laterals each of 25 m length running parallel to the river axis in a confined aquifer of 10m thickness comprising of silt sand can yield $17.31m^3$ /day while located at a distance of 250 m. In such geological situation, several parallel pipes are required to be installed to a common caisson to get desired quantity of filtered water.

3. The correction factor has been determined exactly. For $R/l_2 = 10$, $R/D = 25$, $D = 10m$, $d_p = 1m$, the correction factor $C_f = 0.1175$. For $R/l_2 = 5$, $R/D = 25$, $D = 5m$, $d_p = 1m$, $C_f = 0.1921$. As the correction factor C_f is very

much less than 1, Broom's postulation $\phi = -kD\left(p/\gamma_w + y\right) + C^*$ overestimates flow to the collector system in case the flow is computed based on sheet flow concept.

4. In lieu of correction factor for collector with multiple radials, the present correction factor can be applied.

CONCUSIONS AND SCOPE FOR FUTURE WORK

7.1   CONCLUSIONS

Providing safe and adequate drinking water to the masses has been an important activity for any water utility. Riverbed and riverbank filtration are gaining importance as most of the cities in various parts of the world are expanding on the banks of rivers which are getting polluted due to various anthropogenic activities. However, not much work has been reported in literature for analyzing the problems of riverbed and riverbank filtration mathematically. Aravin and Numerov (1965) have done pioneering work in this direction and have suggested an analytical solution for computing velocity potential and flow to a collector pipe which is placed under a riverbed in homogeneous medium of infinite areal extent. They have identified a relationship between the yield (Q) and various aquifer and physical parameters such as hydraulic conductivity (k), porosity (η), drawdown in the well caisson (D_w), thickness of river bed (D), height above the impervious base at which the collector pipe is laid (d_1), and the length of lateral (l). Mishra and Kansal (2005) have suggested an analytical solution for computing the yield and entrance velocity to a collector pipe placed adjacent to a fully penetrating straight and meandering river reach.

In the present study, applying conformal mapping, the flow characteristics in respect of collector pipes having various cross-sections, have been analyzed. The collector pipe has been treated as a line sink for a circular pipe. The collector which is assumed to be a vertical slit and the collector with square cross section are assumed to have finite potential boundary. The travel time along the shortest path from the river bed to the collector pipe has been analytically determined in the present study. The log cycle reduction in bacteria concentration during travel time has been obtained using Logistic function. The present study, identifies analytical solution based on the Schwartz-Christoffel conformal transformation for computing flow characteristics such as flow, entrance velocity, travel time, and number of log cycle reduction in bacteria concentration under steady state condition in respect of a collector pipe laid under a riverbed. Further, analytical solution has also been suggested for multi-collector pipes with different orientations placed adjacent to fully penetrating straight river reach. The suggested philosophy is illustrated with the help of various examples.

For example, in sandy silt riverbed material having hydraulic conductivity of 0.0864m/day and porosity is 30%, when a line sink collector pipe of 25m length and 0.5m diameter placed at a height of 5m above the impervious base in a riverbed of 10m thickness and the collector pipe has 16% opening area, if a drawdown of 4m is maintained in the well caisson, then, using Aravin and Numerov (1965) method it will yield about $13.95m^3$/day. The same example is solved for collector pipes having finite potential boundary. The yield comes out to be exactly the same. In addition to the yield, the present study also computes the entrance velocity, travel time, and the number of log cycle reduction in bacterial concentration. For example, for this illustrative example, the maximum entrance velocity is 0.00267cm/s and the average entrance velocity is 0.00257cm/s. Magnitude of the average entrance velocity is well below the maximum entrance velocity of 4cm/s. The travel time corresponding to $\eta = 0.3$ is 25.7days. The log cycle reduction n using equation (B.7) is about 1.57. This means the initial bacterial concentration in river water (C_o) will reduce to $C_o*10^{-1.57}$ during water travel from riverbed to the collector pipe.

While carrying out the analysis, one of the challenging stages was to handle the mathematical expressions, which involve elliptic integrals. Further, analytical solution for finding the conformal mapping parameters involve a set of implicit non-linear equations and cannot be easily obtained. The Newton Raphson iterative method has been used to obtain the solution of the non-linear equations for various conformal mapping parameters. The Gaussian-Quadrature method is used to evaluate the improper integrals after applying method of substitution. Based on the derivation of flow characteristics and dimensionless factors in this study, the following inferences are drawn:

Yield of a collector pipe is linearly proportional to

    (i) hydraulic conductivity of the river bed material,

    (ii) drawdown in the well caisson,

    (iii)length of the collector pipe, and

non-linearly dependent on

    (i) the diameter of the collector

    (ii) thickness of the riverbed,

    (iii) height above the impervious base at which the collector pipe is laid.

The entrance velocity is linearly proportional to

    (i) hydraulic conductivity of the riverbed material,

    (ii) drawdown in the well caisson, and

non-linearly dependent on:

(i) the diameter of the collector,

(ii) thickness of the riverbed,

(iii) height above the impervious base at which the collector pipe is laid, and inversely proportional to the fraction of peripheral area perforated.

It has been noticed that for wide range of hydraulic conductivity of the aquifer material, the maximum entrance velocity is less than 4cm/s.

The minimum travel time is directly proportional to porosity of the bed material, square of the riverbed thickness and inversely proportional to hydraulic conductivity of the porous medium in the riverbed and drawdown in the well caisson.

The flow to a multi-collector pipes dependent upon the orientations of collector pipes. In case of a radial collector well with 4 laterals of equal length, the maximum flow occurs when angle between the collector pipes oriented towards the river is $\dfrac{\pi}{3}$ for $\dfrac{R}{l_2} < 5$. For $\dfrac{R}{l_2} \geq 5$, flow to the collector well is the maximum for $\gamma = 0.5$. For the case of a radial collector well with three radials in which one of the collectors orients perpendicularly towards the river and l_3, the flow to the collector well is maximum, if the other two collector pipes are oriented at an angle $\gamma = 0.5$ for $\dfrac{R}{l_2} < 5$; for $\dfrac{R}{l_2} \geq 5$, the flow to the collector well is maximum if $\gamma = \dfrac{2}{3}$.

It is obvious that the water entering to the collector pipe from the river side is more than that from left side of the collector pipe. However, it may be noticed that under steady state condition, the water comes to the collector pipes only from the river side. The present study identifies the analytical solution based on the Schwartz-Christoffel conformal transformation for computing yield of a collector well having two radials each of 25m length running parallel to the river axis at distance of 250m from the riverbank. The correction factor has been determined exactly. As the correction factor C_f is very much less than 1, it may be concluded that the Broom's postulation $\phi = -kD\left(p / \gamma_w + y\right) + C^*$ overestimates flow to the collector system.

7.2 LIMITATIONS AND SCOPE FOR FUTURE WORK

The present study has been carried out under certain assumptions and therefore has following limitations:

111

1. Flow is considered as steady state. However, in actual practice the flow may be under unsteady condition.

2. Aquifer material is assumed as homogeneous and isotropic, whereas, in practice it can be non-homogenous and anisotropic.

3. Flow is considered two dimensional only and satisfies the Laplace equation. However, flow can be three dimensional.

4. The head loss in collector pipe is neglected.

Therefore, one can carry out further research while addressing the above assumptions / limitations. Also, one can carry out the following works to strengthen the suggested philosophy:

1. One can carry out the numerical modelling for the riverbed and riverbank filtration process and check the results with the actual values observed in the field for a real time case study.

2. One can carry out the analysis for estimating the safe distance of collector pipe from the river considering dispersion, adsorption and decay of pollutants.

3. One can consider the various flow regimes like laminar, turbulent and transitional in the collector pipe.

4. One can consider the coupled well-pipe-aquifer hydraulics problem in homogeneous/ non-homogenous porous media.

REFERENCES

1. Abramowitz, M., & Stegun, I. A. (Eds.). (1964). Handbook of mathematical functions: with formulas, graphs, and mathematical tables (No. 55). Courier Corporation p. 1-1044.

2. Aravin, V. I., & Numerov, S. N. (1965). Theory of fluid flow in undeformable porous media. A. A. Moscona (Ed.). Israel Program for Scientific Translations p. 1-511.

3. Bakker, M., Kelson, V. A., & Luther, K. H. (2005). Multilayer analytic element modeling of radial collector wells. Groundwater, 43(6), 926-934.

4. Bear, J. (1972). Dynamics of fluids in porous media. New York. London and Amsterdam: American Elsevier.

5. Berger, P. (2002). Removal of Cryptosporidium using bank filtration. In Riverbank filtration: Understanding contaminant biogeochemistry and pathogen removal (pp. 85-121). Springer Netherlands.

6. Blair, A. H. (1970). Well Screens and Gravel Packsa. Groundwater, 8(1), 10-21.

7. Broom, M. E. (1968). Ground-water resources of Wood County, texas. tex water develop board rep 79, 84 p, Aug. 1968.

8. Byrd, P. F., & Friedman, M. D. (1954). Handbook of elliptic integrals for engeneers and physicists, Springer-Verlag, Berlin.

9. Debrine, B. E. (1970). Electrolytic model study for collector wells under river beds. Water Resources Research, 6(3), 971-978.

10. Dillon, P. J., Miller, M., Fallowfield, H., & Hutson, J. (2002). The potential of riverbank filtration for drinking water supplies in relation to microsystin removal in brackish aquifers. Journal of Hydrology, 266(3), 209-221.

11. Doussan, C., Poitevin, G., Ledoux, E., & Detay, M. (1997). River bank filtration: modelling of the changes in water chemistry with emphasis on nitrogen species. Journal of Contaminant Hydrology, 25(1), 129-156.

12. Driscoll, F. G. (1986). Groundwater and wells. St. Paul, Minnesota: Johnson Filtration Systems Inc., 1986, 2nd ed., 1.

13. Fahimuddin, M. (2007). Performance assessment of a radial collector well near a stream. Ph.D. thesis, Indian Institute of Technology at Roorkee, Roorkee, India.

14. Fitts, C. R. (2002). Groundwater science. Academic Press.

15. Gerba, C. P., Melnick, J. L., & Wallis, C. (1975). Fate of wastewater bacteria and viruses in soil. Journal of the irrigation and drainage division, 101(3), 157-174.

16. Gerritse, R. G. (1998). Biogeochemical changes in aquifers from injected waste water (No. 16/98). CSIRO Land and Water Report.

17. Goldschneider, A. A., Haralampides, K. A., & MacQuarrie, K. T. (2007). River sediment and flow characteristics near a bank filtration water supply: Implications for riverbed clogging. Journal of Hydrology, 344(1), 55-69.

18. Gollnitz, W.D., Clancy, J.L., Whitteberry, B.L., Vogt, J.A., 2003. RBF as a microbial treatment process. J. Am. Water Works Assoc. 95 (12), 56–66.

19. Gradshteyn, I. S., & Ryzhik I. M. 1965). Tables of Integrals, Series and Products, Academic Press, New York.

20. Grischek, T., Schoenheinz, D., & Ray, C. (2003). Siting and design issues for riverbank filtration schemes. In Riverbank Filtration (pp. 291-302). Springer Netherlands.

21. Grischek, T., Schoenheinz, D., Sandhu, C., & Hiscock, K. M. (2005). River bank filtration: its worth in Europe and India. J Indian Water Resour Soc, 25(2), 25-30.

22. Halek, V., and Svec, J. (1979). G.roundwater Hydraulics, Elsevier, New York.

23. Hantush, M. S. (1964). Hydraulics of wells. Advances in hydroscience, V.T.Chow, Ed., Academic Press, New York, Vol. 1, 339-340.

24. Hantush, M. S., & Papadopulos, I. S. (1962). Flow of ground water to collector wells. Journal of the Hydraulics Division, 88(5), 221-244.

25. Harbaugh, A.W., McDonald, M.G., 1996. User's documentation for MODFLOW-96, an update to the US Geological Survey modular finite-difference ground-water flow model. US Geol. Surv., Open-File Rep. 96-485, 56.

26. Harr, M. E. (1962). Groundwater and seepage. McGrawHill Book Company, New York.

27. Hiscock, K. M., & Grischek, T. (2002). Attenuation of groundwater pollution by bank filtration. Journal of Hydrology, 266(3), 139-144.

28. Hülshoff, I., Greskowiak, J., Wiese, B., & Grützmacher, G. (2009). Relevance and opportunities of riverbank filtration to provide safe water for developing and newly industrialised countries. TECHNEAU Integrated Project, European Commission. Report D, 5(9).

29. Huisman, L. (1972). Groundwater Recovery. Winchester Press, New York.

30. Huisman, L., & Olsthoorn, T. N. (1983). Artificial Groundwater Recharge. Pitman, Boston, 320p.

31. Hunt, B. (1983). Mathematical analysis of groundwater resources. Butterworth's, London, U.K.

32. Hunt, B. (2005). Flow to vertical and non-vertical wells in leaky aquifers. Journal of hydrologic engineering, 10(6), 477-484.

33. Hunt, H. (2003). American experience in installing horizontal collector wells. In Riverbank Filtration (pp. 29-34). Springer Netherlands.

34. Irmscher, R., & Teermann, I. (2002). Riverbank filtration for drinking water supply-a proven method, perfect to face todays challenges. Water Supply, 2(5-6), 1-8.

35. IS: 3955 (1967), Indian Standard Code of Practice of Design and Construction of well foundation, Bureau of Indian Standards, New Delhi.

36. Joshi, S. D. (1991). Horizontal well technology. Penn Well Books.

37. Kansal, M.L, Mishra, G.C. and Bishnoi Kailash., (2012). Radial collector well as an alternate source of water supply – a case study. Journal of CSIR, Vol.20(1), 30-35.

38. Kawecki, M. W. (2000). Transient flow to a horizontal water well. Groundwater, 38(6), 842-850.

39. Kelson, V. (2012). Predicting collector well yields with MODFLOW. Groundwater, 50(6), 918-926.

40. Kim, S. H., Ahn, K. H., & Ray, C. (2008). Distribution of discharge intensity along small-diameter collector well laterals in a model riverbed filtration. Journal of irrigation and drainage engineering, 134(4), 493-500.

41. Knappett, P. S., Emelko, M. B., Zhuang, J., & McKay, L. D. (2008). Transport and retention of a bacteriophage and microspheres in saturated, angular porous media: Effects of ionic strength and grain size. water research, 42(16), 4368-4378.

42. Knappett, P.S.K., (2006). Evaluation of effects of gain size and divalent cation concentration on the attenuation of virus and microspheres through crushed silica. Masters thesis, Department of Civil Engineering, University of Waterloo, Waterloo, Ontario, Canada.

43. Kompani-Zare, M., Zhan, H., & Samani, N. (2005). Analytical study of capture zone of a horizontal well in a confined aquifer. Journal of hydrology, 307(1), 48-59.

44. Kothyari, U. C. (2007). Indian practice on estimation of scour around bridge piers—A comment. Sadhana, 32(3), 187-197.

45. Kothyari, U. C., Garde, R. C. J., & Ranga Raju, K. G. (1992). Temporal variation of scour around circular bridge piers. Journal of Hydraulic Engineering, 118(8), 1091-1106.

46. Kuehn, W., Mueller, U., 2000. Riverbank filtration: an overview.J. Am. Water Works Assoc. 92 (12), 60–69

47. Lacey, G. (1929). Stable channels in alluviums. J. Institution of Engineers, Paper No. 4736, 229.

48. Lacey, G. (1946). A general theory of flow in alluvium. Journal of the ICE, 27(1), 16-47.

116

49. Lancellotta, R. (2008). Geotechnical engineering. CRC Press.

50. Li, W. H. (1954). Interaction between well and aquifer. Proa. ASCE, 80.

51. Milojevic, M. (1963). Radial Collector Wells Adjacent to the River Banks. Journal of the Hydraulics Division, 89(6), 133-151.

52. Mishra, G. C., & Fahimuddin, M. (2005). Stream multi aquifer well interactions. Journal of irrigation and drainage engineering, 131(5), 433-439.

53. Mishra, G.C., and Kansal, M.L., (2005). Radial collector well as an alternate source of water supply – a case study. Jornal of Indian Building Congress, 12(1), 3-12.

54. MKnappett, P. S., Emelko, M. B., Zhuang, J., & McKay, L. D. (2008). Transport and retention of a bacteriophage and microspheres in saturated, angular porous media: Effects of ionic strength and grain size. water research, 42(16), 4368-4378.g

55. Mohamed, A., & Rushton, K. (2006). Horizontal wells in shallow aquifers: field experiment and numerical model. Journal of hydrology, 329(1), 98-109.

56. Park, E., & Zhan, H. (2002). Hydraulics of a finite-diameter horizontal well with wellbore storage and skin effect. Advances in water resources, 25(4), 389 - 400.

57. Park, E., & Zhan, H. (2003). Hydraulics of horizontal wells in fractured shallow aquifer systems. Journal of hydrology, 281(1), 147-158.

58. Patel, H. M., Eldho, T. I., & Rastogi, A. K. (2010). Simulation of radial collector well in shallow alluvial riverbed aquifer using analytic element method. Journal of irrigation and drainage engineering, 136(2), 107-119.

59. Patel, H. M., Shah, C. R., & Shah, D. L. (1998). Modeling of radial collector well for sustained yield: a case study. In Proc int conf MODFLOW (Vol. 98, pp. 97-103).

60. Polubarinova-Kochina, P.Ya., 1962. Theory of Groundwater Movement. Princeton University Press, Princeton, NJ.

61. Raghunath, H. M., 2007. Ground Water. New Age International Publishers, India.

62. Ray, C. (2008). Worldwide potential of riverbank filtration. Clean Technologies and Environmental Policy, 10(3), 223-225.

63. Ray, C. (Ed.). (2002). Riverbank Filtration: Understanding Contaminant Biogeochemistry and Pathogen Removal: Understanding Contaminat Biogeochemistry and Pathogen Removal;[proceedings of the NATO Advanced Research Workshop on Riverbank Filtration: Understanding Contaminant Biogeochemistry and Pathogen Removal, Tihany, Hungary, 5-8 September 2001] (Vol. 14). Springer Science & Business Media.

64. Ray, C., & Shamrukh, M. (Eds.). (2010). Riverbank filtration for water security in desert countries. Springer Science & Business Media.

65. Ray, C., 2004. Modeling RBF efficacy for mitigating chemical shock loads. J. Am. Water Works Assoc. 96 (5), 114–128.

66. Ray, C., Grischek, T., Hubbs, S., Drewes, J.E., Haas, D., Darnault, C., 2008. Riverbank Filtration for Drinking Water Supply. ASCE Riverbank Filtration, American Society of Civil Engineers, Riverbank Filtration Task Force, John Wiley & Sons.

67. Ray, C., Grischek, T., Schubert, J., Wang, J. Z., & Speth, T. F. (2002). A Perspective of Riverbank Filtration (PDF). Journal-American Water Works Association, 94(4), 149-160.

68. Ray, C., Melin, G., & Linsky, R. B. (Eds.). (2003). Riverbank filtration: improving source-water quality (Vol. 43). Springer Science & Business Media.

69. Schijven, J., Berger, P., & Miettinen, I. (2003). Removal of pathogens, surrogates, indicators, and toxins using riverbank filtration. In Riverbank Filtration (pp. 73-116). Springer Netherlands.

70. Schmidt, C. K., Lange, F. T., & Brauch, H. J. (2004, October). Assessing the impact of different redox conditions and residence times on the fate of organic micro pollutants during riverbank filtration. In 4th International Conference on Pharmaceuticals and Endocrine Disrupting Chemicals in Water (Vol. 13, No. 15.10, p. 2004).

71. Schmidt, C. K., Lange, F. T., Brauch, H. J., & Kühn, W. (2003). Experiences with riverbank filtration and infiltration in Germany. DVGW-Water Technology Center (TZW), Karlsruhe, Germany, 17.

72. Schubert, J. (2002). Hydraulic aspects of riverbank filtration—field studies. Journal of Hydrology, 266(3), 145-161.

73. Schubert, J. (2003). German experience with riverbank filtration systems. In Riverbank Filtration (pp. 35-48). Springer Netherlands.

74. Sende, S. Sachin, (2008). A study on Riverbank Filtration. Masters thesis, Department of Water Resources Development and Management, Indian Institute of Technology, Roorkee, Roorkee, India

75. Singer, P.C. 1999. Humic substances as precursors for potentially harmful disinfection by-products. Water Science and Technology. 40(9):25.

76. Soliman, M. M. (1965). Boundary Flow Considerations in Design. Journal of the Irrigation and Drainage Division, 91(1), 159-178.

77. Sontheimer, H. (1980). "Experience with riverbank filtration along the Rhine River." Journal American Water Works Association, December 1980: 386-390.

78. Steward, D. R., & Jin, W. (2001). Gaining and losing sections of horizontal wells. Water Resources Research, 37(11), 2677-2685.

79. Sun, D., & Zhan, H. (2006). Flow to a horizontal well in an aquitard–aquifer system. Journal of hydrology, 321(1), 364-376.

80. Tufenkji, N., Ryan, J. N., & Elimelech, M. (2002). Peer reviewed: The promise of bank filtration. Environmental science & technology, 36(21), 422A-428A.

81. Vellaisamy, M, (2007). Pollutant transport through stream. Ph.D. thesis, water resources development & management, IIT Roorkee, India.

82. Verstraeten, I.M., Thurman, E.M., Lindsey, M.E., Lee, E.C., Smith, R.D., (2002) Changes in concentrations of Triazine and Acetamide Herbicides by Bank filtration, ozonation, and chlorination in a public water supply. J. Hydrol. 266 (3/4), 190–208.

83. Weiss, W. J., Bouwer, E. J., Aboytes, R., LeChevallier, M. W., O'Melia, C. R., Le, B. T., & Schwab, K. J. (2005). Riverbank filtration for control of microorganisms: Results from field monitoring. Water research, 39(10), 1990-2001.

84. Weiss, W. J., Bouwer, E. J., Ball, W. P., O'Melia, C. R., Arora, H., & Speth, T. F. (2003a). Reduction in disinfection byproduct precursors and pathogens during riverbank filtration at three Midwestern United States drinking-water utilities. In Riverbank Filtration (pp. 147-173). Springer Netherlands.

85. Weiss, W., Bouwer, E., Ball, W., O'Melia, C., Aboytes, R., & Speth, T. (2004). Riverbank filtration: Effect of ground passage on NOM character. Aqua, 53, 61-83.

86. Weiss, W.J., Bouwer, E.J., Ball, W.P., O'Melia, C.R., Arora, H., Speth, T.F., (2003b). Comparing RBF with bench-scale conventional treatment for precursor reduction. J. Am.Water Works Assoc. 95 (12), 67–80.

87. Weiss, W.J., Bouwer, E.J., Ball, W.P., O'Melia, C.R., LeChevallier, M.W., Arora, H., Speth, T.F., (2003). Riverbank filtration—fate of DBP precursors and selectedmicroorganisms. J. Am. Water Works Assoc. 95(10), 68–81.

88. Zhan, H. (1999). Analytical study of capture time to a horizontal well. Journal of Hydrology, 217(1), 46-54.

89. Zhan, H., & Cao, J. (2000). Analytical and semi-analytical solutions of horizontal well capture times under no-flow and constant-head boundaries. Advances in water resources, 23(8), 835-848.

90. Zhan, H., & Park, E. (2003). Horizontal well hydraulics in leaky aquifers. Journal of Hydrology, 281(1), 129-146.

91. Zhan, H., & Zlotnik, V. A. (2002). Groundwater flow to a horizontal or slanted well in an unconfined aquifer. Water Resources Research, 38(7), 13-1.

92. Zhan, H., Wang, L. V., & Park, E. (2001). On the horizontal-well pumping tests in anisotropic confined aquifers. Journal of Hydrology, 252(1), 37-50.

LACEY'S SCOUR DEPTH AND SILT FACTOR

A.1 GENERAL

During lean flow season (non-monsoon period), the flow in the river attains the minimum and the depth of water in the river is minimum. The thickness of the deposited sediments is the maximum. During the flood period, scouring occurs and the thicknesses of sediments get reduced. The scour depth is estimated using following Lacey (1929) theory

$$D_s = 0.47 \left(\frac{Q}{f_L} \right)^{\frac{1}{3}}$$
(A.1)

where, D_s is the normal scour depth in m below the design flood level, Q the design flood discharge in $\frac{m^3}{s}$, f_L is the Lacey's silt factor related to the median size of bed material d (mm). f_L Values are given in table A.1.

Table A.1.Values of Lacey's Silt Factor   *Source (IS: 3955-1967)*

S. No.	Type of bed soil	Size of particles (mm)	Silt factor (f_L)
1	Coarse silt	0.04	0.35
2	Fine sand	0.08	0.50
		0.15	0.68
3	Medium sand	0.3	0.96
		0.5	1.24
4	Coarse sand	0.7	1.47
		1.0	1.76
		2.0	2.49
5	Gravel	5.0	3.89
		10.0	5.56
		20.0	7.88
6	Boulders	50	12.3
		75	15.2
		190	24.3

The collector pipe should be laid below the scour depth accounting the minimum filter thickness above the collector pipe required for natural filtration through the layer above the pipe. For rapid sand filter, the minimum filtration thickness is taken as 0.8 m.

EXPRESSION FOR NUMBER OF LOG CYCLE REDUCTION IN BACTERIAL CONCENTRATION

B.1 GENERAL

Population growth of bacteria during the time a parcel of water moves from the river to the collector pipe is modeled adopting the modeling of tumor growth; the population growth of bacteria, in a parcel of water which is excluded from the surrounding is expressed as:

$$\frac{dC}{dt} = r\left(1 - \frac{C}{C_0}\right)C - \lambda_L = rC - \lambda_L C - \frac{rC^2}{C_0} \qquad (B.1)$$

Where, C is the concentration of a bacteria (number in unit volume of water), t is the time parameter, C_0 is the initial concentration at time t=0, r is reproduction rate, λ_L is the decay rate. Rewriting equation $(B.1)$

$$\frac{dC}{rC - \lambda_L C - \frac{rC^2}{C_0}} = dt$$

(B.2) Integrating (Abramowitz, and Stegun, 1970, p.12) and simplifying

$$\frac{1}{(r - \lambda_L)} \ln\left[\frac{r\left(\frac{C}{C_0}\right)}{r\left(\frac{C}{C_0}\right) + \lambda_L - r}\right] = t + A \qquad (B.3)$$

Where, A is integration constant. Applying the initial condition i.e. when the parcel of water enters the aquifer medium at $t=0$, $C = C_0$, the constant

$$A = \frac{1}{(r - \lambda_L)} \ln\left[\frac{r}{\lambda_L}\right] \qquad (B.4)$$

Incorporating (B.4) in (B.3)

$$t = \frac{1}{(r - \lambda_L)} \left[\ln\left\{\frac{r\left(\frac{C(t)}{C_0}\right)}{r\left(\frac{C(t)}{C_0}\right) + \lambda_L - r}\right\} - \ln\left\{\frac{r}{\lambda_L}\right\}\right] \qquad (B.5)$$

During the travel time t_r of a parcel of water moving from the stream to the collector pipe, the concentration attains a value $C(t_r)$. Accordingly from equation (B.5), we obtain

$$t_r = \frac{1}{(r-\lambda_L)}\left[\ln\left\{\frac{r\left(\frac{C(t_r)}{C_0}\right)}{r\left(\frac{C(t)}{C_0}\right)+\lambda_L-r}\right\}-\ln\left\{\frac{r}{\lambda_L}\right\}\right] \tag{B.6}$$

Let $\dfrac{C(t_r)}{C_0}$ be equal to 10^{-n}. The variable n is unknown. Incorporating $\dfrac{C(t_r)}{C_0}=10^{-n}$ in $\quad$ (B.6)

$$t_r = \frac{1}{(r-\lambda_L)}\left[\ln\left\{\frac{r10^{-n}}{r10^{-n}+\lambda_L-r}\right\}-\ln\left\{\frac{r}{\lambda_L}\right\}\right]=\frac{1}{(r-\lambda_L)}\left[\ln\left\{\frac{\lambda_L10^{-n}}{r10^{-n}+\lambda_L-r}\right\}\right]$$

$$=\frac{1}{(r-\lambda_L)}\left[\ln\left\{\frac{1}{r/\lambda_L+(1-r/\lambda_L)10^n}\right\}\right]=\frac{1}{(\lambda_L-r)}\left[\ln\left\{r/\lambda_L+(1-r/\lambda_L)10^n\right\}\right]$$

or

$$(\lambda_L-r)t_r=\left[\ln\left\{r/\lambda_L+(1-r/\lambda_L)10^n\right\}\right]$$

$$10^n=\frac{r/\lambda_L-e^{-(r-\lambda_L)t_r}}{(r/\lambda_L)-1}$$

$$n=\log_{10}\frac{r/\lambda_L-e^{-(r-\lambda_L)t_r}}{(r/\lambda_L)-1} \tag{B.7}$$

The variable n is the number of log cycle reduction in bacteria concentration during the travel time t_r.

C.1 GENERAL

The Schwarz-Christoffel transformation is a method of mapping a polygon consisting of straight-line boundaries from one plane onto the upper/lower half of another plane. The mapping is conformal implying that the angle of intersection between two curves in the original plane is maintained in magnitude and sense when transformed to the other plane. The technique is applied for solving Laplace equation governing two dimensional steady groundwater flows. The confined flow domain is required to be homogeneous and isotropic for applying the conformal mapping technique. This transformation can be considered as the mapping of a polygon from one plane onto a similar polygon in another plane in such a manner that the sides of the polygon in one plane extend through the real axis of the other plane. This is accomplished by opening the polygon at some convenient point preferably at one of the vertices. The vertex that is taken to infinity does not take part in the transformation there by the complexity of transformation is reduced. Thus the transformation maps conformally the region interior to the polygon into the entire upper/lower half of auxiliary plane. The mapping is applicable for closed as shown in Fig. (C.1) as well as for open polygon as shown in Fig. (C.2). If a polygon is located in $z(= x + iy)$ plane, the transformation that maps it conformally onto upper half of the auxiliary $t(= r + is)$ plane is:

$$z(t) = M \int_{0}^{t} \frac{d\zeta}{(\zeta - a)^{1-\alpha}(\zeta - b)^{1-\beta}(\zeta - c)^{1-\gamma}\ldots} + N \qquad (C.1)$$

Applying Leibniz rule for differentiation of an integral (Abramowitz and Stegun, 1970) that is value of the integrand at the upper limit multiplied by differential of the upper limit with respect to the independent variable

$$\frac{dz}{dt} = M(t-a)^{\alpha-1}(t-b)^{\beta-1}(t-c)^{\gamma-1}\ldots \qquad (C.2)$$

$a,b,c\ldots\ldots$ are mapping parameters; only two of them can be assigned values on the real axis of the t-plane. The complex constant N depends on the lower limit of integration. The complex constant M and other parameters are determined from geometry of polygon in z-plane.
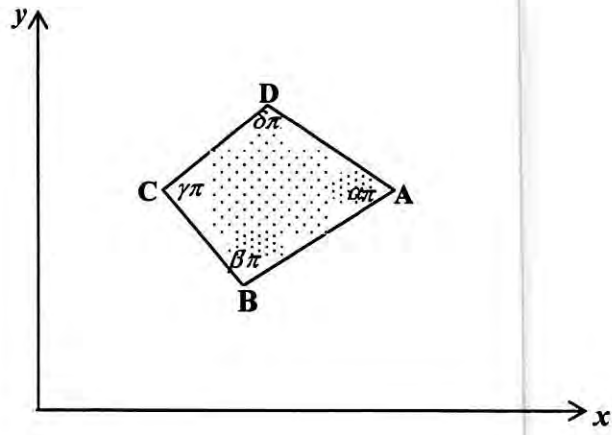
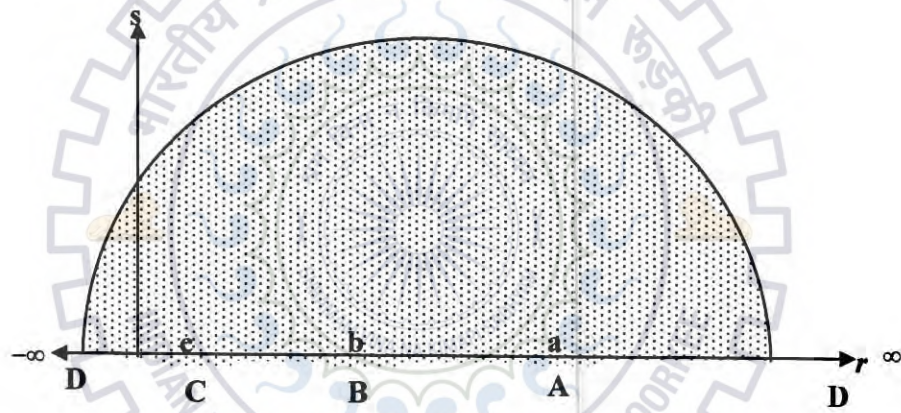Fig. (*C*.1) Closed polygon in z-plane
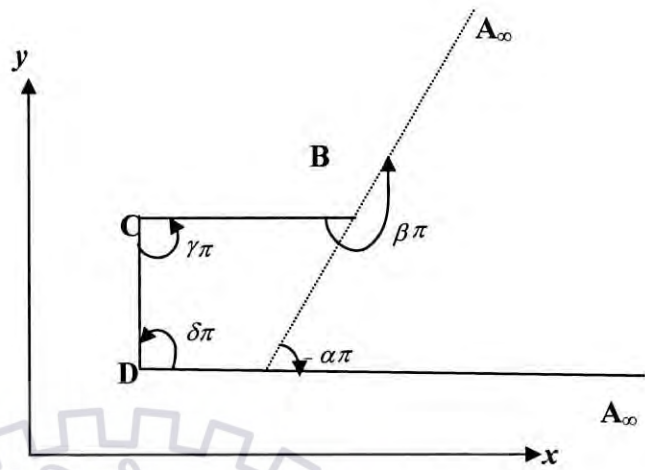

Fig. (C.2) Upper half auxiliary t-plane
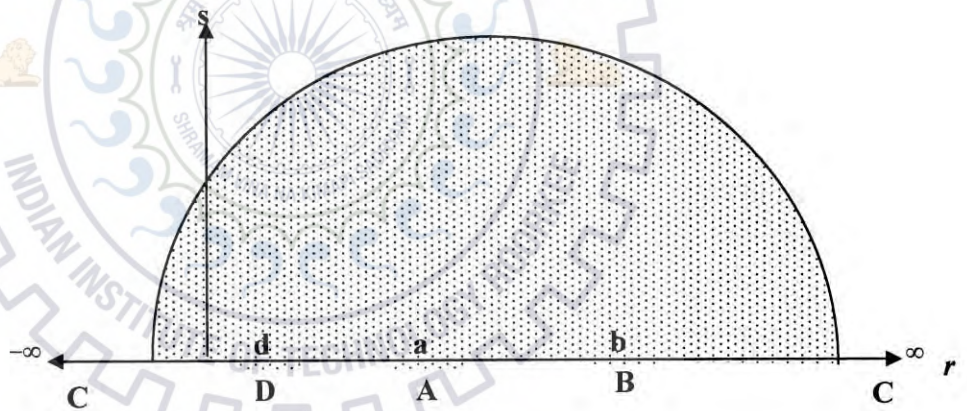
126

Fig. (C.3) Open polygon in z-plane

Fig. (C.4) Upper half auxiliary *t*-plane

If an open polygon is located in the *z* plane as shown in Fig. (C.3) and if vertex *C* is taken to infinity, then the transformation that maps it conformally onto upper half of the auxiliary *t*-plane is

$$z(t) = M \int_0^t \frac{d\zeta}{(\zeta - a)^{1+\alpha} (\zeta - b)^{1-\beta} (\zeta - d)^{1-\delta} \dots} + N \tag{C.3}$$

and

$$\frac{dz}{dt} = M (t - a)^{-(\alpha+1)} (t - b)^{\beta-1} (t - d)^{\delta-1} \dots \tag{C.4}$$

127

Where, ζ =dummy variable; $\alpha, \beta, \gamma \dots$ are the interior angles (fractions of π) of the polygon in the z plane, and $a, b, c \ (-\infty < a < b < c < \dots < \infty)$ are the points on the real axis of the of the t-plane corresponding to the respective vertices.

D.1 GENERAL

Since, the mapping steps result in a set of non-linear equations, which require a suitable technique to compute the unknown parameters. The implicit nature of the non-linear equations restricts the range of its applicability. So such non-linear equations are solved by iterative method given by Newton-Rapshon.

The set of non-linear equations are derived in chapter 4. All the sets are represented by:

$F_i\left(X_1, X_2, \cdots \cdots \cdots X_n\right) = 0$, where $i = 1, 2, \cdots \cdots \cdots n$ constitute the variables $X_1, X_2, \cdots \cdots \cdots X_n$. Let '$X$' and '$F$' denote entire values of vector X_i and functions F_i, then in the neighborhood of X, e.g. of the functions F_i can be expanded in Taylor series.

$$F_i\left(X + \delta x\right) = F_i\left(X\right) + \sum_{j=1}^{n} \frac{\partial F_i}{\partial x_j} \Delta x_j + 0.\delta x^2 \qquad (D.1)$$

In matrix notation, the above equation can be written as:

$$F_i\left(X + \delta x\right) = F_i\left(X\right) + J.\Delta x_j + 0.\delta x^2 \qquad (D.2)$$

Neglecting the term of the order δx^2 and higher and setting $F_i\left(X + \delta x\right) = 0$.

We have $J.\Delta x = F(X)$ is an equation of matrix of set of non-linear equations. This matrix equation can be solved by LU decomposition and correction is then added to the solution vector as: $X_{new} = X_{old} + \Delta x$

Where J is known as the Jacobian matrix and represented as:

$$J = \begin{bmatrix} \dfrac{\partial F_1}{\partial x_1} & \dfrac{\partial F_1}{\partial x_2} & \dfrac{\partial F_1}{\partial x_3} & \cdots & \cdots & \cdots & \cdots & \dfrac{\partial F_1}{\partial x_n} \\ \dfrac{\partial F_2}{\partial x_1} & \dfrac{\partial F_2}{\partial x_2} & \dfrac{\partial F_2}{\partial x_3} & \cdots & \cdots & \cdots & & \dfrac{\partial F_2}{\partial x_n} \\ \cdots & \cdots & \cdots & & & & & \\ \cdots & \cdots & \cdots & & & & & \\ \dfrac{\partial F_n}{\partial x_1} & \dfrac{\partial F_n}{\partial x_2} & \dfrac{\partial F_n}{\partial x_3} & & & & & \dfrac{\partial F_n}{\partial x_n} \end{bmatrix}$$

where,

$$\frac{\partial F_i}{\partial x_i} = \frac{F_i\left(x_1, x_2, x_3, \cdots \cdots \cdots \cdots + \Delta h, \cdots \cdots, x_n\right) - Fi\left(x_1, x_2, x_3, \cdots \cdots, x_n\right)}{\Delta h} \qquad (D.3)$$

and $\Delta x_i = -F[J]^{-1}$

or $X_i = X_i + \Delta x$, X_i are the variables in the non-linear equations.